



---

seit 1558

Friedrich-Schiller-Universität Jena  
Biologisch-Pharmazeutische Fakultät  
Institute für Pharmazie  
Lehrstuhl für Pharmazeutische Technologie

# **Predicting Skin Permeability of Neutral Species and Ionic Species**

**Dissertation**

**zur Erlangung des akademischen Grades doctor rerum naturalium**

**(Dr. rer. nat.)**

**vorgelegt dem Rat der Biologisch-Pharmazeutischen Fakultät**

**der Friedrich-Schiller-Universität Jena**

**von Keda Zhang**

**Master of Science in Medizinische Chemie (M.Sc.)**

**Geboren am 25. August 1986, in Hubei, V. R. China**



---

seit 1558

Friedrich-Schiller-University Jena  
Faculty of Biology and Pharmacy  
Institute of Pharmacy  
Department of Pharmaceutical Technology

# **Predicting Skin Permeability of Neutral Species and Ionic Species**

**Dissertation**

**For the obtainment of the academic degree doctor rerum naturalium**

**(Dr. rer. nat.)**

**Presented to the Council of the Faculty of Biology and Pharmacy of  
the Friedrich-Schiller-University Jena**

**Submitted by**

**Keda Zhang**

**Master of Science in Medicinal Chemistry (M.Sc.)**

**Born on 25<sup>th</sup> of August, 1986, in Hubei, P. R. China**

# **Reviewers**

**Reviewer 1: Prof. Dr. Alfred Fahr, Friedrich-Schiller-University Jena**

**Reviewer 2: Prof. Dr. Gerhard Scriba, Friedrich-Schiller-University Jena**

**Reviewer 3: Prof. Dr. Rolf Schubert, Albert-Ludwigs-University Freiburg**

**Date of Defense: 30. 11. 2012**

*“Try not to become a man of success  
but rather to become a man of value.”*

**Albert Einstein (1879-1955)**

# Contents

<b>1. Introduction</b> .....	1
1.1 Structure of Skin.....	3
1.1.1 Epidermis (and Stratum Corneum) .....	4
1.1.2 Dermis .....	6
1.2 Transdermal Permeation Pathways.....	7
1.3 Measurement of Lipid Membrane-Water Partition .....	9
1.3.1 Immobilized Artificial Membrane (IAM) Chromatography .....	10
1.3.2 Immobilized Liposome Chromatography (ILC) .....	12
1.3.3 Liposome Electrokinetic Chromatography (LEKC) .....	14
1.4 Linear Free-Energy Relationship (LFER).....	15
1.5 Aims of this Study .....	17
<b>2. Publication Overview</b> .....	20
<b>3. Publications</b> .....	23
3.1 Publication 1 .....	23
3.2 Publication 2.....	33
3.3 Publication 3 .....	35
<b>4. Discussion</b> .....	68
4.1 Comparison of Partitioning Systems .....	68
4.1.1 Comparison Methods of LEER Coefficients .....	69
4.1.2 Comparison of Lipid Membrane-Water Systems with Organic Solvent-Water Systems .....	70
4.1.3 Uniqueness of Cerasome on Modeling the Stratum Corneum in Partitions.....	70
4.1.4 Correlation between Skin Permeation and Partitioning Systems.....	71
4.2 LFER Analysis for Skin Permeability of Both Species .....	72
4.2.1 Assessment of Predictive Power .....	72
4.2.2 Effects of Ionization on the Overall Permeation and the Separate Partition and Diffusion.....	73
4.3 Application of the Potts-Guy Model.....	74
4.4 Contribution of this Study .....	75

<b>5. Summary</b> .....	77
<b>6. References</b> .....	82
<b>7. Abbreviations</b> .....	89
<b>8. Acknowledgements</b> .....	91
<b>Curriculum Vitae</b> .....	93

# 1. Introduction

---

The skin forms the body's extremely efficient barrier, which prevents the loss of excessive water from the body and ingress of xenobiotics during exposure to the biologically hostile environment. Nevertheless, compounds frequently contacting with human skin can be dermally absorbed to the extents associated with their chemical structures (Flynn, 1990; Potts and Guy, 1992). Moreover, transdermal delivery provides an appealing alternative to other modes of administration in view of the advantages it owns, including sustained and controlled delivery, direct access to target site, the avoidance of first pass metabolism and improved patient acceptance and compliance and so on (Brown et al., 2006).

Skin permeability is a critical parameter for estimating the dermal absorption for compounds through the skin. Over the past decades, experimentally measured values of skin permeability for many compounds have been reported. However, measurements do not exist for more compounds with the potential for dermal absorption. Hence, various predictive models based on the different assumptions of the fundamental mechanisms underlying skin permeation have been proposed in order to estimate the unavailable permeability (Mitragotri et al., 2011). Among these models, the best known and most applied type is the quantitative structure-permeability relationship (QSPR) proposed by Potts and Guy (1992), generally written as follows:

$$\log K_p = a + b \cdot \log P - c \cdot MV \quad (1.1)$$

where  $K_p$  is the skin permeability of the compound through the skin, commonly equated with the stratum corneum (SC) permeability as the dominant resistance to permeation of most compounds comes from the SC (Michaels et al., 1975);  $P$  describes the partition in model vehicles that mimic the SC, and  $MV$  is the molecular volume, which is sometimes approximated by molecular weight

## Introduction

(MW); a, b and c are the constants. Such a QSPR equation was in reality deduced on the basis of Fick's first law that describes steady-state diffusion through membrane:

$$K_p = K_{sc} \cdot D_{sc}/h_{sc} \quad (\text{or} \quad \log K_p = \log K_{sc} + \log D_{sc} - \log h_{sc}) \quad (1.2)$$

Here,  $K_{sc}$ ,  $D_{sc}$  and  $h_{sc}$  are the partition coefficient, the diffusion coefficient and the diffusion path length in the SC treated as a pseudo-homogenous membrane, respectively. Because both  $K_{sc}$  and  $D_{sc}$  are not easily determined, their values have to be estimated from some more readily available parameters in practice. In general,  $P$  in various model vehicles is used instead of  $K_{sc}$ , while  $D_{sc}$  is supposed to depend inversely upon molecular volume (Flynn, 1990; Potts and Guy, 1992). Thus, it is the case in Eq. 1.1. Octanol is by far a widely-used model solvent for the SC, partially due to the facts that the octanol-water partition coefficient ( $P_{oct}$ ) for chemicals can be easily found out in the literature, or calculated from molecular structure (Mannhold and van de Waterbeemd, 2001), and correlate well with the partition coefficient in lipid bilayers (Burns et al., 2002; Diamond and Katz, 1974). As a representative instance, Potts and Guy (1992) took advantage of experimental skin permeability data compiled by Flynn (1990) from aqueous solution on about 90 compounds to generate a renowned equation on the lines of Eq. 1.1:

$$\log K_p = -6.3 + 0.71 \log P_{oct} - 0.0061MW \quad (R^2 = 0.67) \quad (1.3)$$

However, such models were constructed upon  $K_p$  data sets for neutral species only. And in some cases, ionization of basic and acidic penetrating chemicals was selectively ignored. This is due to the fact that it is extremely difficult to set up an equation for skin permeation that includes both neutral species and ionic species. On the one hand, ionizable solutes exist both as separated ions (anions and cations) and as ion-pairs in octanol; the experimentally measured  $P_{oct}$  values for separated ions are those for a neutral combination of anion and cation, and single-ion  $P_{oct}$  values have to be obtained after adjustment using some extra-thermodynamic convention (Abraham and



## Introduction

Acree, 2010d). On the other hand,  $P_{\text{oct}}$  fails to encode some important recognition forces between ionic species and biological membranes (Avdeef et al., 1998). Consequently, the liposome-water partition has been developed as a promising model for the SC-water partition because of the lipid bilayer microstructure of liposome (Wang et al., 2009; Xian et al., 2008). However, this aspect of study is, up to now, too rough to answer the fundamental questions, e.g., whether or not liposome can model the SC in partition processes, and further whether or not Eq. 1.1 using liposome-water partition parameters provides a reasonable prediction for  $\log K_p$  of ionic species.

One feasible method for predicting  $\log K_p$  of ionic species is through the linear-free energy relationship (LFER) developed by Abraham and Acree (2010a, b, c, d). The LFER can be used to predict biological membrane permeability of both neutral and ionic species, and has been applied to blood-brain barrier (BBB) permeability (Abraham, 2011). It is also the key analytical method of this study. This LFER full of intelligence will be introduced in great detail below.

### **1.1 Structure of Skin**

The skin covers the entire outer surface of the body. Structurally, the skin consists of two distinct layers: the epidermis and the dermis. The epidermis is the outer layer, serving as the physical and chemical barrier between the interior body and the exterior environment; the dermis is the deeper layer, providing mechanical support and protection to the underlying muscle, bones and organs, as well as the structural support of the skin. Beneath the dermis lies hypodermis or subcutaneous fatty tissue, which binds the skin to the underlying structures and stores energy in the form of fat. Hair, nails, sebaceous glands, eccrine and apocrine sweat glands are known as the appendages of the skin. These appendages can be found to disperse throughout the skin, varying in number and size according to the anatomical site of the body. The cross-section of the skin is shown in Fig. 1.1.

## Introduction

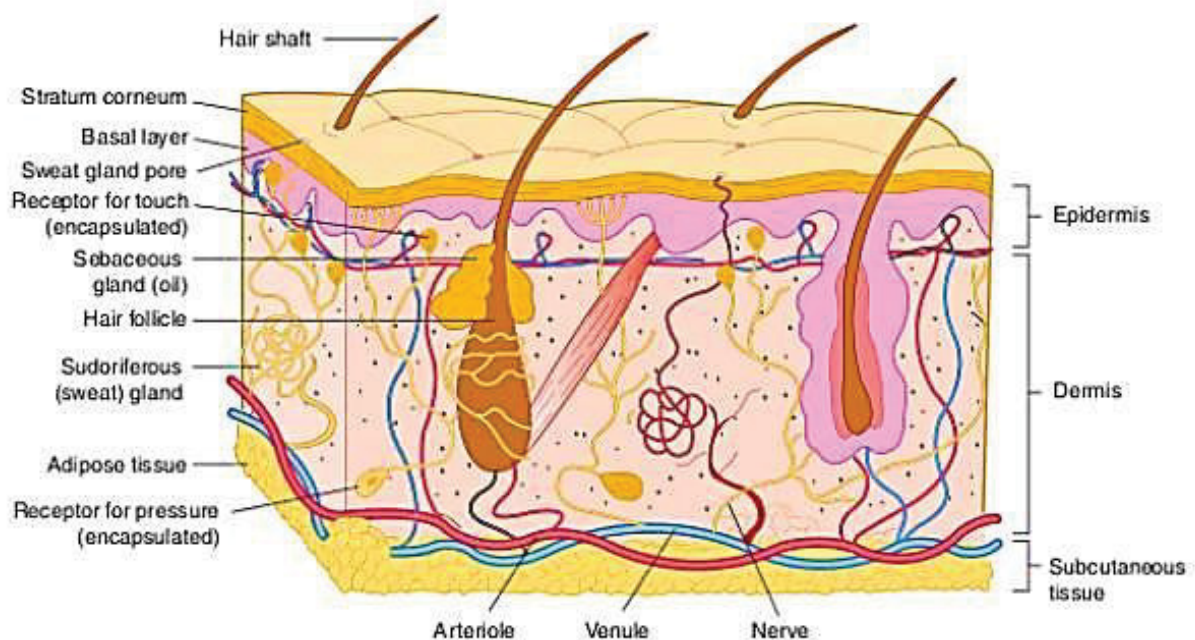


*Figure 1.1 A cross-sectional diagram of the skin, source: <http://body-disease.com/page/19/>*

### ***1.1.1 Epidermis (and Stratum Corneum)***

The epidermis is a thin, stratified squamous epithelium mainly composed of keratinocytes, which synthesize the protein keratin. The epidermis is in a constant state of transition, as the inner cells moving upward to the surface continuously replace the outer cells until being shed, accompanied by their differentiation (or keratinization). The differentiation process is essentially characterized by an accumulation of three types of species, i.e., cytokeratins, other proteins in the keratohyalin granules and lipids, and a degradation of all of the internal organelles. The five distinct layers of the epidermis are formed by the differing stages of differentiation, from bottom to top, including the basal layer (stratum basale), the spinous layer (stratum spinosum), the granular layer (stratum granulosum), the clear layer (stratum lucidum) and the horny layer (stratum corneum). The cells become wider and flatter as they move from the stratum basale towards the surface (see Fig. 1.2). Over most of the body, the epidermis is on the order of 100  $\mu\text{m}$  thick. The complete renewal of the epidermis takes roughly 3-4 weeks in normal individuals.

## Introduction

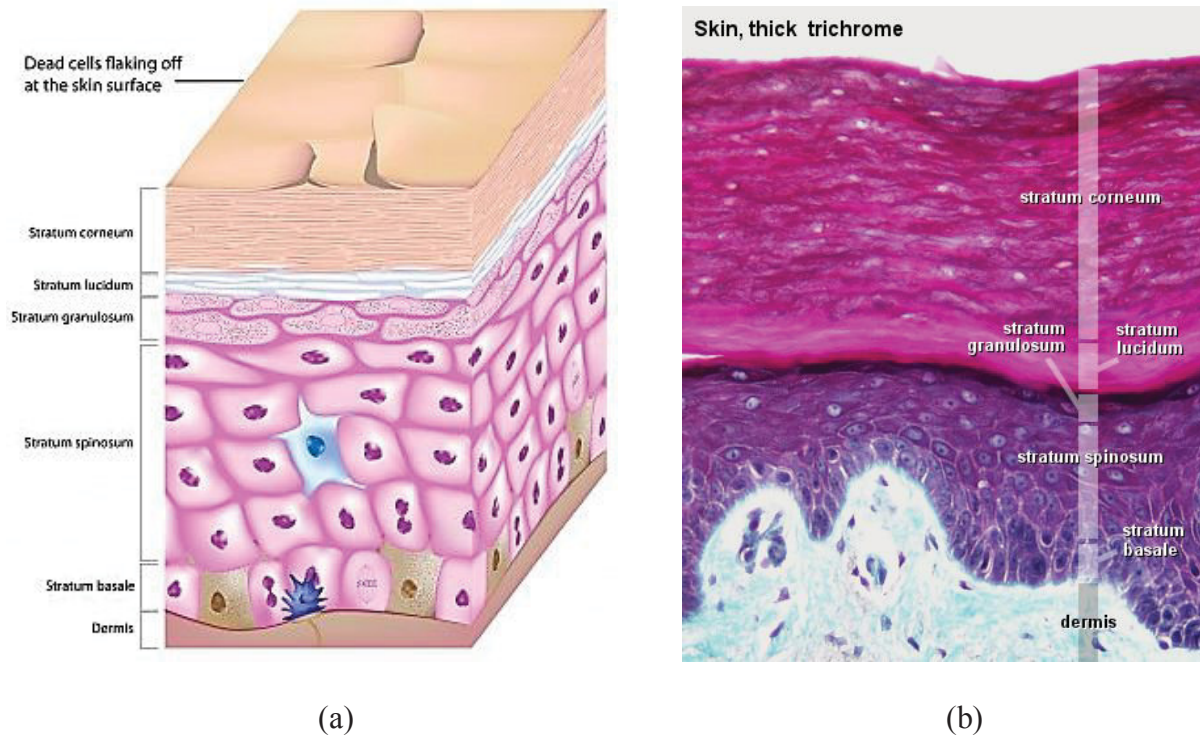


**Figure 1.2** Cross-section of the epidermis:

(a) A artificial sketch, modified from source: <http://totalskinmanagement.com/skin-structure/>

(b) A micrographic picture for thick epidermis using trichrome, from the kind share of Lutz Slomianka: <http://www.lab.anhb.uwa.edu.au/mb140/>. Note that the stratum lucidum is a transitional and translucent layer between the stratum granulosum and the stratum corneum, and is not usually seen in thin epidermis.

The stratum corneum is the final outcome of the differentiation process, which is made up of layers of extremely flattened, hexagonal-shaped, cornified and dead cells known as corneocytes. The corneocytes are stacked 15-25 layers deep in most areas of the skin, each of which is about 30  $\mu\text{m}$  in diameter and 0.5-0.8  $\mu\text{m}$  in thickness (Holbrook and Odland, 1974). Each corneocyte is filled with densely packed keratin proteins, bounded by a protein envelope and embedded into an intercellular lipid matrix. Virtually all of the lipids in the stratum corneum are in the intercellular space, being present in stacked lipid bilayers, except for a small part in residual cell membranes. This compact and continuous structure provides the primary permeability barrier of the skin. The lipid content takes up 10-20% of the stratum corneum's dry weight, while the proteins contribute 70-80% to the weight (Lu and Flynn, 2009). The stratum corneum mainly contains three types of

## Introduction

lipids: ceramides, cholesterol, and saturated fatty acids. These lipids account for about 50%, 25%, 10% of the lipid mass, respectively (Law et al., 1995). Cholesterol esters, cholesterol sulfate, and glucosylceramides are present in minor amounts (Michniak-Koln et al., 2005).

Moreover, in health skin at ordinary relative humidity, the water content of stratum corneum is normally roughly 15-20% (Lu and Flynn, 2009). The water-retaining keratin certainly plays an important role in consequence here. Should the skin become fully hydrated, the stratum corneum can absorb up to three times its dry weight of water.

### ***1.1.2 Dermis***

The dermis lies below and immediately connects with the epidermis, often referred to as the true skin. As the major portion of the skin, it varies in thickness from 0.6 mm on the eyelids to 3 mm on the back, palms and soles. Its structure is held together by a tough meshwork of structural fibers, e.g., collagen, elastin, and reticulin. The space between these fibers is mostly filled with a mucopolysaccharidic gel called the ground substance. Collagen represents approximately 75% of the dermis composition, providing strength and toughness (Lu and Flynn, 2009).

The dermis may be divided into two sublayers without a shape boundary: the papillary layer and the reticular layer. The papillary layer is the thin upper layer in contact with the deep surface of the epidermis, consisting of loose, relatively cell-rich connective tissue. Note that the interface between the epidermis and the dermis is not flat but papillose. The papillary layer bulges into the epidermis, which houses the capillary plexus that nurture the epidermis. The thick reticular layer is the lower layer, which appears denser and contains fewer cells. In the papillary layer, collagen fibers are finer and more arranged, while coarser collagen fibers often aggregate into bundles and form an interlacing network in the reticular layer. The dermis basically comprises fibroblasts that synthesize the structural fibers, mast cells that are considered to synthesize the ground substance, and macrophages that are involved in immune response. The microcirculation that subserves the

## Introduction

skin is entirely located in the dermis. Also, embedded in the dermis are the dermal sensory nerve endings and a widespread lymphatic network. In addition, sweat glands, hair follicles associated with sebaceous glands, and small amounts of striated muscle are anchored within the dermis.

### **1.2 Transdermal Permeation Pathways**

As is well known, the stratum corneum serves as the predominant permeability barrier of the skin (Blank and Scheuplein, 1969; Scheuplein, 1965; Scheuplein and Blank, 1971, 1973). In general, the stratum corneum barrier is simplified as an idealized “bricks-and-mortar” model (Elias, 1983; Michaels et al., 1975). This model is composed of an array of corneocytes (bricks) with the space between them filled with lamellar lipids (mortar), as illustrated in Fig. 1.3. It has constituted the base for understanding the nature of the permeation of chemicals through intact stratum corneum to date. The model indicates that one substance permeates across the barrier, either by movement alternately through the intercellular lipid matrices and corneocytes (i.e., transcellular route), or by movement continuously through the intercellular lipid matrices (i.e., intercellular route). However, a substantial amount of evidence points to the fact that the intercellular pathway is, in reality, the major permeation route for most compounds, both lipophilic and hydrophilic. These observations include increased permeabilities after extraction or alteration of the SC lipids (Mitragotri et al., 1996; Scheuplein, 1967; Scheuplein and Blank, 1971), high lipids-water partition coefficients and low corneocyte-water partition coefficients (Raykar et al., 1988), and correlation between transport enhancement by chemicals and ultrasound and their action site, i.e., the lipid phase (Mitragotri et al., 1995; Potts and Francoeur, 1990). More directly, Bodde et al. (1991) and Nemanic and Elias (1980) visualized the permeation pathways of an inorganic ion  $\text{Hg}^{2+}$  and *n*-butanol, respectively, using vapor fixation and electron microscopy, and confirmed that both substances preferentially traverse the stratum corneum between corneocytes rather than through them. Moreover, Lu and Flynn (2009) explained that “the intracellular space is dense, offering little freedom of movement

## Introduction

to organic molecules that may become dissolved within it. Moreover, because of its remarkable ionic character, the intracellular keratin mass borders on being thermodynamically impenetrable.”

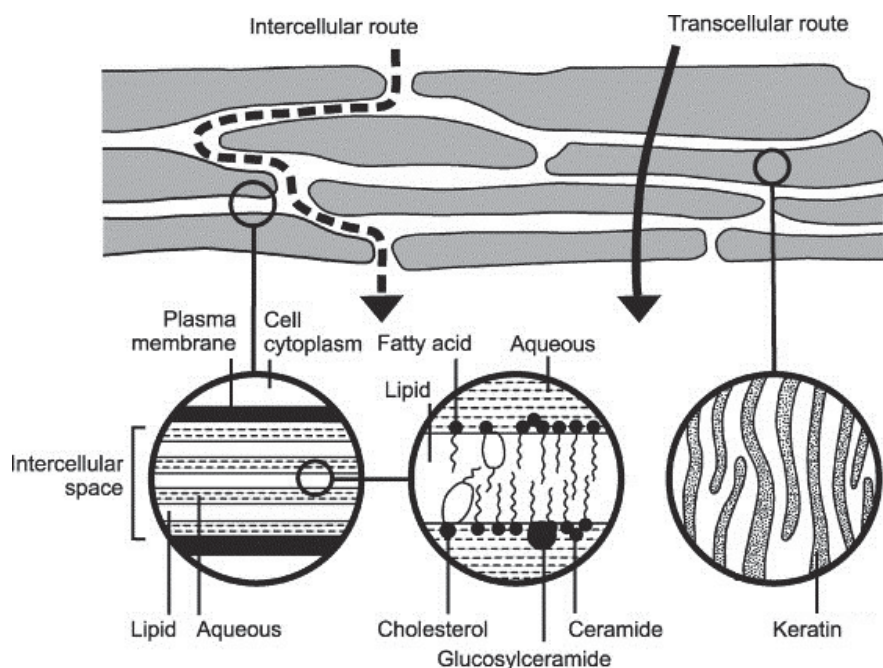


**Figure 1.3** Schematic diagram of the bricks-and-mortar model of the stratum corneum with possible drug penetration pathways through intact stratum corneum. Also shown is a lamellar model of intercellular domain showing the main stratum corneum lipids; modified from Williams and Barry (1992).

Although the intercellular pathway is the principal permeation route of the stratum corneum, it is known that the permeability coefficients of excessively hydrophilic compounds could not be explained by the intercellular lipid-based pathway only (Ackermann and Flynn, 1987; Peck et al., 1994). Hence, workers believe that transdermal transport of very hydrophilic compounds mainly takes place via an “aqueous pore” pathway instead of the lipid pathway (Ackermann and Flynn, 1987; Menon and Elias, 1997; Peck et al., 1994; Williams and Elias, 1987). And, these “aqueous pores” are thought to be created by the defects in the intercellular lipid bilayers, including multi-molecular nucleated defects, molecular packing defects, missing lipids and transient fluctuation (Mitragotri, 2003; Sznitowska et al., 1998). Very hydrophilic compounds can be characterized by  $\log P_{\text{oct}}$  values of less than  $-2.0$ .

## Introduction

In addition to “aqueous pores”, the appendages (i.e., hair follicles and sweat ducts) also offer a transdermal transport pathway for hydrophilic compounds. But due to the extremely small area fraction (about 0.1%) of the skin covered by the appendages transport through them is generally neglected. Upon mathematical modeling, Mitragotri (2003) proposed that the contribution of the appendages is dominant for large hydrophilic compounds (MW > 100,000 Da) only.

In brief, the intercellular lipid bilayers function as the non-polar pathway for transport across the barrier, while “aqueous pores” present in the lipid bilayers and the appendages constitute the polar pathway. Both pathways exist simultaneously, but their respective contributions to the total permeation depend on the physiochemical properties of the permeant, especially the lipophilicity.

### **1.3 Measurement of Lipid Membrane-Water Partition**

Liposomes have been used as model membranes to study the interaction between solutes and biological membranes since their first introduction by Bangham and his coworkers (Bangham et al., 1965a; Bangham et al., 1965b). This is obviously because liposomes significantly reproduce the lipidic assembly mode (i.e., anisotropic highly-ordered bilayers) in biological membranes, in which the lipid domain is the principal pathway for passive diffusion of drugs and physiological matters. The partitioning behavior of solutes between liposomal membranes and aqueous phases can provide a reasonable estimate for their *in vivo* affinity to biological membranes.

However, the application of liposome-water partitions has ever been severely restricted by the conventional techniques (collectively called shake-equilibrium method) to characterize them, which differ from each other in terms of the means for separating liposomal and aqueous phases after partition equilibrium (e.g., dialysis, ultrafiltration, centrifugation), because these techniques are labor-intensive and time-consuming and therefore are of little use in routine work. In recent years, high-throughput chromatographic techniques have been developed for rapid and efficient determination of chemicals partitioning into lipid layers, mainly including immobilized artificial

## Introduction

membrane (IAM) chromatography, immobilized liposome chromatography (ILC) and liposome electrokinetic chromatography (LEKC). They exhibit many attractive advantages, such as speed, small sample amount, automation, low sample purity requirement and high reproducibility. The current techniques used to characterize lipid membrane-water partitions and their advantages and disadvantages are summarized in Table 1.1. Here, the chromatographic techniques will be introduced in detail.

**Table 1.1** Current techniques for analyzing the lipid membrane-water partitions and their characters.

Techniques	Advantages	Disadvantages	Others
Shake Equilibrium	Standard approaches	Time-consuming; tedious; laborious; unwieldy	Traditional techniques (e. g. dialysis method, centrifugation method, ultrafiltration method)
Potentiometric Titration	Relatively higher speed; $\log P_{lip}$ values for both ionic and neutral species <sup>a</sup>	Only suitable for ionizable solutes; time-consuming; tedious; laborious	—
Immobilized Artificial Membrane (IAM) Chromatography	Speed; high-reproducibility; small sample amount; low purity requirement	Lipid monolayer with lack of lateral mobility of lipids and density of phospholipid head-groups	Set up on high-performance liquid chromatography (HPLC)
Immobilized Liposome Chromatography (ILC)	Speed, high-reproducibility; small sample amount; low purity requirement	Unstable; irreproducible column preparation; unsuitable for lipophilic solutes (long retention times for many neutral molecules)	Set up on HPLC
Liposome Electrokinetic Chromatography (LEKC)	Speed; high-reproducibility; small sample amount; low purity requirement	Unsuitable for neutral solutes with neutral liposomes used	Set up on capillary electrophoresis (CE)

<sup>a</sup>  $\log P_{lip}$  represents the partition coefficient between liposome and water.

### ***1.3.1 Immobilized Artificial Membrane (IAM) Chromatography***

Immobilized artificial membrane (IAM) chromatography is a chromatographic technique set up on high-performance liquid chromatography (HPLC). Originally developed by Pidgeon and his coworkers (Pidgeon, 1990a, b; Pidgeon and Venkataram, 1989) in the 1990s, the IAM stationary



## Introduction

phase consists of a monolayer of phospholipids covalently immobilized on an inert silica support. The resulting IAM surface is a chemically stable chromatographic material in both aqueous and organic solvents, which mimics the lipid environment of a fluid cell membrane on a solid matrix. Fig. 1.4 illustrates the structures of Pidgeon's IAM stationary phases (Ong and Pidgeon, 1995). IAM chromatography is quite useful for the analytical and preparative separation of membrane-associated proteins (Pidgeon et al., 1991), and has recently gained acceptance for monitoring the interaction of solutes with biological membranes (Taillardat-Bertschinger et al., 2003).

IAM chromatography measures the "phospholipophilicity" of solutes, including neutral and ionic species, where the lipophilicity index is the capacity factor (as  $\log k_{IAMw}$ ) at 100% aqueous solution being mobile phase. For hydrophilic compounds,  $\log k_{IAMw}$  can be measured directly by using aqueous mobile phase. But for lipophilic compounds,  $\log k_{IAMw}$  values have to be deduced by extrapolating a linear curve made from the capacity factors ( $\log k$ ) at different concentrations of an organic modifier (e.g., methanol) to pure aqueous mobile phase, due to their long retention times at aqueous mobile phase. The relationship between  $\log k_{IAMw}$  and  $\log k$  is described by Eq. 1.4, where  $\phi$  is the volume fraction of organic solvent and  $S$  is the constant for a specific organic modifier. When  $\phi$  is zero, that is, the mobile phase is pure aqueous solution,  $\log k$  is equal to  $\log k_{IAMw}$ . Here,  $\log k$  was calculated in accordance with the common definition of "capacity factor" in chromatography.

$$\log k = - S \cdot \phi + \log k_{IAMw} \quad (1.4)$$

Certainly, nothing is perfect. Covalent immobilization of phospholipid ligands brings forth the chemical stability of IAM surface, but it also reduces lipids' lateral mobility. Further, Ong et al. (1996) reported that the density of the polar phospholipid head groups in IAM is less than that in liposomes. It is also known that the polar head-groups are an important factor for substances partitioning in lipid membranes (Avdeef et al., 1998; Mitragotri et al., 1999). Moreover, IAM is

## Introduction

present in the form of lipid monolayers. A more adequate phase for modeling the environment of biological membranes is perhaps provided by lipid bilayers, composed of mobile lipid molecules forming a hydrophobic region sandwiched between two interfacial hydrophilic layers.

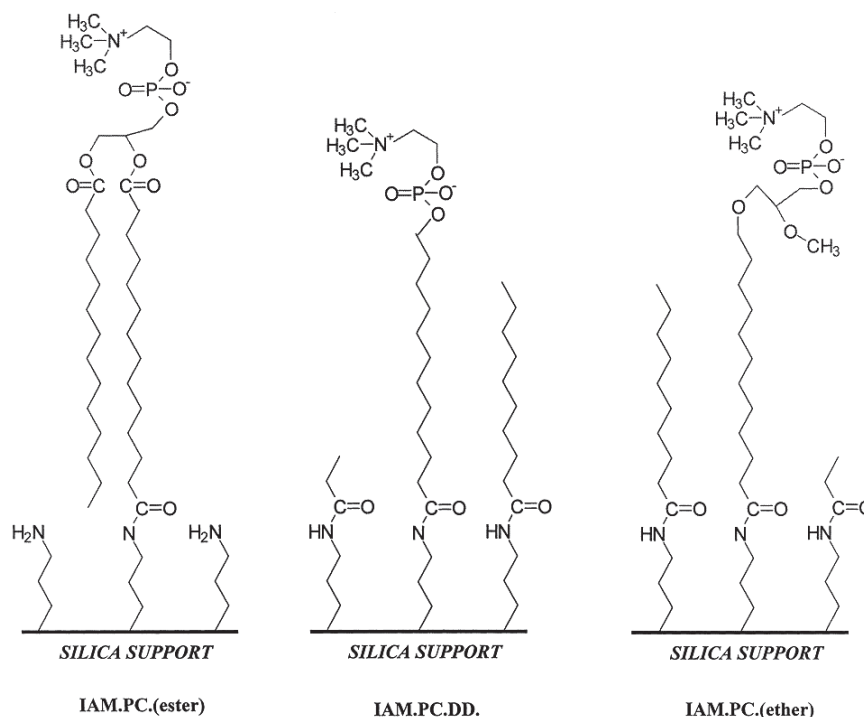


**Figure 1.4** Structures of Pidgeon's immobilized artificial membrane (IAM) stationary phases; modified from Ong and Pidgeon (1995) and Kaliszan (1999).

### 1.3.2 Immobilized Liposome Chromatography (ILC)

Immobilized liposome chromatography (ILC) is also a HPLC-based technique, where liposomes are directly immobilized into gel beads as a stationary phase. Similarly to IAM chromatography, ILC can also be used for the study of biological membrane-solute interactions (Beigi et al., 1995; Lundahl and Beigi, 1997). This approach has been extended to comprise immobilized biological membrane vesicles (e.g., human red cell membrane vesicles) for quantitative binding analyses of substrates and inhibitors interacting with transport proteins (Brekkan et al., 1996; Lundqvist et al., 1997).

## Introduction

How to immobilize liposomes in gel beads is always a subject of focus for ILC, on which the stability of immobilized liposome stationary phases as well as the density of phospholipids in the gel does depend (Wiedmer et al., 2004). Several methods for liposome immobilization have been reported, including: (a) hydrophobic ligands (e.g., alkylsulfide) able to interact with hydrophobic parts of phospholipids were coupled to the matrix of gel beads (Khaleque et al., 2000; Sandberg et al., 1987); (b) large liposomes were sterically entrapped in the gel-bead pores, either by direct formation inside the beads upon dialysis of mixed detergent-lipid micelles (Wallsten et al., 1989), or by freeze-thawing of small liposomes introduced into the gel that resulted in their fusion and growth (Yang and Lundahl, 1994); (c) liposomes can also be covalently bound to gel matrix with the help of appropriate gel ligands (Yang et al., 1999); (d) liposomes containing biotin-attached phospholipids were immobilized in avidin- or streptavidin-derivatized gels by the strong avidin-biotin binding (Yang et al., 1998). Among these techniques, the avidin-biotin technique produces the most stable stationary phases, partly because of the narrow size distribution of liposomes that was obtained, and the resultant homogeneous liposome-immobilized gels (Wiedmer et al., 2004). The tendency for phospholipid densities in the gel obtained by different immobilization methods: hydrophobic interactions  $\approx$  freeze-thawing (steric) > avidin-biotin bonding > covalent bonding > dialysis (steric) (Wiedmer et al., 2004).

The lipophilicity index from ILC is expressed as the capacity factor (as  $\log K_s$ ) measured by HPLC using aqueous buffer eluent, which is calculated according to Eq. 1.5:

$$K_s = (V_R - V_0)/A \quad (1.5)$$

where  $V_R$  and  $V_0$  are the retention volumes of the analyte and an unretained compound (usually being small and hydrophilic), and  $A$  is the amount of immobilized phospholipids.

Although ILC overcomes the disadvantages of IAM chromatography, where the fluidic lipid bilayers are anchored to gel beads, the intrinsic instability of liposome vesicles inevitably causes

## Introduction

the difficulty of the long-term storage of liposome-immobilized stationary phases as well as the leakage of phospholipids during chromatographic runs. In addition, the preparation of the phases is short of reproducibility. More importantly, the use of organic modifiers in the mobile phases is avoided in ILC, which can destroy the phospholipid membrane, so that the retention of lipophilic compounds in the stationary phases is prolonged in normal measurements of  $\log K_s$ .

### 1.3.3 Liposome Electrokinetic Chromatography (LEKC)

Unlike IAM chromatography and ILC, liposome electrokinetic chromatography (LEKC) utilizes the capillary electrophoresis (CE) instrument, but in this case liposomes are present in the buffer solutions. The liposomes function as a pseudo-stationary phase and provide partitioning sites for solutes. Fig. 1.5 illustrates the mechanism of migration and separation of two uncharged solutes,  $S_1$  and  $S_2$  in LEKC where the liposomes are negatively charged. The electrophoretic migration of the liposomes is toward the anode, but the stronger electroosmotic flow drives the liposomes and the solutes toward the cathode where they are detected. Uncharged solutes are separated according to differences in liposome-water partitions (Burns and Khaledi, 2002).

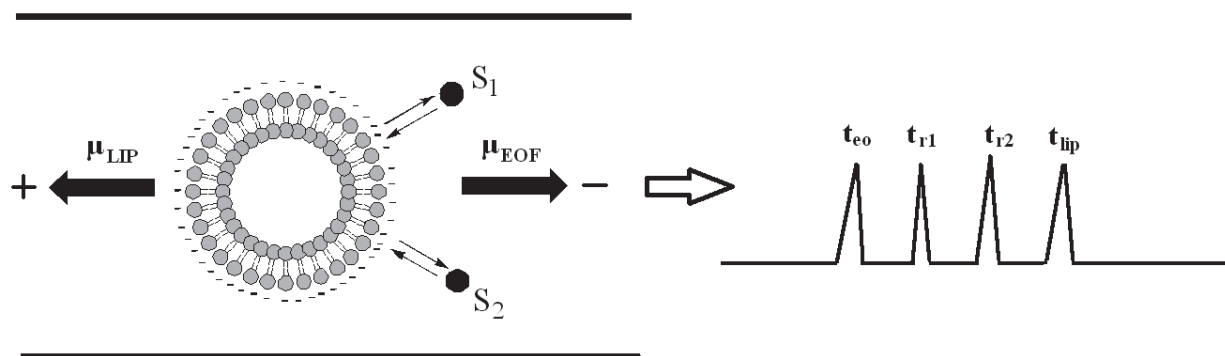


**Figure 1.5** Schematic presentation of the migration pattern in LEKC with a negatively charged liposome.  $S_1$  and  $S_2$  represent two uncharged solutes partitioning into the liposome.  $\mu_{LIP}$  and  $\mu_{EOF}$  are the mobilities of the liposome and the electroosmotic flow at a high voltage, respectively. As a result,  $t_{eo}$ ,  $t_{r1}$ ,  $t_{r2}$ , and  $t_{lip}$  are the retention times of an unretained marker (e.g., methanol), two solutes, and a liposome marker (e.g., decanophenone), respectively. Modified from Burns and Khaledi (2002).

## Introduction

A substantial number of publications on predicting analyte-membrane interactions by LEKC have been seen since the first use of LEKC on the separation of compounds (Zhang et al., 1995), as reviewed by Wiedmer and Shimmo (2009). The retention factor (as  $\log k$ ) is the lipophilicity index derived in LEKC. Two different procedures were performed in LEKC system to determine  $\log k$  of charged solutes and neutral solutes respectively, since charged solutes possess their own electrophoretic mobility under voltage as compared to neutral solutes, as described in Eq. 1.6 for neutral solutes and in Eq. 1.7 for charged solutes.

$$k = (t_r - t_0) / t_0 (1 - t_r/t_{lip}) \quad (1.6)$$

$$k = (t_r - t_{eo}) / t_{eo} (1 - t_r/t_{lip}) \quad (1.7)$$

In the equations,  $t_r$ ,  $t_{eo}$  and  $t_{lip}$  are the retention times of the solute, the electroosmotic flow marker (e.g., methanol) and the liposome marker (e.g., decanophenone) in LEKC system, respectively;  $t_0$  is the retention time of charged solutes in pure buffer solution.  $t_{eo}$  and  $t_0$  represent the unretained times of neutral solutes and charged solutes, respectively.

LEKC is a powerful tool for the study of drug-membrane interactions, which provides some particular advantages over those HPLC-based techniques. For example, the preparation of HPLC columns is generally tedious, time-consuming and costly so that adjusting the composition of the stationary phases to simulate specific biological membranes is not a trivial task. On the contrary, any type of liposomes can be used in LEKC whenever it is needed. Moreover, there is no storage problem for the liposomes in LEKC, since they may be easily and reproducibly prepared prior to use. Nevertheless, LEKC has an obvious disadvantage that when the net charge of the liposomes is neutral, uncharged solutes are impossibly distinguished.

### **1.4 Linear Free-Energy Relationship (LFER)**

## Introduction

A LFER equation proposed by Abraham (1993) has been widely used to characterize a number of equilibrium systems, including *in vivo* and *in vitro* partition processes and transport processes, and to predict the corresponding equilibrium coefficients (Acree et al., 2012), including partition coefficients (e.g.,  $\log P_{\text{oct}}$  and liposome-water partition coefficient,  $\log P_{\text{lip}}$ ) and rate coefficients (e.g.,  $\log K_p$  and blood brain barrier permeability,  $\log P_{\text{BBB}}$ ), see Eq. 1.8:

$$SP = c + eE + sS + aA + bB + vV \quad (1.8)$$

Here and elsewhere, SP represents an equilibrium coefficient for a series of solutes in a given system. The independent variables are physicochemical properties or descriptors of the solutes as follows: E is the excess molar refraction in  $(\text{cm}^3 \text{mol}^{-1})/10$ , S is the solute dipolarity/polarizability, A and B are the overall hydrogen bond acidity and basicity, respectively, and V is the McGowan characteristic molecular volume in  $(\text{cm}^3 \text{mol}^{-1})/100$ . Eq. 1.8 was set up for processes that involve neutral species only. Abraham and Acree (2010a, b, c, d) found that it was necessary to introduce a new descriptor for cations,  $J^+$ , and a new descriptor for anions,  $J^-$ , in order to extend Eq. 1.8 to include ions and ionic species, leading to Eq. 1.9:

$$SP = c + eE + sS + aA + bB + vV + j^+J^+ + j^-J^- \quad (1.9)$$

Note that  $J^+$  is zero for anions,  $J^-$  is zero for cations, and both are zero for neutral species, in which case Eq. 1.9 reverts to Eq. 1.8. All the solute descriptors can be calculated or estimated as detailed previously (Abraham, 2011; Abraham and Acree, 2010a, b, c). The descriptors for ions and ionic species are on the same scales as those for neutral species, so that Eq. 1.9 can include ions, ionic species and neutral species. In this study, the term “ions” refers to permeant ions such as  $\text{Na}^+$  and  $\text{Cl}^-$ , and the term “ionic species” refers to ions derived from protonation of bases and deprotonation of acids. Some examples of the descriptors used in Eq. 1.2 are shown in Table 1.2. The coefficients in Eq. 1.9 (i.e., c, e, s, a, b, v,  $j^+$  and  $j^-$ ) are obtained by multiple linear regression

## Introduction

(MLR). They are not only fitting coefficients, but serve to characterize the given system. So far, Eq. 1.9 has been proved to be a pretty good model that incorporates neutral and ionic species for the partitions between organic solvents and water (Abraham and Acree, 2010d), the diffusions in water and ethanol (Hills et al., 2011) and the permeation through BBB (Abraham, 2011).

**Table 1.2** Descriptors for some neutral species, ions and ionic species<sup>a</sup>

Species	E	S	A	B	V	J <sup>+</sup>	J <sup>-</sup>
Na <sup>+</sup>	-0.020	2.31	1.22	0.00	0.0330	0.316	0.000
K <sup>+</sup>	0.000	2.57	1.21	0.00	0.0920	0.357	0.000
NH <sub>4</sub> <sup>+</sup>	-0.011	1.77	1.80	0.00	0.3399	0.370	0.000
MeNH <sub>3</sub> <sup>+</sup>	0.100	2.90	1.35	0.00	0.3708	0.722	0.000
Me <sub>2</sub> NH <sub>2</sub> <sup>+</sup>	0.039	2.41	1.00	0.00	0.5117	0.877	0.000
Me <sub>4</sub> N <sup>+</sup>	-0.100	1.31	0.68	0.00	0.7635	1.255	0.000
Cl <sup>-</sup>	0.100	3.52	0.00	2.32	0.2280	0.000	2.363
I <sup>-</sup>	0.380	3.55	0.00	1.34	0.4080	0.000	1.251
Acetate <sup>-</sup>	0.415	2.20	0.00	2.93	0.4433	0.000	2.075
Benzoate <sup>-</sup>	0.880	3.64	0.00	2.88	0.9102	0.000	2.395
Phenoxide <sup>-</sup>	0.955	2.80	0.00	2.12	0.7536	0.000	1.676
Propanone	0.179	0.70	0.04	0.49	0.5470	0.000	0.000
DMSO	0.522	1.72	0.00	0.97	0.6126	0.000	0.000
Ethanol	0.246	0.42	0.37	0.48	0.4491	0.000	0.000
Acetic acid	0.265	0.64	0.62	0.44	0.4648	0.000	0.000

<sup>a</sup> the data taken from Abraham (2011).

### **1.5 Aims of this Study**

The motivation for this study originated from an ambitious thought to construct a mathematical model for predicting skin permeability of both neutral and ionic species on the basis of simplicity, mechanistic relevance and predictive ability. As was introduced, there are two potential solutions: one is the Potts-Guy model, Eq. 1.1, based on liposome-water partition parameters, and the other is the LFER model, Eq. 1.9, from Abraham and Acree. In line with the above, the major aims of this study can be divided into three, albeit interconnected themes, as follows:

## Introduction

**1) To compare liposome-water partitions and organic solvent-water partitions with the SC-water partition using LFERs in physicochemical nature.**

For this purpose, I measured the retention factors for a diversity of compounds (including neutral and ionized) in LEKC, where cerasomes consisting mainly of SC lipids and regular phospholipid liposomes consisting of 3-*sn*-phosphatidylcholine (POPC) and 3-*sn*-Phosphatidyl-L-serine (PS) (80:20, mol/mol) were employed as the investigated liposomes, respectively. Cerasome was used specifically to simulate the SC in the present study, given that the lipid composition of liposomes had a remarkable effect on their chemical similarity with the SC in terms of their phase behaviors and lateral diffusion coefficients (Johnson et al., 1997; Kitson et al., 1994; Ongpipattanakul et al., 1994).

**2) To investigate the feasibility of Eq. 1.1 that employs partition into liposomes as a model for the partition into SC to predict  $\log K_p$  of both neutral and ionic species.**

To this end, the retention factors of solutes measured in liposome electrokinetic chromatography using cerasomes (also called cerasome EKC) were considered as an estimate of  $\log K_{sc}$  in Eq. 1.1. The explanatory power of such a model for skin permeation was investigated for both species in this study.

**3) To construct a LFER model for skin permeation of both species.**

Previously, Eq. 1.8 was applied to observed  $\log K_p$  of 119 neutral solutes (Abraham and Martins, 2004), leading to Eq. 1.9, with  $K_p$  in units of  $\text{cm s}^{-1}$ :

$$\log K_p = -5.426 - 0.106E - 0.473S - 0.473A - 3.000B + 2.296V \quad (R^2 = 0.832) \quad (1.10)$$

Now that descriptors can be calculated or estimated for ionic species, Eq. 1.10 can be extended to include both species, thus leading to a model for the prediction of skin permeation of ions and



## Introduction

ionic species as well as neutral species, from known solute descriptors. To achieve this purpose, I have measured the  $\log K_p$  values for 18 ionized solutes across human epidermis in this study, and have combined these data with literature  $\log K_p$  values in order to derive such a LFER model.

## 2. Publication Overview

---

### 2.1 *Research Article*

**Linear Free Energy Relationship (LFER) Analysis of Retention Factors in Cerasome Electrokinetic Chromatography (EKC) Intended for Predicting Drug Skin Permeation**

*Keda Zhang, Ming Chen, Gerhard K. E. Scriba, Michael H. Abraham, Alfred Fahr, Xiangli Liu*

Journal of Pharmaceutical Sciences, 2012, 101(6): 2034-2044.

**Abstract:** The retention factors for a great variety of compounds (including neutral and charged solutes) were measured in cerasome EKC system. The LFER model gave an account of these retention factors for both neutral and ionic species ( $R^2 = 0.814$ ,  $SD = 0.29$  log units). The equation was compared with those for a number of solvent-water partitions. It was shown that cerasome is quite different from organic solvents on interaction with solutes and hence that it could be a very useful model for the SC in partitions.

**Own contribution to the manuscript:**

- 1) Measurements of the retention factors for all the compounds in cerasome EKC.
- 2) Data evaluation, interpretation and presentation of the results.
- 3) Writing of the first version of the manuscript.

## **2.2 Research Article**

### **Human Skin Permeation of Neutral Species and Ionic Species: Extended**

#### **Linear Free-Energy Relationship Analyses**

*Keda Zhang, Ming Chen, Gerhard K. E. Scriba, Michael H. Abraham, Alfred Fahr, Xiangli Liu*

Journal of Pharmaceutical Sciences, 2012, 101(6): 2034-2044

**Abstract:** The permeabilities  $\log K_p$  of nine acids and nine bases through human epidermis were measured in this work. Combining these data with the experimental  $\log K_p$  data for neutral species from the Abraham-Martins database and reliable data for ionic species in literature, a LFER equation for skin permeation was deduced, with  $R^2 = 0.861$  and  $SD = 0.462$  log units. This equation can be used to predict  $\log K_p$  for both species, as well as partly ionized solutes. In addition, skin-water partition was compared with cerasome/organic solvent-water partitions using LFERs. The results show that partition into cerasome is a useful model for partition into skin.

#### **Own contribution to the manuscript:**

- 1) Measurements of skin permeability for all 18 compounds.
- 2) Data evaluation, interpretation and presentation of the results.
- 3) Writing of the first version of the manuscript.

## **2.3 Research Article**

### **Comparison of Lipid Membrane-Water Partitions with Various Organic Solvent-Water Partitions of Neutral Species and Ionic Species**

*Keda Zhang, Kewei Yang, Gerhard K. E. Scriba, Michael H. Abraham, Alfred Fahr, Xiangli Liu*

Journal of Pharmaceutical Sciences, being revised.

**Abstract:** The retention factors for a reasonable number of neutral and charged solutes were determined in LEKC, where liposomes (POPC<sub>80</sub>/PS<sub>20</sub>) were used. The LFER analysis was applied to these retention factors as well as the capacity factors in a reported neutral IAM system, which is used as a surrogate for neutral liposome-water partition. Some lipid membrane-water partitions whose ionic LFER equations are available, including the above two systems, were compared to a number of organic solvent-water partitions using LFERs. The results show that lipid membranes exhibit a fairly different chemical environment from those of organic solvents. Further, partitions into cerasome and phospholipid liposomes were compared to skin permeation. It was found that the cerasome-water partition exhibits a better chemical correlation to skin permeation.

#### **Own contribution to the manuscript:**

- 1) Measurements of the retention factors for all the compounds in LEKC.
- 2) Data evaluation, interpretation and presentation of the results.
- 3) Writing of the first version of the manuscript.

## 3. Publications

---

### **3.1 Publication 1**

**Linear Free-Energy Relationship (LFER) Analysis of Retention Factors in  
Cerasome Electrokinetic Chromatography (EKC) Intended for Predicting  
Drug Skin Permeation**

*Keda Zhang, Ming Chen, Gerhard K. E. Scriba, Michael H. Abraham, Alfred Fahr, Xiangli Liu*

Journal of Pharmaceutical Sciences, 2012, 101(6): 2034-2044

**Pages in the dissertation: 24 ~ 32 (9 pages)**

# DRUG DISCOVERY INTERFACE

## Linear Free Energy Relationship Analysis of Retention Factors in Cerasome Electrokinetic Chromatography Intended for Predicting Drug Skin Permeation

KEDA ZHANG,<sup>1</sup> MING CHEN,<sup>1</sup> GERHARD K. E. SCRIBA,<sup>2</sup> MICHAEL H. ABRAHAM,<sup>3</sup> ALFRED FAHR,<sup>1</sup> XIANGLI LIU<sup>1</sup>

<sup>1</sup>Department of Pharmaceutical Technology, Friedrich-Schiller-Universität Jena, 07743 Jena, Germany

<sup>2</sup>Department of Pharmaceutical Chemistry, Friedrich-Schiller-Universität Jena, 07743 Jena, Germany

<sup>3</sup>Department of Chemistry, University College London, London WC1H 0AJ, UK

Received 12 January 2011; revised 27 February 2011; accepted 1 March 2011

Published online 31 March 2011 in Wiley Online Library (wileyonlinelibrary.com). DOI 10.1002/jps.22549

**ABSTRACT:** The retention factors of neutral, positively charged, and negatively charged solutes were determined in a liposome electrokinetic chromatography (EKC) system, where cerasome was used as the investigated liposome. The Abraham linear free energy relationship (LFER) for neutral and ionized solutes gave a good account of the retention factors ( $N = 71$ ,  $R^2 = 0.814$ , and  $SD = 0.29$  log units). It was shown that the calculated retention factors for 16 neutral acids were about four times higher than those of the corresponding anions, whereas the calculated retention factors for neutral bases were less than those for the corresponding cations by a factor of 0.36. The LFER equation for neutral species, anions, and cations was compared with those for partition from water into a number of solvents and for *n*-octanol–water distribution coefficients. It was shown that the cerasome EKC system is substantially different to the other systems and consequently it could be a very useful additional model system, possibly for predicting skin permeation. It was further shown that there are considerable advantages in the use of Abraham LFERs that can encompass not only neutral molecules but also ionic species. © 2011 Wiley-Liss, Inc. and the American Pharmacists Association *J Pharm Sci* 100:3105–3113, 2011

**Keywords:** liposome electrokinetic chromatography (LEKC); cerasome; retention factors; log *P*; skin; liposomes; physicochemical properties; linear free energy relationship; QSPR; ionic species

### INTRODUCTION

Skin permeability is a critical parameter for transdermal delivery of drugs and the risk assessment of chemicals in contact with the skin, both in the pharmaceutical and the cosmetic fields. Because of the fact that measurement of the penetration of chemicals through skin either *in vivo* or *in vitro* is time consuming and laborious, and may also give rise to ethical difficulties,<sup>1</sup> the prediction of skin permeability using various model systems is an area of great significance and of increasing interest.

As Flynn proposed a working model of the skin to assess the permeation of chemicals based on their physicochemical properties,<sup>1,2</sup> a great deal of work has been conducted on experimental and theoretical models to predict skin permeation. The most recent developments have used immobilized artificial membrane<sup>3–6</sup> (IAM) and micellar electrokinetic chromatography<sup>7,8</sup> (MEKC). Both systems involve ordered lipid aggregates that are similar to biomembranes and, hence, could be useful models for permeation through the stratum corneum. Subsequently, liposome electrokinetic chromatography (LEKC) was developed as a logical consequence after the introduction of micelles in electrokinetic chromatography (EKC). Compared with IAM and MEKC, LEKC provides not only the measurement advantages, such as speed, small sample amount, automation, lack of sample purity requirement, and high reproducibility,

Correspondence to: Xiangli Liu (Telephone: +49-3641-949903; Fax: +49-3641-949902; E-mail: Xiangli.Liu@uni-jena.de), Michael H. Abraham (Telephone: +44-20-7679-4639; Fax: +44-20-7679-7463; E-mail: m.h.abraham@ucl.ac.uk)

*Journal of Pharmaceutical Sciences*, Vol. 100, 3105–3113 (2011)  
© 2011 Wiley-Liss, Inc. and the American Pharmacists Association

but also a distinct lipophilicity index in pharmacokinetic studies, as liposomes possess spherical lipid bilayer microstructures that make them more suitable models for the dynamic and fluid bilayer environment of biomembranes. LEKC has been used to evaluate the penetration of chemicals through skin in recent years and the derived quantitative structure–permeability relationship models showed adequate predictive ability for skin permeation, as  $\log K_p$ .<sup>9,10</sup>

However, LEKC research on skin permeation has mostly been performed using the conventional phospholipid system, phosphatidylcholine (PC)/phosphatidylserine (PS), which is quite distinct from lipid compositions in the stratum corneum layer. The stratum corneum, the thin, outer dead layer of the epidermis, is the main barrier to percutaneous absorption of most chemicals.<sup>1</sup> Hence, the use of appropriate liposomes to mimic the stratum corneum lipids is of vital importance.

To compare different partitioning systems (including biological and artificial ones) and unravel the structural determinants governing the partitioning of solutes in these systems, we use the Abraham linear free energy relationship (LFER)<sup>11–13</sup>:

$$SP = c + eE + sS + aA + bB + vV \quad (1)$$

where  $E$ ,  $S$ ,  $A$ ,  $B$ , and  $V$  are solute descriptors.  $E$  is the excess molar refraction in  $(\text{cm}^3 \text{mol}^{-1})/10$ ,  $S$  is the solute dipolarity/polarizability,  $A$  and  $B$  are the overall solute hydrogen bond acidity and hydrogen bond basicity, and  $V$  is the McGowan characteristic volume of the solute in  $(\text{cm}^3 \text{mol}^{-1})/100$ .  $SP$  represents a set of solute properties in a given system, for example,  $SP$  could be the  $n$ -octanol–water distribution coefficient  $\log D_{\text{oct}}$ , the skin permeability  $\log K_p$ , or the retention factor  $\log k$  in LEKC for a series of solutes. Equation 1 has been successfully tested in a wide range of systems, including a large number of partitions from water to organic solvent,<sup>12,14,15</sup> various artificial membrane models,<sup>9,13,16</sup> as well as biological processes.<sup>17–19</sup> The coefficients in Eq. 1 ( $c$ ,  $e$ ,  $s$ ,  $a$ ,  $b$ , and  $v$ ) are obtained by multiple linear regression (MLR) analysis and are used to characterize the given system.

In the present study, all the measurements were performed at pH 7.4, where some of the solutes summarized in Table 1 are present as ionic species: cations from protonated amines and anions from deprotonated carboxylic acids. Equation 1 was set up for neutral solutes only<sup>12–19</sup> and to extend it to ionic species Abraham and Acree<sup>20–23</sup> developed Eq. 2. This equation contains the same five descriptors as in Eq. 1, together with a new descriptor for cations,  $J^+$ , and a new descriptor for anions,  $J^-$ .

$$SP = c + eE + sS + aA + bB + vV + j^+J^+ + j^-J^- \quad (2)$$

Note that  $J^+ = 0$  for anions,  $J^- = 0$  for cations, and both  $J^+$  and  $J^- = 0$  for neutral compounds. In other words, Eq. 2 reverts to Eq. 1 when Eq. 2 is constructed only for neutral species.

The aims of the present work are to measure LEKC retention factors in the presence of cerasome, a material that closely resembles stratum corneum lipids, and to investigate the possibility of constructing an LFER equation for the LEKC retention factors as a necessary preliminary to assess the LEKC system (called cerasome EKC system in this work) as a model for skin permeation, especially with respect to the possibility of incorporating ionic species in the LFER equation.

## MATERIALS AND METHODS

### Materials

The (4-methylbenzyl)alkylamines were synthesized according to known procedures.<sup>24</sup> All other compounds in Table 1 were obtained from Sigma–Aldrich (Steinheim, Germany) and were of highest available purity. Sodium dihydrogen phosphate and disodium hydrogen phosphate were purchased from Sigma–Aldrich, methanol (high-performance liquid chromatography grade) was purchased from Carl Roth (Karlsruhe, Germany), and decanophenone was from Alfa Aesar (Karlsruhe, Germany).

Cerasome (product name: Cerasome 9005) was kindly donated by Lipoid GMBH (Ludwigshafen, Germany). This cerasome is composed of hydrogenated lecithin, cholesterol, ceramides (NP and NS), and fatty acids (palmitic acid and oleic acid) in distilled water with a small amount of ethanol as preservative (around 10%). The concentration of the total lipids is 6.60 (g/100g). The particle size and pH value of cerasome offered by Lipoid GMBH are 48.1 nm and 7.3, respectively. The cerasome was stored between 15°C and 25°C, as recommended in the product information sheet.

### Preparation of Cerasome Dispersion Used in LEKC

Cerasome was diluted 50 times with 10 mM phosphate buffer (pH 7.4). The diluted cerasome dispersion was filtered (200 nm, nylon; MedChrom, Flörsheim-Dalsheim, Germany) at room temperature. The average particle size and the zeta potential of filtered cerasome measured using a Zetasizer Nano ZS (Malvern, Herrenberg, Germany) were 49.5 ( $\pm 0.5$ ) nm with polydispersity index of 0.105 and  $-68.0$  ( $\pm 1.0$ ) mV, respectively. Cerasome dispersion (150 mL) was prepared once as described above and utilized in all the cerasome EKC experiments.

**Table 1.** Physicochemical Parameters of the Investigated Compounds

No.	Solutes	pKa <sup>a</sup>	Charge State	log P <sub>oct</sub> <sup>a</sup>	log D <sub>7.4</sub> <sup>b</sup>	log k <sub>7.4</sub> <sup>c</sup>	E <sup>d</sup>	S <sup>d</sup>	A <sup>d</sup>	B <sup>d</sup>	V <sup>d</sup>	J <sup>+d</sup>	J <sup>-d</sup>
1	Cortexolone	N	Neutral	2.52	2.52	-1.11	1.910	3.45	0.36	1.60	2.7389	0.0000	0.0000
2	Cortexone	N	Neutral	2.88	2.88	-0.82	1.740	3.50	0.14	1.31	2.6802	0.0000	0.0000
3	Corticosterone	N	Neutral	1.94	1.94	-1.27	1.860	3.43	0.40	1.63	2.7389	0.0000	0.0000
4	Cortisone	N	Neutral	1.47	1.47	-1.57	1.960	3.50	0.36	1.87	2.7546	0.0000	0.0000
5	Dexamethasone	N	Neutral	1.83	1.83	-1.40	2.040	3.51	0.71	1.92	2.9132	0.0000	0.0000
6	Digitoxin	N	Neutral	1.86	1.86	-1.12	3.460	5.56	1.67	4.35	5.6938	0.0000	0.0000
7	Estriol	N	Neutral	2.54	2.54	-1.37	1.970	1.74	1.06	1.63	2.2575	0.0000	0.0000
8	Hydrocortisone	N	Neutral	1.55	1.55	-1.47	2.030	3.49	0.71	1.90	2.7976	0.0000	0.0000
9	Hydrocortisone-21-acetate	N	Neutral	2.19	2.19	-1.41	1.890	2.88	0.46	2.16	3.0951	0.0000	0.0000
10	17-Hydroxyprogesterone	N	Neutral	3.17	3.17	-0.90	1.640	3.35	0.25	1.31	2.6802	0.0000	0.0000
11	Prednisolone	N	Neutral	1.62	1.62	-1.50	2.210	3.10	0.71	1.92	2.7546	0.0000	0.0000
12	Testosterone	N	Neutral	3.29	3.29	-0.85	1.540	2.59	0.32	1.19	2.3827	0.0000	0.0000
13	Bibenzyl	N	Neutral	4.80	4.80	0.72	1.220	1.04	0.00	0.33	1.6060	0.0000	0.0000
14	4-Chloro-2-methylphenol	9.60	Neutral	2.78	2.78	-0.74	0.890	0.91	0.63	0.22	1.0384	0.0000	0.0000
15	4-Chloro-3,5-dimethylphenol	9.70	Neutral	3.27	3.27	-0.51	0.925	0.96	0.64	0.21	1.1793	0.0000	0.0000
16	3,4-Dimethylphenol	10.32	Neutral	2.23	2.23	-1.34	0.830	0.90	0.55	0.38	1.0569	0.0000	0.0000
17	1-Fluoro-2,4-dinitrobenzene	N	Neutral	1.47	1.47	-1.63	1.006	1.69	0.00	0.45	1.0825	0.0000	0.0000
18	2-Naphthol	9.57	Neutral	2.70	2.70	-0.70	1.520	1.08	0.61	0.40	1.1441	0.0000	0.0000
19	Resorcinol	9.15	Neutral	0.80	0.79	-1.49	0.980	1.11	1.09	0.52	0.8338	0.0000	0.0000
20	Styrene	N	Neutral	2.95	2.95	-0.62	0.849	0.65	0.00	0.16	0.9552	0.0000	0.0000
21	Toluene	N	Neutral	2.73	2.73	-0.83	0.601	0.52	0.00	0.14	0.8573	0.0000	0.0000
22	4-BrC <sub>6</sub> H <sub>4</sub> OH	9.31	Neutral	2.59	2.58	-0.87	1.080	1.17	0.67	0.20	0.9501	0.0000	0.0000
23	3-CH <sub>3</sub> C <sub>6</sub> H <sub>4</sub> OH	10.09	Neutral	1.96	1.96	-1.48	0.822	0.88	0.57	0.34	0.9160	0.0000	0.0000
24	4-CH <sub>3</sub> C <sub>6</sub> H <sub>4</sub> OH	10.26	Neutral	1.95	1.95	-1.43	0.820	0.87	0.57	0.31	0.9160	0.0000	0.0000
25	C <sub>6</sub> H <sub>5</sub> COCH <sub>3</sub>	N	Neutral	1.58	1.58	-1.64	0.818	1.01	0.00	0.48	1.0139	0.0000	0.0000
26	2-ClC <sub>6</sub> H <sub>4</sub> NH <sub>2</sub>	2.64	Neutral	1.91	1.91	-1.50	1.033	0.92	0.25	0.31	0.9390	0.0000	0.0000
27	2-ClC <sub>6</sub> H <sub>4</sub> NO <sub>2</sub>	N	Neutral	2.52	2.52	-1.27	1.020	1.24	0.00	0.24	1.0130	0.0000	0.0000
28	3-ClC <sub>6</sub> H <sub>4</sub> OH	9.11	Neutral	2.50	2.49	-1.05	0.909	1.06	0.69	0.15	0.8975	0.0000	0.0000
29	4-ClC <sub>6</sub> H <sub>4</sub> OH	9.40	Neutral	2.39	2.39	-1.01	0.915	1.08	0.67	0.20	0.8975	0.0000	0.0000
30	4-ClC <sub>6</sub> H <sub>4</sub> CH <sub>2</sub> OH	N	Neutral	1.96	1.96	-1.36	0.911	0.96	0.40	0.50	1.0384	0.0000	0.0000
31	2-H <sub>2</sub> NC <sub>6</sub> H <sub>4</sub> Ph	3.82	Neutral	2.84	2.84	-1.06	1.600	1.48	0.26	0.41	1.4240	0.0000	0.0000
32	3-O <sub>2</sub> NC <sub>6</sub> H <sub>4</sub> OH	8.40	Neutral	2.00	1.96	-0.83	1.050	1.57	0.79	0.23	0.9493	0.0000	0.0000
33	PhCH <sub>2</sub> CN	N	Neutral	1.56	1.56	-1.61	0.751	1.03	0.00	0.50	1.0120	0.0000	0.0000
34	PhCH <sub>2</sub> OH	N	Neutral	1.10	1.10	-1.66	0.803	0.87	0.39	0.56	0.9160	0.0000	0.0000
35	PhNH <sub>2</sub>	4.60	Neutral	0.90	0.90	-1.73	0.955	0.96	0.26	0.41	0.8162	0.0000	0.0000
36	PhNHEt	5.12	Neutral	2.16	2.16	-1.52	0.945	0.85	0.17	0.43	1.0980	0.0000	0.0000
37	PhNO <sub>2</sub>	N	Neutral	1.85	1.85	-1.49	0.871	1.11	0.00	0.28	0.8906	0.0000	0.0000
38	PhOH	9.95	Neutral	1.47	1.47	-1.56	0.805	0.89	0.60	0.30	0.7751	0.0000	0.0000
39	Acridine	5.58	Neutral	3.40	3.39	-0.51	2.356	1.32	0.00	0.58	1.4133	0.0000	0.0000
40	Aspirin	3.48	Anion	1.13	-2.79	-2.20	0.931	3.91	0.04	3.03	1.2664	0.0000	2.1227
41	Flurbiprofen	3.91	Anion	3.81	0.32	-1.21	1.590	4.56	0.07	3.36	1.8174	0.0000	2.5383
42	Ibuprofen	4.43	Anion	3.87	0.90	-1.19	0.880	3.50	0.08	3.31	1.7556	0.0000	2.4188
43	Ketoprofen	4.29	Anion	2.77	-0.34	-1.32	1.800	5.49	0.01	3.39	1.9564	0.0000	2.4851
44	Mefenamic acid	4.33	Anion	5.12	2.05	-1.17	1.800	4.71	0.09	3.14	1.8996	0.0000	2.6427
45	Naproxen	4.15	Anion	3.06	-0.19	-1.43	1.660	5.07	0.02	3.11	1.7606	0.0000	2.4260
46	4-BrC <sub>6</sub> H <sub>4</sub> COOH	3.97	Anion	2.86	-0.57	-1.16	1.150	3.47	0.04	2.61	1.0852	0.0000	2.2504
47	1-C <sub>10</sub> H <sub>7</sub> COOH	3.69	Anion	3.10	-0.61	-1.61	1.610	4.13	0.05	2.87	1.2792	0.0000	2.4041
48	3-ClC <sub>6</sub> H <sub>4</sub> COOH	3.83	Anion	2.71	-0.86	-1.58	0.990	3.25	0.04	2.68	1.0326	0.0000	2.2010
49	4-ClC <sub>6</sub> H <sub>4</sub> COOH	3.98	Anion	2.65	-0.77	-1.39	0.990	3.31	0.04	2.60	1.0326	0.0000	2.1873
50	4-IC <sub>6</sub> H <sub>4</sub> COOH	3.96	Anion	3.13	-0.31	-1.32	1.460	4.00	0.03	2.63	1.1684	0.0000	2.3116
51	C <sub>6</sub> H <sub>5</sub> COOH	4.20	Anion	1.96	-1.24	-1.16	0.880	3.05	0.02	2.75	0.9102	0.0000	2.1385
52	C <sub>6</sub> H <sub>5</sub> (CH <sub>2</sub> ) <sub>2</sub> COOH	4.25	Anion	1.89	-1.26	-1.37	0.900	3.43	0.03	3.02	1.1920	0.0000	2.1879
53	C <sub>6</sub> H <sub>5</sub> (CH <sub>2</sub> ) <sub>3</sub> COOH	4.72	Anion	2.42	-0.26	-1.67	0.910	3.59	0.04	3.01	1.3329	0.0000	2.2184
54	C <sub>6</sub> H <sub>5</sub> (CH <sub>2</sub> ) <sub>4</sub> COOH	4.55	Anion	2.85	0.00	-1.63	0.920	3.63	0.04	3.10	1.4718	0.0000	2.2794
55	C <sub>6</sub> H <sub>5</sub> (CH <sub>2</sub> ) <sub>7</sub> COOH	5.03	Anion	4.09	1.72	-1.31	0.940	3.87	0.07	3.26	1.8965	0.0000	2.4256
56	4-MeC <sub>6</sub> H <sub>4</sub> CH <sub>2</sub> NHMe	9.93	Cation	1.96	-0.57	-0.63	0.630	2.64	1.47	0.00	1.2604	1.2622	0.0000
57	4-MeC <sub>6</sub> H <sub>4</sub> CH <sub>2</sub> NHEt	10.04	Cation	2.38	-0.26	-0.63	0.610	2.69	1.48	0.00	1.4013	1.2647	0.0000
58	4-MeC <sub>6</sub> H <sub>4</sub> CH <sub>2</sub> NHPr	9.98	Cation	2.96	0.38	-0.56	0.590	2.68	1.45	0.00	1.5422	1.2605	0.0000
59	4-MeC <sub>6</sub> H <sub>4</sub> CH <sub>2</sub> NHBu	9.98	Cation	3.49	0.91	-0.44	0.570	2.68	1.46	0.00	1.6831	1.2405	0.0000
60	4-MeC <sub>6</sub> H <sub>4</sub> CH <sub>2</sub> NH(CH <sub>2</sub> ) <sub>4</sub> Me	10.08	Cation	4.26	1.58	-0.08	0.550	2.66	1.41	0.00	1.8240	1.2522	0.0000
61	4-MeC <sub>6</sub> H <sub>4</sub> CH <sub>2</sub> NH(CH <sub>2</sub> ) <sub>5</sub> Me	10.17	Cation	4.96	2.19	0.26	0.540	2.45	1.29	0.00	1.9649	1.2268	0.0000
62	4-MeC <sub>6</sub> H <sub>4</sub> CH <sub>2</sub> NH(CH <sub>2</sub> ) <sub>6</sub> Me	10.02	Cation	5.12	2.50	0.95	0.530	2.51	1.47	0.00	2.1058	1.1215	0.0000

Continued



Table 1. Continued

No.	Solutes	pKa <sup>a</sup>	Charge State	log P <sub>oct</sub> <sup>a</sup>	log D <sub>7.4</sub> <sup>b</sup>	log k <sub>7.4</sub> <sup>c</sup>	E <sup>d</sup>	S <sup>d</sup>	A <sup>d</sup>	B <sup>d</sup>	V <sup>d</sup>	J <sup>+d</sup>	J <sup>-d</sup>
63	Acebutolol	9.52	Cation	2.02	-0.10	-1.01	1.450	6.69	3.62	0.00	2.7771	2.2965	0.0000
64	Alprenolol	9.59	Cation	3.10	0.91	0.06	1.100	4.46	1.78	0.00	2.1802	2.2574	0.0000
65	Metoprolol	9.63	Cation	1.95	-0.28	-0.79	1.020	5.35	2.16	0.00	2.2819	2.3476	0.0000
66	Oxprenolol	9.57	Cation	2.51	0.34	-0.50	1.160	5.09	2.35	0.00	2.2389	2.2029	0.0000
67	Penbutolol	9.92	Cation	4.62	2.10	0.74	0.775	4.66	1.98	0.00	2.6195	1.9630	0.0000
68	Pindolol	9.54	Cation	1.75	-0.39	-0.83	1.550	4.60	2.36	0.00	2.0305	2.2661	0.0000
69	Propafenone	9.62	Cation	3.64	1.42	0.45	1.550	5.67	2.97	0.00	2.8467	2.3467	0.0000
70	Propranolol	9.53	Cation	3.48	1.35	0.47	1.690	4.31	2.07	0.00	2.1695	2.4319	0.0000
71	Timolol	9.21	Cation	1.83	0.01	-0.82	1.320	5.67	2.83	0.00	2.3974	2.2692	0.0000

<sup>a</sup>Taken from Refs. 31, 32 and Biolum Software (Version 1.5; Biobyte Corporation, Claremont, U.S.A.).

<sup>b</sup>Calculated according to  $\log D = \log P_{\text{oct}} - \log(1 + 10^{\text{pKa} - \text{pH}})$  for bases and  $\log D = \log P_{\text{oct}} - \log(1 + 10^{\text{pH} - \text{pKa}})$  for acids.

<sup>c</sup>Calculated from retention time data using Eqs. 3 and 4;  $n = 3$ ,  $s.d \leq 0.01$  for neutrals and bases, and  $s.d \leq 0.05$  for acids.

<sup>d</sup>Taken from Refs. 20–23, or calculated from the equations in Ref. 21.

### Storage of Cerasome Dispersion

Cerasome vesicles dispersed in 10 mM phosphate buffer (pH 7.4) were unstable between 15°C and 25°C (the storage temperature for original cerasome). During storage, the average particle size increased slightly 24 h after dilution of the cerasome product and cerasome aggregates were observed. Therefore, the cerasome dispersion was stored at 4°C (the general storage temperature of liposome).<sup>25</sup> Under these conditions, the cerasome dispersion was stable for at least 14 days determining the particle size before the cerasome EKC experiments each day.

### Capillary Electrophoresis Apparatus

The cerasome EKC experiments were carried out on a HPCE 1600AX (Agilent, Waldbronn, Germany) equipped with a diode array detector. An uncoated fused silica capillary of 50 μm inner diameter (ID) and 375 μm outer diameter (OD), with a total length of 58.5 cm (50 cm in effective length to the detector) was used throughout the study. The samples were analyzed at an applied positive voltage of 20 kV, at a temperature of 37°C. Sample injection was performed hydrodynamically at 50 mbar for 3 s. Detection wavelengths were 210, 225, and 245 nm. Methanol was used as electroosmotic flow marker and decanophenone was used as liposome marker.<sup>26,27</sup> The prepared cerasome dispersion and 10 mM phosphate buffer (pH 7.4) were used as the running solutions, respectively, in the cerasome EKC and capillary zone electrophoresis (CZE) systems.

### LEKC Procedures

A new fused silica capillary was pretreated for 15 min with 1.0 M NaOH, 5 min with Milli-Q water, 15 min with 1.0 M HCl, and 5 min with Milli-Q water. In order to equilibrate the physical absorption of cerasome vesicles on the inner wall, the capillary was rinsed for 30 min each day with the cerasome dispersion before sample injections were performed.<sup>26</sup> At the end of

each day, the capillary was rinsed with 10 mM phosphate buffer (pH 7.4) at 50 mbar overnight.

For charged solutes, the retention time  $t_r$  (from LEKC) in the presence of cerasome, and the retention time  $t_0$  (from CZE) in the absence of cerasome were determined in order to calculate the retention factor  $k$ , as described by Eq. 3, whereas only LEKC measurements are needed for neutral solutes, as shown by Eq. 4:<sup>27</sup>

$$k = \frac{(t_r - t_0)}{t_0 (1 - t_r/t_{\text{lip}})} \quad (3)$$

$$k = \frac{(t_r - t_{e0})}{t_{e0} (1 - t_r/t_{\text{lip}})} \quad (4)$$

where  $t_r$ ,  $t_{e0}$ , and  $t_{\text{lip}}$  are the retention times of the solute, the electroosmotic flow marker (methanol), and the cerasome marker (decanophenone) in cerasome EKC system, respectively;  $t_0$  is the retention time of ionized solutes in the bulk aqueous phase (CZE; buffer solution without cerasomes); the retention factor  $\log k$  can be regarded as a lipophilicity index in the liposome–water system because the  $\log k$  value of a solute is linearly related to its partition coefficient between the aqueous phase and the liposome phase.<sup>28</sup> The equation for calculating the retention factors of ionizable solutes is different from that for neutral solutes, owing to the fact that migration of charged solutes in LEKC system involves the electrophoretic mobility in the aqueous phase as well as their interaction with liposome carriers, but migration of neutral solutes is only related to their partition with liposome.<sup>27</sup> Thus, the retention time of solutes in the aqueous buffer without cerasome (CZE) was considered as the unretained time instead of the migration time of the electroosmotic flow marked by methanol for ions.

The  $\log k$  measurements of all the solutes were repeated three times. Before sample injection, the

capillary was rinsed for 3 min with the corresponding running solution (buffer solution or cerasome dispersion). CZE measurements for each charged solute were carried out immediately following LEKC measurements after rinsing the capillary with buffer solution for 3 min.<sup>26</sup> This was performed in order to maintain cerasome vesicles adsorbed to the inner capillary wall so that CZE experiments were performed under the same wall conditions.<sup>29,30</sup>

Solutes were dissolved in methanol to prepare stock solutions, which were diluted with the corresponding running solution before injection to approximately  $2.0\text{--}3.0 \times 10^{-4}$  mol L<sup>-1</sup>. Decanophenone dissolved in methanol was added where appropriate, as the cerasome maker. All solutions were filtered (200 nm) prior to use.

## RESULTS AND DISCUSSION

A set of 71 compounds with a broad structural diversity was selected and their retention factors,  $\log k_{7.4}$ , were determined using cerasome EKC. The  $\log k_{7.4}$  values and other physicochemical parameters, including acid dissociation constants p*K*<sub>a</sub>,<sup>31,32</sup> *n*-octanol–water distribution coefficients at pH 7.4,  $\log D_{7.4}$ , *n*-octanol–water partition coefficients,  $\log P_{\text{oct}}$ ,<sup>31,32</sup> as well as the values of the solute descriptors are shown in Table 1. The space distributions of structural parameters (*E*, *S*, *A*, *B*, and *V*) are shown in Figure 1. As *J*<sup>+</sup> and *J*<sup>-</sup> specific to ions have no exact physicochemical definition, they are not discussed here.

Abraham<sup>33</sup> has recently shown that Eq. 2 can be applied to the permeation of neutral molecules and ionic species from saline through the blood–brain barrier. We follow exactly the same procedure. Appropriate solute descriptors were used for whatever species is present at pH 7.4, as shown in Table 1. Abraham and Acree<sup>20–23</sup> have obtained solute descriptors for many anions derived from acids by deprotonation and for

many cations derived from bases by addition of a proton. In cases where the descriptors were not determined, we used the equations set out by Abraham and Acree<sup>21</sup> for the calculation of descriptors. Once descriptors for the relevant species are available, the dependent variable, in this case  $\log k_{7.4}$ , can be regressed against them for the LFER model. Thus to reveal the solute factors that influence the partitioning of chemicals in cerasome EKC system, the MLR of  $\log k_{7.4}$  against the solute descriptors yielded the LFER model that includes both neutral and ionic species, as follows:

$$\begin{aligned} \log k_{7.4} = & -1.922(\pm 0.258) + 0.200(\pm 0.245)E \\ & -0.629(\pm 0.179)S - 0.109(\pm 0.236)A \\ & -1.451(\pm 0.328)B + 1.757(\pm 0.320)V \\ & + 0.334(\pm 0.356)J^+ + 1.958(\pm 0.400)J^- \\ N = 71, R^2 = 0.814, SD = 0.293, F = 39 \quad (5) \end{aligned}$$

In this and the following equations, 95% confidence limits are given in parentheses; *N* is the number of compounds, *R* is the correlation coefficient, *SD* is the standard deviation, and *F* is the Fisher's test. The standardization of Eq. 5 gives the relative contributions of each variable to the total LFER model, which is 3.67% for *E*, 26.13% for *S*, 1.15% for *A*, 24.59% for *B*, and 44.45% for *V*, indicating that the significant factors influencing partitioning in cerasome EKC are *S*, *B*, and *V*, whereas *E* and *A* are of no statistical significance. Eq. 6 shows the LFER model when *E* and *A* are removed.

$$\begin{aligned} \log k_{7.4} = & -1.844(\pm 0.218) - 0.587(\pm 0.166)S \\ & -1.427(\pm 0.326)B + 1.782(\pm 0.322)V \\ & + 0.164(\pm 0.289)J^+ + 1.912(\pm 0.373)J^- \\ N = 71, R^2 = 0.803, SD = 0.297, F = 53 \quad (6) \end{aligned}$$

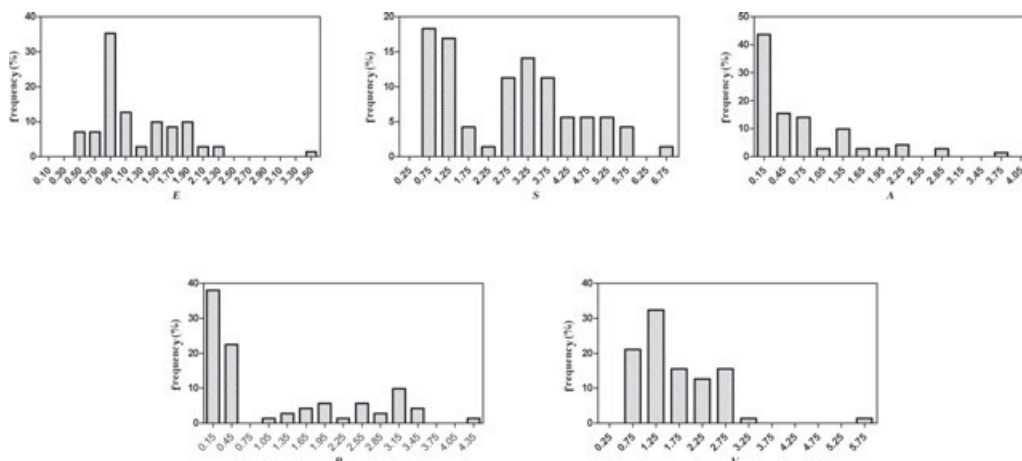


**Figure 1.** Space distributions of structural parameters for the selected set of 71 compounds.

**Table 2.** Coefficients in Eq. 2 for Partition Between Water and Solvents

Solvent	No.	<i>c</i>	<i>e</i>	<i>s</i>	<i>a</i>	<i>b</i>	<i>v</i>	<i>j</i> <sup>+</sup>	<i>j</i> <sup>-</sup>
Methanol	1	0.276	0.334	-0.714	0.243	-3.320	3.549	-2.609	3.027
Ethanol	2	0.222	0.471	-1.035	0.326	-3.596	3.857	-3.170	3.085
1-Propanol	3	0.139	0.405	-1.029	0.247	-3.767	3.986	-3.077	2.834
1-Butanol	4	0.152	0.438	-1.177	0.096	-3.919	4.122	-3.605	2.685
1-Hexanol	5	0.115	0.492	-1.164	0.054	-3.971	4.131	-3.100	2.940
Propanone	6	0.313	0.312	-0.121	-0.608	-4.753	3.942	-2.288	0.078
Acetonitrile	7	0.413	0.077	0.326	-1.566	-4.391	3.364	-2.243	0.101
NMP <sup>a</sup>	8	0.147	0.532	0.275	0.840	-4.794	3.674	-1.797	0.105
DMSO <sup>b</sup>	9	-0.194	0.327	0.791	1.260	-4.540	3.361	-3.387	0.132
EG <sup>c</sup>	10	-0.270	0.578	-0.511	0.715	-2.619	2.729	-1.300	2.363
PC <sup>d</sup>	11	0.004	0.168	0.504	-1.283	-4.407	3.421	-1.989	0.341
Wet 1-octanol, log <i>P</i>	12	0.088	0.562	-1.054	0.034	-3.460	3.814	-3.023	2.580
Wet 1-octanol, log <i>D</i> <sub>7.4</sub>	13	-0.027	0.868	-1.053	-0.257	-3.383	3.577	-1.438	3.389
Cerasome, log <i>k</i> <sub>7.4</sub>	14	-1.922	0.200	-0.629	-0.109	-1.451	1.757	0.334	1.958

<sup>a</sup>*N*-methylpyrrolidinone.<sup>b</sup>Dimethylsulfoxide.<sup>c</sup>Ethylene glycol.<sup>d</sup>Propylene carbonate.

As  $J^+$  and  $J^-$  are specific to ions, they were excluded in the contribution calculation for log  $k_{7.4}$  values of the whole set. The relative contribution of  $J^+$  could be calculated while considering only cations, that is, compounds #56–71, whereas that of  $J^-$  could be calculated while considering only anions, that is, compounds #40–55. In Eq. 5, the relative contributions of  $J^+$  and  $J^-$  are 8.37% and 32.26%, respectively, which indicates that the importance of  $J^+$  for cationic partitioning is much lower than that of  $J^-$  for anionic partitioning in cerasome EKC system.

It is of considerable interest to compare retention factors for neutral compounds that are ionizable with those for the corresponding anions or cations. We have measured log  $k_{7.4}$  for 16 anions derived from carboxylic acids and we are now in a position to use Eq. 5 to calculate for the 16 neutral carboxylic acids, using descriptors for the neutral species. These can then be compared with log  $k_{7.4}$  for the anions. Over the 16 compounds, the average difference log  $k$  (neutral carboxylic acids) – log  $k_{7.4}$  (carboxylate anions) = 0.60 log units, so that on average the retention factor for the neutral carboxylic acids is four times that for the carboxylate anions. In the case of 16 protonated base cations, the average difference log  $k$  (neutral base) – log  $k_{7.4}$  (protonated base cation) = -0.44 log units, so that the retention factor for the neutral bases is only 0.36 times that for the protonated base cations. This is a particularly important example of the extra information that can be obtained by LFER methods when LFERs using descriptors for ionic species are applied.

To compare the factors that influence the cerasome EKC system with those in the traditional *n*-octanol–water system, the LFER model was also applied to the distribution coefficients (log  $D_{7.4}$ ) of the

same set, yielding Eq. 7:

$$\begin{aligned} \log D_{7.4} = & -0.027 (\pm 0.368) + 0.868 (\pm 0.350) E \\ & -1.053 (\pm 0.256) S - 0.257 (\pm 0.337) A \\ & -3.383 (\pm 0.468) B + 3.577 (\pm 0.456) V \\ & -1.438 (\pm 0.509) J^+ + 3.389 (\pm 0.572) J^- \\ N = 71, R^2 = 0.919, SD = 0.419, F = 102 \quad (7) \end{aligned}$$

with the relative contributions of 7.35% for *E*, 20.82% for *S*, 1.29% for *A*, 27.27% for *B*, and 43.05% for *V*. The relative contributions of  $J^+$  and  $J^-$  for log  $D_{7.4}$  are 16.63% and 27.84% for ionized solutes, respectively. After removal of the term *A* with no statistical significance, Eq. 8 was obtained:

$$\begin{aligned} \log D_{7.4} = & -0.089 (\pm 0.362) + 0.870 (\pm 0.354) E \\ & -1.085 (\pm 0.255) S - 3.424 (\pm 0.470) B \\ & + 3.601 (\pm 0.460) V - 1.643 (\pm 0.436) J^+ \\ & + 3.503 (\pm 0.557) J^- \\ N = 71, R^2 = 0.916, SD = 0.423, F = 116 \quad (8) \end{aligned}$$

A very useful way to compare the coefficients in a set of equations is to carry out a principle components analysis (PCA). The seven coefficients in equations of the type of Eq. 2 were transformed into seven principle components that contain exactly the same information, but which are orthogonal to each other. The comparison of the systems is shown in Table 2.<sup>22,23</sup> The first two principle components contain 75% of the total information. A plot of the scores of PC2 against PC1 will reveal how “close” the equations are in terms

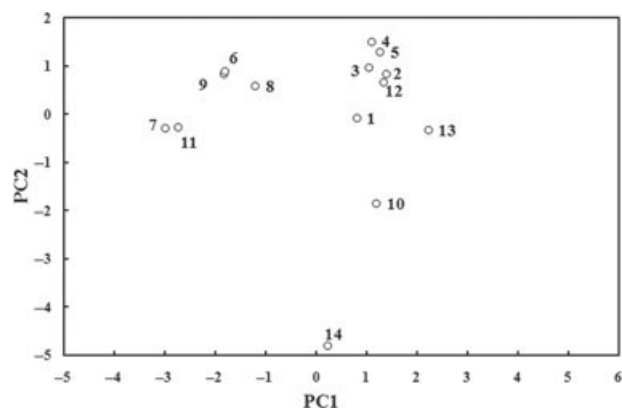


**Figure 2.** Plot of the scores of PC2 against the scores of PC1 for the coefficients of the equations in Table 2. PC1 and PC2 are the first two principle components from principle component analysis for these coefficients.

of chemical interactions (see Fig. 2). As might be expected, the points for the hydroxylic solvents, #1–5, #10, and #12, cluster together. Perhaps surprisingly,  $\log D_{7.4}$  is quite close to this group. The aprotic solvents, #6–9 and #11, form a quite separate cluster. Very interestingly, the point (#14) for the cerasome  $\log k_{7.4}$  coefficients is far away from all the other points on the PC2 versus PC1 plot, so that the cerasome  $\log k_{7.4}$  data leads to a quite new model for the comparison of uptake from water to organic phases. In future, we shall investigate the cerasome model for the analysis of skin permeation.

The coefficients  $c$ – $v$  for partitioning of neutral molecules and ionic species from water to wet octanol<sup>23</sup> were constrained to be exactly the same as the coefficients in the corresponding equation for neutral species. We should therefore expect that our equation for  $\log D_{7.4}$  would also have the same coefficients,  $c$ – $v$ . Within reasonable experimental error, this is the case, see Table 2.

From our previous equations, it can be seen that both  $J^+$  and  $J^-$  have a significant effect on partitioning of charged compounds in cerasome EKC and  $n$ -octanol-water systems, although values of the coefficients are completely different. This implies that the different contributions of the terms  $j^+ \times J^+$  and  $j^- \times J^-$  in these two partitioning systems might be the biggest difference between them. To confirm this, a plot of  $\log k_{7.4}$  against  $\log D_{7.4}$  was constructed. As shown in Figure 3, the data points for neutrals, anions, and cations lie on three distinct lines, with no direct correlation existing between  $\log k_{7.4}$  and  $\log D_{7.4}$  for the whole set of compounds ( $R^2 = 0.117$ ). This also indicates that the charge factor of the solutes plays a crucial role on the difference of partitioning mechanisms in both systems. Thus, a MLR of  $\log k_{7.4}$  against  $\log D_{7.4}$  and the ionic descriptors was carried out as shown in Eq. 7:

$$\begin{aligned} \log k_{7.4} = & 0.372 (\pm 0.089) \log D_{7.4} + 0.743 (\pm 0.129) J^+ \\ & + 0.262 (\pm 0.0128) J^- - 1.948 (\pm 0.225) \\ N = 71, R^2 = & 0.712, SD = 0.354, F = 55 \end{aligned} \quad (9)$$

As expected, this equation shows a significant improvement on the correlation between  $\log k_{7.4}$  and  $\log D_{7.4}$ , where  $R^2 = 0.117$  over all solutes. This also demonstrates the necessity of addition of the ionic descriptors in LFER models.

## CONCLUSION

Liposome electrokinetic chromatography is a powerful tool for investigating the interactions between chemicals and lipid bilayers. In this study, the retention factors of 71 solutes including neutral and ionic species were determined using a LEKC system, where cerasome was used as the liposome material. The developed Abraham LFER model was applied to

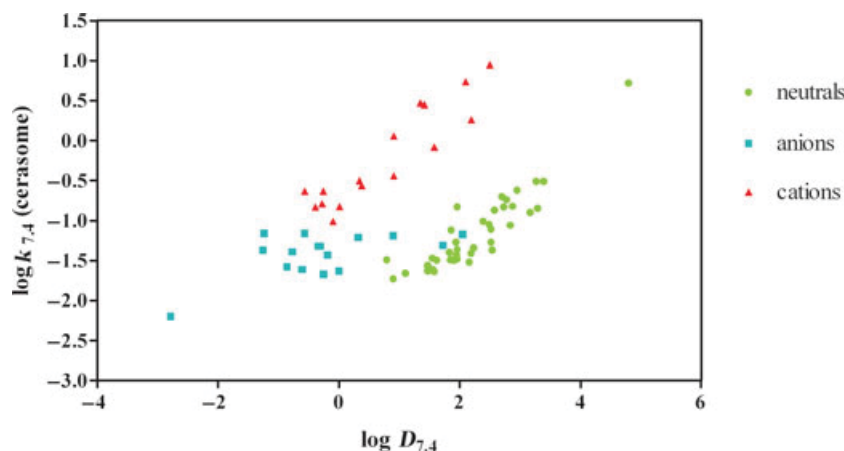


**Figure 3.** Correlation between the retention factors  $\log k_{7.4}$  in cerasome EKC and the  $n$ -octanol–water distribution coefficients  $\log D_{7.4}$  for all solutes.

the retention factors by MLR analysis. The resulting LFER model revealed the structural parameters  $S$ ,  $B$ , and  $V$  as the three prominent factors in cerasome EKC system, whereas the effects of  $E$  and  $A$  are of minor importance or even negligible. A detailed analysis showed that the retention factors for neutral acids are about four times that for carboxylate anions, whereas the factor is only 0.36 times for neutral bases as compared with the protonated base cations. A comparison between the LFER models for  $\log k_{7.4}$  and various water-organic solvent partitions revealed that  $\log k_{7.4}$  reflects quite different solute interactions. Therefore, it could provide the basis of a new model, possibly for skin permeation. The relationship between  $\log k_{7.4}$  and  $\log D_{7.4}$  is very poor but is considerably improved by the incorporation of descriptors for ionic partitioning.

## REFERENCES

- Exposure Assessment Group. 1992. Dermal exposure assessment: Principles and applications. Washington, D. C.: U. S. Environmental Protection Agency, Office of Health and Environmental Assessment. Report No.: EPA/600/8-91/011B.
- Flynn GL. 1990. Physicochemical determinants of skin absorption. In Principles of route-to-route extrapolation for risk assessment; Gerrity TR, Henry CJ, Eds. New York: Elsevier, pp 93-127.
- Turowski M, Kaliszan R. 1997. Keratin immobilized on silica as a new stationary phase for chromatographic modelling of skin permeation. *J Pharmaceut Biomed Anal* 15(9-10):1325-1333.
- Yang CY, Cai SJ, Liu H, Pidgeon C. 1997. Immobilized artificial membranes—Screens for drug membrane interactions. *Adv Drug Deliv Rev* 23(1-3):229-256.
- Nasal A, Sznitowska M, Bucinski A, Kaliszan R. 1995. Hydrophobicity parameter from high-performance liquid-chromatography on an immobilized artificial membrane column and its relationship to bioactivity. *J Chromatogr A* 692(1-2):83-89.
- Lazaro E, Rafols C, Abraham MH, Roses M. 2006. Chromatographic estimation of drug disposition properties by means of immobilized artificial membranes (IAM) and C18 columns. *J Med Chem* 49(16):4861-4870.
- Martinez-Pla JJ, Martin-Biosca Y, Sagrado S, Villanueva-Camanas RM, Medina-Hernandez MJ. 2004. Evaluation of the pH effect of formulations on the skin permeability of drugs by biopartitioning micellar chromatography. *J Chromatogr A* 1047(2):255-262.
- Martinez-Pla JJ, Martin-Biosca Y, Sagrado S, Villanueva-Camanas RM, Medina-Hernandez MJ. 2003. Biopartitioning micellar chromatography to predict skin permeability. *Biomed Chromat* 17(8):530-537.
- Wang YJ, Sun J, Liu HZ, Liu JF, Zhang LQ, Liu K, He ZG. 2009. Predicting skin permeability using liposome electrokinetic chromatography. *Analyst* 134(2):267-272.
- Xian DL, Huang KL, Liu SQ, Xiao JY. 2008. Quantitative retention-activity relationship studies by liposome electrokinetic chromatography to predict skin permeability. *Chinese J Chem* 26(4):671-676.
- Abraham MH, Ibrahim A, Zissimos AM. 2004. Determination of sets of solute descriptors from chromatographic measurements. *J Chromatogr A* 1037(1-2):29-47.
- Abraham MH, Zhao YH. 2005. Characterisation of the water/*o*-nitrophenyl octyl ether system in terms of the partition of nonelectrolytes and of ions. *Phys Chem Chem Phys* 7(12):2418-2422.
- Sprunger L, Blake-Taylor BH, Wairegi A, Acree WE Jr., Abraham MH. 2007. Characterization of the retention behavior of organic and pharmaceutical drug molecules on an immobilized artificial membrane column with the Abraham model. *J Chromatogr A* 1160(1-2):235-245.
- Abraham MH, Acree WE, Jr. 2005. Characterisation of the water-isopropyl myristate system. *Int J Pharm* 294(1-2):121-128.
- Abraham MH. 2003. The determination of air/water partition coefficients for alkyl carboxylic acids by a new indirect method. *J Environ Monit* 5(5):747-752.
- Gil-Agusti M, Esteve-Romero J, Abraham MH. 2006. Solute-solvent interactions in micellar liquid chromatography: Characterization of hybrid micellar systems of sodium dodecyl sulfate-pentanol. *J Chromatogr A* 1117(1):47-55.
- Zhao YH, Le J, Abraham MH, Hersey A, Eddershaw PJ, Luscombe CN, Butina D, Beck G, Sherborne B, Cooper I, Platts JA. 2001. Evaluation of human intestinal absorption data and subsequent derivation of a quantitative structure-activity relationship (QSAR) with the Abraham descriptors. *J Pharm Sci* 90(6):749-784.
- Abraham MH, Martins F. 2004. Human skin permeation and partition: General linear free-energy relationship analyses. *J Pharm Sci* 93(6):1508-1523.
- Zhao YH, Abraham MH, Hersey A, Luscombe CN. 2003. Quantitative relationship between rat intestinal absorption and Abraham descriptors. *Eur J Med Chem* 38(11-12):939-947.
- Abraham MH, Acree WE Jr. 2010. Solute descriptors for phenoxide anions and their use to establish correlations of rates of reaction of anions with iodomethane. *J Org Chem* 75(9):3021-3026.
- Abraham MH, Acree WE Jr. 2010. Equations for the transfer of neutral molecules and ionic species from water to organic phases. *J Org Chem* 75(4):1006-1015.
- Abraham MH, Acree WE Jr. 2010. The transfer of neutral molecules, ions and ionic species from water to ethylene glycol and to propylene carbonate; descriptors for pyridinium cations. *New J Chem* 34(10):2298-2305.
- Abraham MH, Acree WE Jr. 2010. The transfer of neutral molecules, ions and ionic species from water to wet octanol. *Phys Chem Chem Phys* 12(40):13182-13188.
- Meindl WR, Von Angerer E, Schoenenberger H, Ruckdeschel G. 1984. Benzylamines: Synthesis and evaluation of antimycobacterial properties. *J Med Chem* 27(9):1111-1118.
- Mehanna MM, Elmaradny HA, Samaha MW. 2009. Ciprofloxacin liposomes as vesicular reservoirs for ocular delivery: Formulation, optimization, and *in vitro* characterization. *Drug Dev Ind Pharm* 35(5):583-593.
- Carrozzino JM, Khaledi MG. 2004. Interaction of basic drugs with lipid bilayers using liposome electrokinetic chromatography. *Pharm Res* 21(12):2327-2335.
- Burns ST, Khaledi MG. 2002. Rapid determination of liposome-water partition coefficients (K<sub>lw</sub>) using liposome electrokinetic chromatography (LEKC). *J Pharm Sci* 91(7):1601-1612.
- Taillardat-Bertschinger A, Carrupt PA, Testa B. 2002. The relative partitioning of neutral and ionised compounds in sodium dodecyl sulfate micelles measured by micellar electrokinetic capillary chromatography. *Eur J Pharm Sci* 15(2):225-234.
- Hautala JT, Wiedmer SK, Riekkola ML. 2004. Anionic liposomes in capillary electrophoresis: Effect of calcium on 1-palmitoyl-2-oleyl-sn-glycero-3-phosphatidylcholine/phosphatidylserine-coating in silica capillaries. *Anal Bioanal Chem* 378(7):1769-1776.

30. Hautala JT, Linden MV, Wiedmer SK, Ryhanen SJ, Saily MJ, Kinnunen PK, Riekkola ML. 2003. Simple coating of capillaries with anionic liposomes in capillary electrophoresis. *J Chromatogr A* 1004(1–2):81–90.
31. Liu X, Hefesha H, Scriba G, Fahr A. 2008. Retention behavior of neutral and positively and negatively charged solutes on an immobilized-artificial-membrane (IAM) stationary phase. *Helv Chim Acta* 91(8):1505–1512.
32. Liu X, Tanaka H, Yamauchi A, Testa B, Chuman H. 2005. Determination of lipophilicity by reversed-phase high-performance liquid chromatography: Influence of 1-octanol in the mobile phase. *J Chromatogr A* 1091(1–2):51–59.
33. Abraham MH. The permeation of neutral molecules, ions, and ionic species through membranes: Brain permeation as an example. *J Pharm Sci* (in press).

### **3.2 Publication 2**

#### **Human Skin Permeation of Neutral Species and Ionic Species:**

#### **Extended Linear Free-Energy Relationship Analyses**

*Keda Zhang, Ming Chen, Gerhard K. E. Scriba, Michael H. Abraham, Alfred Fahr, Xiangli Liu*

Journal of Pharmaceutical Sciences, 2012, 101(6): 2034-2044

**Pages in the dissertation: 34 ~ 44 (11 pages)**

## Human Skin Permeation of Neutral Species and Ionic Species: Extended Linear Free-Energy Relationship Analyses

KEDA ZHANG,<sup>1</sup> MING CHEN,<sup>1</sup> GERHARD K. E. SCRIBA,<sup>2</sup> MICHAEL H. ABRAHAM,<sup>3</sup> ALFRED FAHR,<sup>1</sup> XIANGLI LIU<sup>1</sup>

<sup>1</sup>Department of Pharmaceutical Technology, Friedrich-Schiller-Universität Jena, 07743 Jena, Germany

<sup>2</sup>Department of Pharmaceutical Chemistry, Friedrich-Schiller-Universität Jena, 07743 Jena, Germany

<sup>3</sup>Department of Chemistry, University College London, London WC1H 0AJ, United Kingdom

Received 21 September 2011; revised 27 January 2012; accepted 31 January 2012

Published online 13 March 2012 in Wiley Online Library (wileyonlinelibrary.com). DOI 10.1002/jps.23086

**ABSTRACT:** The permeability,  $K_p$ , of some ionized solutes (including nine acids and nine bases) through human epidermis membrane was measured in this work. Combined with the experimental  $K_p$  data set for neutral species created by Abraham and Martins and reliable  $K_p$  data for ionic species from the literature, a linear free-energy relationship (LFER) analysis was conducted. The values of  $\log K_p$  for 118 compounds have been correlated with solute descriptors to yield an LFER equation that incorporates neutral species and ionic species, with  $R^2 = 0.861$  and  $SD = 0.462$  log units. The equation can be used to predict  $K_p$  for neutral species and ionic species, as well as partly ionized solutes. Predicted values for the passive permeation of the sodium ion and the tetraethylammonium ion are in good accord with the experimental values. It was observed that neutral acids and bases are more permeable than their ionized forms, and that the ratio depends on the actual structure. The correlation between human skin permeation and water–organic solvent/artificial membrane partitions was investigated by comparison of the coefficients in the LFER equations. Partition into cerasome is a reasonable model for partition into skin, and using cerasome as a surrogate for the partitioning process, we separate permeation into partition and diffusion processes. We show that the poor permeability of ionic species is largely due to slow diffusion through the stratum corneum. This is especially marked for a number of protonated base cations. © 2012 Wiley Periodicals, Inc. and the American Pharmacists Association *J Pharm Sci* 101:2034–2044, 2012

**Keywords:** transdermal drug delivery; permeability; skin; permeation; partition; diffusion; ionic species; physicochemical properties; linear free-energy relationship; LFER; QSPR

### INTRODUCTION

Much work on physicochemical models for drug permeation through human skin has been carried out using the *n*-octanol/water partition coefficient ( $\log P_{\text{oct}}$ ) as a lipophilicity index plus molecular weight (or volume).<sup>1</sup> However, these models were just built on human skin permeability ( $K_p$ ) data sets for neutral solutes, and in some cases, ionization of basic and acidic compounds was ignored selectively. This is due to the fact that it is extremely difficult to construct an equation incorporating neutral species

and ionic species for skin permeation. On the one hand, ionizable species can exist both as separate ions (anions and cations) and as ion pairs in octanol; the experimentally measured  $\log P_{\text{oct}}$  values for the separated ions are those for a neutral combination of anions and cations and single ion  $\log P_{\text{oct}}$  values have to be obtained using some extrathermodynamic convention.<sup>2</sup> On the other hand,  $\log P_{\text{oct}}$ , as a widely used lipophilicity index, could not encode some important recognition forces between charged solutes and biological membranes. In our study, the term “ions” refer to permanent ions such as  $\text{Na}^+$  and  $\text{Cl}^-$ , and the term “ionic species” refers to ions derived from protonation of basic compounds and deprotonation of acidic compounds.

One feasible method for the prediction of  $K_p$  for ions and ionic species is through the linear free-energy relationship (LFER) proposed by Abraham.

Correspondence to: Xiangli Liu (Telephone: +49-3641-949903; Fax: +49-3641-949902; E-mail: xiangli.liu@uni-jena.de); Michael H. Abraham (Telephone: +44-20-7679-4639; Fax: +44-20-7679-7463; E-mail: m.h.abraham@ucl.ac.uk)

*Journal of Pharmaceutical Sciences*, Vol. 101, 2034–2044 (2012)  
© 2012 Wiley Periodicals, Inc. and the American Pharmacists Association



The general LFER equation, Eq. 1, has been successfully applied to a large number of equilibrium systems, including water–solvent partitions,<sup>3–5</sup> water–artificial membrane partitions,<sup>6–9</sup> and biological membrane permeations.<sup>10–12</sup> Nevertheless, Eq. 1 was established to deal with processes that involved only neutral solutes. In order to extend Eq. 1 to include ions and ionic species, Abraham and Acree<sup>13</sup> incorporated an additional term  $j^+J^+$  for cations and an additional term  $j^-J^-$  for anions, as shown in Eq. 2:

$$SP = c + eE + sS + aA + bB + vV \quad (1)$$

$$SP = c + eE + sS + aA + bB + vV + j^+J^+ + j^-J^- \quad (2)$$

Here and elsewhere, the dependent variable SP represents a property of a series of solutes in a given system, including partition coefficients (e.g.,  $\log P_{\text{oct}}$ ) and rate coefficients (e.g.,  $\log K_p$ ). The independent variables are the solute descriptors as follows:  $E$  is the excess molar refraction in units of  $(\text{cm}^3/\text{mol})/10$ ,  $S$  is the combined dipolarity/polarizability,  $A$  and  $B$  are the overall solute hydrogen bond acidity and basicity, and  $V$  is McGowan's characteristic molecular volume in units of  $(\text{cm}^3/\text{mol})/100$ ;  $J^+$  and  $J^-$  are the additional descriptors that refer to the ion–solvent interaction for cations and anions, respectively. That is to say,  $J^+$  is zero for anions,  $J^-$  is zero for cations, and both of them are zero for neutral species. The methods of computation or estimation of the seven solute descriptors have been detailed previously.<sup>14</sup> The coefficients in Eq. 2 are obtained using multiple linear regression analysis and serve to characterize the system of interest.

Equation 2 has been proved to be a good model that includes both neutral species and ionic species for the partition of solutes in water/organic solvents,<sup>2,13,15</sup> and in water/liposome (cerasome),<sup>16</sup> as well as the permeation through the blood–brain barrier.<sup>14</sup>

Previously, Eq. 1 was applied to observed  $\log K_p$  of 119 neutral solutes,<sup>11</sup> leading to Eq. 3, with  $K_p$  in units of  $\text{cm s}^{-1}$ :

$$\log K_p = -5.426 - 0.106E - 0.473S - 0.473A - 3.000B + 2.296V \quad (3)$$

Now that descriptors can be estimated for ionic species, Eq. 3 can be extended to include both species, thus leading to a model for the prediction of skin permeation of ions and ionic species as well as neutral species, from known solute descriptors. The aim of this study is to set up an LFER model for human skin permeation of neutral and ionic species. To achieve this aim, we have measured the  $\log K_p$  values for 18 ionized solutes through human epidermis, and have combined these data with literature  $\log K_p$  values in order to derive such an LFER model.

## MATERIALS AND METHODS

### Chemicals

A series of (4-methylbenzyl)alkylamines hydrochloride was synthesized according to a known procedure.<sup>17</sup> All other compounds shown in Table 1 as well as potassium dihydrogen phosphate and dipotassium hydrogen phosphate were purchased from Sigma–Aldrich (Steinheim, Germany) and were of highest available purity. Methanol and acetonitrile [high-performance liquid chromatography (HPLC) gradient grade] used in HPLC measurements were purchased from BDH Prolabo (VWR, Dresden, Germany).

### Measurement of Solubility

The solutes in Table 1 were added to 0.02 M phosphate buffer (pH 7.4) until saturation occurs, indicated by undissolved excess solute. The resulting suspension was stirred with a magnetic bar overnight in an air bath of 32°C by using an incubator. The sample was rapidly filtered to remove the undissolved material by using a syringe filter (200 nm, nylon; MedChrom, Flörsheim-Dalsheim, Germany). The concentration of the saturated solution (solubility of the solute) was determined by HPLC analysis.

### Epidermis Preparation

Human abdominal skin was obtained from women aged 30–50 years old and subjected to plastic surgery. The subcutaneous fatty tissue was removed from the skin using disposable scalpels and surgical scissors with curved blade within 2 h after operation, and then the remaining full-thickness skin was frozen at –20°C with aluminum foil packing as soon as possible, for 3-month usage. Before permeation experiments for each compound, some frozen skin disks of 25 mm diameter were punched out and thawed at room temperature, followed by a water bath at 60°C for 90 s. The epidermis sheets were separated by scratching the connective part between dermis and epidermis with toothless tweezers. These epidermis sheets were bathed in the receptor medium for at least 30 min prior to use.

### In Vitro Permeation Studies

The *in vitro* permeation studies were conducted for the compounds in Table 1. The epidermis sheet was mounted in a single-wall Franz cell (Gauer Glas, Püttlingen, Germany) with an effective diffusion area of 1.76 cm<sup>2</sup> and a receptor chamber of 12 mL, following a visual check for skin integrity with a magnifier. In skin permeation experiments, 0.02 M phosphate buffer pH 7.4 was used as the donor and receptor medium. The donor solution for each

**Table 1.** Experimental Values of Log  $K_p$  at 32°C for the Compounds Used in This Work, and Other Physicochemical Parameters

No.	Compound	Log $P_{oct}^a$	Solubility <sup>b</sup>	pKa <sup>a</sup>	pH (Obs)	$F_n^c$	$F_i^c$	Log $K_p^d$ (Obs)
1	C <sub>6</sub> H <sub>5</sub> COOH	1.96	4.78	4.20	3.97	0.629	0.371	-5.31 ± 0.02
2	C <sub>6</sub> H <sub>5</sub> (CH <sub>2</sub> ) <sub>2</sub> COOH	1.89	11.85	4.52	4.16	0.696	0.304	-5.28 ± 0.01
3	C <sub>6</sub> H <sub>5</sub> (CH <sub>2</sub> ) <sub>3</sub> COOH	2.42	4.81	4.72	5.00	0.344	0.656	-5.50 ± 0.06
4	C <sub>6</sub> H <sub>5</sub> (CH <sub>2</sub> ) <sub>4</sub> COOH	2.85	3.29	4.55	6.01	0.034	0.966	-5.82 ± 0.02
5	C <sub>6</sub> H <sub>5</sub> (CH <sub>2</sub> ) <sub>7</sub> COOH	4.09	1.54	5.03	6.84	0.015	0.985	-5.60 ± 0.05
6	Flurbiprofen	3.81	2.75	3.91	6.75	0.001	0.999	-6.20 ± 0.02
7	Ibuprofen	3.87	2.57	4.43	6.61	0.007	0.993	-6.03 ± 0.02
8	Ketoprofen	3.12	3.89	4.29	6.42	0.007	0.993	-5.71 ± 0.06
9	Naproxen	3.06	2.68	4.15	6.71	0.003	0.997	-6.73 ± 0.03
10	4-MeC <sub>6</sub> H <sub>4</sub> CH <sub>2</sub> NHMe	1.96	–	9.93	7.40	0.003	0.997	-7.71 ± 0.07
11	4-MeC <sub>6</sub> H <sub>4</sub> CH <sub>2</sub> NHEt	2.38	–	10.04	7.40	0.002	0.998	-6.97 ± 0.08
12	4-MeC <sub>6</sub> H <sub>4</sub> CH <sub>2</sub> NHPr	2.96	130.80	9.98	7.40	0.003	0.997	-6.97 ± 0.03
13	4-MeC <sub>6</sub> H <sub>4</sub> CH <sub>2</sub> NHBu	3.49	82.02	9.98	7.40	0.003	0.997	-6.72 ± 0.04
14	4-MeC <sub>6</sub> H <sub>4</sub> CH <sub>2</sub> NH(CH <sub>2</sub> ) <sub>4</sub> Me	4.26	22.87	10.08	7.40	0.002	0.998	-6.00 ± 0.07
15	4-MeC <sub>6</sub> H <sub>4</sub> CH <sub>2</sub> NH(CH <sub>2</sub> ) <sub>5</sub> Me	4.96	16.43	10.17	7.40	0.002	0.998	-5.87 ± 0.02
16	4-MeC <sub>6</sub> H <sub>4</sub> CH <sub>2</sub> NH(CH <sub>2</sub> ) <sub>6</sub> Me	5.12	6.07	10.02	7.40	0.002	0.998	-5.79 ± 0.03
17	Alprenolol	3.10	–	9.59	7.40	0.006	0.994	-7.10 ± 0.06
18	Propranolol	3.48	–	9.53	7.40	0.007	0.993	-7.90 ± 0.10

<sup>a</sup>Data from Zhang et al.<sup>16</sup><sup>b</sup>Solubility in units of mg/mL of the compounds in 0.02 M phosphate buffer pH 7.4.<sup>c</sup> $F_n$  and  $F_i$  are the fraction of neutral and ionic species in a given pH.<sup>d</sup>Values are the average ± SD,  $n = 3-6$ ;  $K_p$  in units of cm/s.

compound was freshly prepared by diluting the respective saturated solution to a concentration of 80% of solubility, except for four extremely soluble compounds (#10, 11, 17, and 18 in Table 1), which were dissolved in 0.02 M phosphate buffer pH 7.4 at a concentration of 271.6 mg/mL for #10, 81.2 mg/mL for #11, 72.2 mg/mL for #17, and 92.9 mg/mL for #18. The stratum corneum (SC) side of epidermis sheet was placed upward to the air and the underside supported by a dialysis membrane (Medicell, London, United Kingdom) was in contact with the receptor medium. The Franz cell was moved into an incubator set at 32°C, with the receptor medium stirred by a magnetic bar. After equilibration for 60 min, the Franz cell was overturned repeatedly up to the removal of all air bubbles in receptor chamber. Donor solution (0.5 mL) was added into the donor chamber, and then the opening of the Franz cell was enclosed with Parafilm® (Pechiney Plastic Packaging, Chicago, Illinois). The receptor liquid was sampled by 0.3 mL with a following replacement (receptor medium) at fixed times. For each compound, the skin permeability was measured in no less than three parallel experiments.

### HPLC Analysis

The quantitative analyses of the compounds were carried out with a System Gold® HPLC (Beckman Coulter, Fullerton, California) equipped with an HPLC pump System-Gold-125 solvent module, a System-Gold-507e autosampler, and a System-Gold-UV/VIS-168 detector. The HPLC column used was a Symmetry® C18 (4.6 × 100 mm<sup>2</sup> internal diameter 3.5 μm) from Waters (Milford, Massachusetts).

The isocratic elution method was performed at room temperature in HPLC measurements. The mobile phases consisted of 0.02 M phosphate buffer pH 7.0 and methanol in proportions ranging from 80:20 to 20:80. The phosphate buffer was filtered through a 0.45 μm HA Millipore filter (Millipore, Milford, Massachusetts) under vacuum before being mixed with methanol. The injection volume was 20 μL, and the flow rate was 1 mL/min. The compounds were detected using the ultraviolet-visible detector at the maximum absorption wavelength  $\lambda_{max}$ . For each compound, the calibration linear curve was constructed in a constant concentration range (0.5–100 μg/mL), with a square regression coefficient of 0.999–1.000. In addition, each sample was injected in triplicate.

### Data Treatment

The cumulative amount ( $Q$ ) of each compound permeated through human epidermis was plotted as a function of time ( $t$ ). The permeability  $K_p$  was calculated by dividing the steady-state flux ( $J$ ) that is the slope for the linear portion of the accumulation curve by the concentration of the donor solution ( $C$ ), in accordance with the following equation:

$$K_p = \frac{J}{C} = \frac{dQ}{dt \times C} \quad (4)$$

## RESULTS AND DISCUSSION

The values of log  $K_p$  for some ionizable compounds (including nine acids and nine bases) across human

epidermis membrane were measured in this study (Table 1). A donor solution of high concentration (80% of the solubility for most compounds) was applied in *in vitro* permeation studies in order to achieve an easy-to-monitor transdermal process. But as a result, the 0.02 M phosphate buffer pH 7.4 used as the donor medium failed to control the pH after addition of some solutes. The actual pH values of donor solutions were determined prior to permeation experiments (shown in Table 1). The fraction of neutral and ionic species ( $F_n$  and  $F_i$ ) were calculated for each compound in the donor solution and given in Table 1. It can be seen that some of the acids were partly ionized, instead of complete ionization as expected. The bases were fully ionized thanks to the use of the respective hydrochloride salt. In this work, the “complete ionization” was defined so that the fraction of ionic species at a given pH is more than 0.990. Meanwhile, we also used the experimental  $\log K_p$  data of the ionic species of five nonsteroidal anti-inflammatory drugs (NSAIDs) obtained by Singh and Roberts<sup>18</sup> (Table 2), considering the similar experimental conditions and that the reported  $\log K_p$  values ( $\text{cm s}^{-1}$ ) for naproxen ( $-6.71$ ) and indomethacin ( $-7.22$ ) are, respectively, very close to our measurement ( $-6.73$ ) and the value ( $-7.00$ ) obtained by Hirvonen et al.,<sup>19</sup> where the  $K_p$  value for propranolol is  $-7.87$  (in our work,  $-7.90$ ). It should be noted that in Ref. 18, the reported value of  $K_p$  at 0% ionization for piroxicam is incorrect—it should be  $0.34 \times 10^{-2}$  cm/h, not  $3.40 \times 10^{-2}$  cm/h. This may be recalculated using the same method by the investigators, and also seen in their Figure 2.

The experimental  $\log K_p$  data set for neutral species previously collected by Abraham and Martins<sup>11</sup> were carefully appraised in terms of whether the given experimental conditions allowed an exact calculation of the ionization extent of permeants in the donor solutions. Donor solutions are usually buffered for ionizable compounds, but if the compound concentration is too high, the buffering capacity may not be enough to lead to the desired concentrations of ionized or neutral species. Only if the pH of the donor solutions is determined after the addition of the ionizable compound to the buffer solution can the fraction of neutral or ionized species be determined accurately. In a number of cases, we had to omit the data obtained for ionizable compounds because of an uncertain ionic fraction. The data for a series of phenolic compounds whose  $\text{p}K_a$  values are between 8.0 and 10.0 were determined by Roberts et al.<sup>20</sup> using distilled water as the donor medium, so we can estimate that at their threshold concentrations for skin damage offered by the workers, the compounds exist almost entirely in the neutral form. The  $\log K_p$  data for four phenylene-diamine hair dyes are also available from Bronaugh and Congdon,<sup>21</sup> who used a borate buffer pH 9.7 to prevent ionization.

Singh and Roberts<sup>18</sup> gave values of  $K_p$  for five NSAIDs, both for the neutral species and for the fully ionized species, where the ratio of  $K_p$  for the neutral form to the ionized anion averages 70 except for piroxicam where the ratio is 29. However, piroxicam is a rather unusual compound, and is a “weak” zwitterion with a weakly acidic phenolic group ( $\text{p}K_a$  5.46) and a weakly basic pyridyl nitrogen ( $\text{p}K_a$  1.86).<sup>22</sup> So, we can regard the ratio as 70 in general. Then, for five phenyl fatty acids (#1–5) in Table 1, we can analyze the observed  $K_p$  data for the mixture of neutral and ionic species, using the neutral–anion ratio of 70 together with Eq. 5 to obtain the “observed” values for the neutral and the ionic species, as shown in Table 2. Note that in Table 2, the naproxen anion is included twice. One is our observed value for the anion and the other is the value observed by Singh and Roberts.<sup>18</sup> We need to include both of these because it is the data by Singh and Roberts<sup>18</sup> on the neutral and ionized species that help us to obtain the ratio as 70.

$$K_p = K_p(i) \times F_i + K_p(n) \times F_n \quad (5)$$

Abraham and Martins<sup>11</sup> left out a number of hydrophilic compounds on the grounds that they might permeate by a different mechanism. We can see no reason to omit these, and so we include urea, mannitol, ouabain, and the tetraethylammonium ion; we deal with the latter later on, as a test compound to see if we can predict the  $K_p$  value. We were unable to include sucrose and raffinose because of the difficulty in assigning descriptors to these two compounds.

Roy and Flynn<sup>23</sup> studied the influences of pH on  $K_p$  of fentanyl and sufentanyl, and measured their  $K_p$  as a function of pH. In their work, they used the value of  $K_p$  at pH 2.88 as that of ionic species for both compounds. At first sight, it seems to be rather reasonable. But we found that the  $K_p$  values at pH 2.88 and at pH 5.08 of each compound are quite different, where the ionic fractions are over 0.999. Furthermore, for these two compounds, the predictions of  $K_p$  at different pH using the  $K_p$  values of neutral and ionic species shown by the investigators in their Table VI would be much lower than the experimental values at the pH range from 5.0 to 8.0. Hence, we have to omit these data in view of data reliability.

In a few cases, large initial lag times were observed, but all the  $K_p$  values that we have used have been obtained from steady-state portions of the permeation–time plots.

All the compounds and species (compounds #1–85 from Abraham and Martins<sup>11</sup>; compounds #86–108 from our work; compounds #109–118 from Singh and Roberts<sup>18</sup>) used in our analysis are shown in Table 2. The chemical structures of the hydrocortisone esters, 1a–1k, are given in Figure 1. The  $K_p$  values are all in centimeter per second. We can now apply Eq. 2,

**Table 2.** Compounds and Species Used in This Work, Their Solute Descriptors, Experimental Log  $K_p$  Values, and Log  $K_p$  Values Calculated from Eq. 6

No.	Solute	$E^a$	$S^a$	$A^a$	$B^a$	$V^a$	$J^{+a}$	$J^{-a}$	Obs <sup>b</sup>	Calc <sup>b</sup>
1	Water	0.000	0.45	0.82	0.35	0.1673	0.0000	0.0000	-6.28	-6.48
2	Methanol	0.278	0.44	0.43	0.47	0.3082	0.0000	0.0000	-6.38	-6.41
3	Ethanol	0.246	0.42	0.37	0.48	0.4491	0.0000	0.0000	-6.08	-6.12
4	Propan-1-ol	0.236	0.42	0.37	0.48	0.5900	0.0000	0.0000	-5.93	-5.82
5	Butan-1-ol	0.224	0.42	0.37	0.48	0.7309	0.0000	0.0000	-5.70	-5.53
6	Pentan-1-ol	0.219	0.42	0.37	0.48	0.8718	0.0000	0.0000	-5.30	-5.24
7	Hexan-1-ol	0.210	0.42	0.37	0.48	1.0127	0.0000	0.0000	-4.92	-4.95
8	Heptan-1-ol	0.211	0.42	0.37	0.48	1.1536	0.0000	0.0000	-4.57	-4.66
9	Octan-1-ol	0.199	0.42	0.37	0.48	1.2950	0.0000	0.0000	-4.30	-4.36
10	Nonan-1-ol	0.193	0.42	0.37	0.48	1.4354	0.0000	0.0000	-4.30	-4.07
11	Decan-1-ol	0.191	0.42	0.37	0.48	1.5763	0.0000	0.0000	-4.15	-3.78
12	dl-Butan-2,3-diol	0.341	0.93	0.61	0.88	0.7896	0.0000	0.0000	-7.38	-6.81
13	2-Ethoxyethanol	0.237	0.52	0.31	0.81	0.7896	0.0000	0.0000	-6.68	-6.32
14	Phenol	0.805	0.89	0.60	0.30	0.7751	0.0000	0.0000	-5.27	-5.31
15	2-Methylphenol	0.840	0.86	0.52	0.30	0.9160	0.0000	0.0000	-4.88	-4.98
16	3-Methylphenol	0.822	0.88	0.57	0.34	0.9160	0.0000	0.0000	-4.89	-5.11
17	4-Methylphenol	0.820	0.87	0.57	0.31	0.9160	0.0000	0.0000	-4.83	-5.03
18	3,4-Dimethylphenol	0.830	0.86	0.56	0.39	1.0569	0.0000	0.0000	-4.52	-4.94
19	4-Ethylphenol	0.800	0.90	0.55	0.36	1.0569	0.0000	0.0000	-4.53	-4.87
20	2-Isopropyl-5-methylphenol	0.822	0.79	0.52	0.44	1.3387	0.0000	0.0000	-4.35	-4.45
21	2-Chlorophenol	0.853	0.88	0.32	0.31	0.8975	0.0000	0.0000	-4.56	-4.99
22	4-Chlorophenol	0.915	1.08	0.67	0.20	0.8975	0.0000	0.0000	-4.52	-4.91
23	4-Bromophenol	1.080	1.17	0.67	0.20	0.9501	0.0000	0.0000	-4.52	-4.86
24	4-Chloro-3-methylphenol	0.920	1.02	0.67	0.22	1.0384	0.0000	0.0000	-4.34	-4.64
25	4-Chloro-3,5-dimethylphenol	0.925	0.96	0.64	0.21	1.1793	0.0000	0.0000	-4.31	-4.29
26	Resorcinol	0.980	1.11	1.09	0.52	0.8338	0.0000	0.0000	-6.70	-6.05
27	2-Naphthol	1.520	1.08	0.61	0.40	1.1441	0.0000	0.0000	-4.65	-4.98
28	Benzyl alcohol	0.803	0.87	0.39	0.56	0.9160	0.0000	0.0000	-5.30	-5.64
29	4-Hydroxybenzyl alcohol	0.998	1.20	0.86	0.81	0.9747	0.0000	0.0000	-6.26	-6.51
30	2-Phenylethanol	0.811	0.86	0.31	0.65	1.0569	0.0000	0.0000	-5.20	-5.56
31	5,5-Diethylbarbituric acid	1.030	1.14	0.47	1.18	1.3739	0.0000	0.0000	-7.29	-6.52
32	5-Ethyl-5-butylbarbituric acid	1.030	1.14	0.47	1.18	1.6557	0.0000	0.0000	-7.05	-5.94
33	Aniline	0.955	0.96	0.26	0.41	0.8162	0.0000	0.0000	-4.73	-5.45
34	Benzaldehyde	0.820	1.00	0.00	0.39	0.8730	0.0000	0.0000	-3.93	-5.20
35	Benzene	0.610	0.52	0.00	0.14	0.7164	0.0000	0.0000	-4.27	-4.62
36	Butanone	0.166	0.70	0.00	0.51	0.6879	0.0000	0.0000	-5.42	-5.70
37	Caffeine	1.500	1.82	0.08	1.25	1.3632	0.0000	0.0000	-7.08	-6.97
38	Diethylcarbamazine	0.645	1.30	0.00	1.55	1.7241	0.0000	0.0000	-6.15	-6.67
39	Diethylether	0.041	0.25	0.00	0.45	0.7309	0.0000	0.0000	-5.37	-5.23
40	Digitoxin	3.460	5.63	1.33	4.35	5.6938	0.0000	0.0000	-8.15	-8.68
41	Urea	0.501	1.49	0.83	0.84	0.4646	0.0000	0.0000	-7.93	-7.71
42	Mannitol	0.836	2.33	0.87	1.77	1.3062	0.0000	0.0000	-8.42	-8.90
43	Ouabain	4.000	6.50	0.90	3.56	4.1615	0.0000	0.0000	-9.66	-10.04
44	Ethylbenzene	0.613	0.51	0.00	0.15	0.9982	0.0000	0.0000	-3.00	-4.06
45	5-Ethyl-5-(3-methylbutyl)barbital	1.030	1.11	0.47	1.23	1.7966	0.0000	0.0000	-5.98	-5.77
46	5-Ethyl-5-phenylbarbital	1.630	1.80	0.73	1.15	1.6999	0.0000	0.0000	-6.68	-6.22
47	Fluocinonide	1.950	2.48	0.31	2.51	3.4603	0.0000	0.0000	-6.33	-6.43
48	5-Fluorouracil	0.720	0.84	0.57	1.02	0.7693	0.0000	0.0000	-6.82	-7.21
49	Glycerol trinitrate	0.586	2.11	0.00	0.35	1.2300	0.0000	0.0000	-5.21	-4.84
50	4-Hydroxy-methylphenylacetate	0.908	1.46	0.59	0.68	1.2722	0.0000	0.0000	-5.26	-5.57
51	4-Hydroxyphenylacetamide	1.280	2.03	0.86	0.94	1.1724	0.0000	0.0000	-6.89	-6.86
52	Isoquinoline	1.211	1.00	0.00	0.54	1.0443	0.0000	0.0000	-5.11	-5.29
53	8-Methoxypsoralen	1.611	1.70	0.00	0.80	1.4504	0.0000	0.0000	-5.12	-5.51
54	Methyl 4-hydroxybenzoate	0.900	1.37	0.69	0.45	1.1313	0.0000	0.0000	-5.12	-5.23
55	Methylphenylether	0.708	0.75	0.00	0.29	0.9160	0.0000	0.0000	-4.68	-4.72
56	Toluene	0.601	0.52	0.00	0.14	0.8573	0.0000	0.0000	-3.64	-4.32
57	4-Chloro-m-phenylenediamine	1.358	1.50	0.23	0.69	1.0384	0.0000	0.0000	-6.54	-6.02
58	o-Phenylenediamine	1.260	1.40	0.24	0.73	0.9160	0.0000	0.0000	-6.70	-6.33
59	p-Phenylenediamine	1.300	1.73	0.31	0.84	0.9160	0.0000	0.0000	-6.98	-6.80
60	Aldosterone	2.010	3.47	0.40	1.90	2.6890	0.0000	0.0000	-7.45	-6.88
61	Corticosterone	1.860	3.43	0.40	1.63	2.7389	0.0000	0.0000	-6.84	-6.02
62	Dexamethasone	2.040	3.51	0.71	1.92	2.9132	0.0000	0.0000	-7.27	-6.59

(Continued)

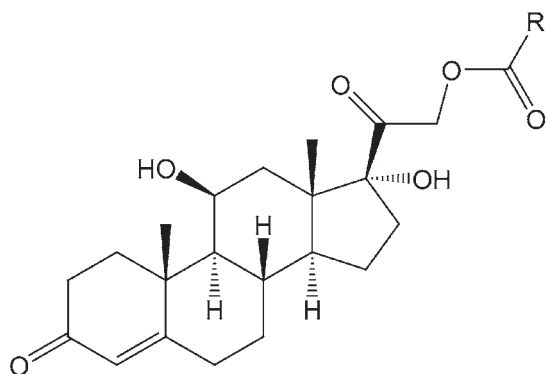
Table 2. Continued

No.	Solute	$E^a$	$S^a$	$A^a$	$B^a$	$V^a$	$J^{+a}$	$J^{-a}$	Obs <sup>b</sup>	Calc <sup>b</sup>
63	Estradiol	1.800	1.77	0.86	1.10	2.1988	0.0000	0.0000	-5.61	-5.10
64	Hydrocortisone	2.030	3.49	0.71	1.90	2.7976	0.0000	0.0000	-7.22	-6.77
65	Progesterone	1.450	3.29	0.00	1.14	2.6215	0.0000	0.0000	-4.90	-4.71
66	Testosterone	1.540	2.59	0.32	1.19	2.3827	0.0000	0.0000	-5.54	-5.13
67	Benzyl nicotinate	1.262	1.60	0.00	0.80	1.6393	0.0000	0.0000	-4.87	-5.04
68	Butyl nicotinate	0.658	1.07	0.00	0.73	1.4542	0.0000	0.0000	-4.86	-4.93
69	Ethyl nicotinate	0.667	1.10	0.00	0.73	1.1724	0.0000	0.0000	-5.28	-5.53
70	Hexyl nicotinate	0.628	1.07	0.00	0.73	1.7360	0.0000	0.0000	-4.83	-4.34
71	2-Hydroxypropyl nicotinate	0.840	1.38	0.35	1.19	1.3720	0.0000	0.0000	-7.55	-6.61
72	Methyl nicotinate	0.710	1.13	0.00	0.71	1.0315	0.0000	0.0000	-5.77	-5.78
73	Methyltriglycol nicotinate	0.730	1.42	0.00	1.79	2.0530	0.0000	0.0000	-6.83	-6.70
74	Triglycol nicotinate	0.950	1.58	0.37	1.78	1.9121	0.0000	0.0000	-8.08	-7.18
75	1a	2.310	3.32	1.01	2.84	3.4924	0.0000	0.0000	-8.14	-7.90
76	1b	2.210	3.77	0.46	2.86	3.7742	0.0000	0.0000	-7.73	-7.39
77	1c	1.990	3.11	0.46	2.61	3.5922	0.0000	0.0000	-7.23	-6.77
78	1d	2.100	3.15	1.06	2.61	3.4513	0.0000	0.0000	-6.69	-7.28
79	1e	2.020	3.58	1.06	2.61	3.8740	0.0000	0.0000	-6.24	-6.60
80	1f	2.210	4.15	0.96	2.78	3.9151	0.0000	0.0000	-6.13	-7.22
81	1g	2.020	3.49	0.83	2.64	3.7174	0.0000	0.0000	-6.12	-6.89
82	1h	1.870	2.90	0.46	2.16	3.2360	0.0000	0.0000	-6.02	-6.19
83	1i	1.930	3.49	0.46	2.61	4.0149	0.0000	0.0000	-5.82	-6.06
84	1j	1.810	3.02	0.46	2.16	3.6587	0.0000	0.0000	-5.30	-5.37
85	1k	1.770	3.05	0.46	2.16	3.9405	0.0000	0.0000	-4.76	-4.79
86	4-MeC <sub>6</sub> H <sub>4</sub> CH <sub>2</sub> NHMe, cation	0.650	2.58	1.42	0.00	1.2604	1.2835	0.0000	-7.71	-7.01
87	4-MeC <sub>6</sub> H <sub>4</sub> CH <sub>2</sub> NHEt, cation	0.640	2.66	1.44	0.00	1.4013	1.2994	0.0000	-6.97	-6.79
88	4-MeC <sub>6</sub> H <sub>4</sub> CH <sub>2</sub> NHPr, cation	0.630	2.63	1.37	0.00	1.5422	1.3290	0.0000	-6.97	-6.52
89	4-MeC <sub>6</sub> H <sub>4</sub> CH <sub>2</sub> NHBu, cation	0.620	2.62	1.34	0.00	1.6831	1.3349	0.0000	-6.72	-6.23
90	4-MeC <sub>6</sub> H <sub>4</sub> CH <sub>2</sub> NH(CH <sub>2</sub> ) <sub>4</sub> Me, cation	0.610	2.60	1.34	0.00	1.8240	1.3136	0.0000	-6.00	-5.88
91	4-MeC <sub>6</sub> H <sub>4</sub> CH <sub>2</sub> NH(CH <sub>2</sub> ) <sub>5</sub> Me, cation	0.600	2.60	1.36	0.00	1.9649	1.2956	0.0000	-5.87	-5.56
92	4-MeC <sub>6</sub> H <sub>4</sub> CH <sub>2</sub> NH(CH <sub>2</sub> ) <sub>6</sub> Me, cation	0.590	2.63	1.36	0.00	2.1058	1.2969	0.0000	-5.70	-5.29
93	Alprenolol, cation	1.100	4.46	1.78	0.00	2.1802	2.2574	0.0000	-7.10	-8.02
94	Propranolol, cation	1.690	4.31	2.07	0.00	2.1695	2.4319	0.0000	-7.90	-8.47
95	Flurbiprofen anion	1.590	4.56	0.07	3.36	1.8174	0.0000	2.5383	-6.20	-6.47
96	Ibuprofen, anion	0.880	3.50	0.08	3.31	1.7556	0.0000	2.4188	-6.03	-6.22
97	Ketoprofen, anion	1.800	5.49	0.01	3.39	1.9564	0.0000	2.4851	-5.71	-6.83
98	Naproxen, anion	1.660	5.07	0.02	3.11	1.7606	0.0000	2.4260	-6.73	-6.43
99	C <sub>6</sub> H <sub>5</sub> COOH, anion	0.880	3.05	0.02	2.75	0.9102	0.0000	2.1385	-6.96	-6.95
100	C <sub>6</sub> H <sub>5</sub> COOH	0.730	0.90	0.59	0.40	0.9317	0.0000	0.0000	-5.11	-5.25
101	C <sub>6</sub> H <sub>5</sub> (CH <sub>2</sub> ) <sub>2</sub> COOH, anion	0.900	3.43	0.03	3.02	1.1920	0.0000	2.1879	-6.98	-7.15
102	C <sub>6</sub> H <sub>5</sub> (CH <sub>2</sub> ) <sub>2</sub> COOH	0.750	1.18	0.60	0.60	1.2135	0.0000	0.0000	-5.13	-5.33
103	C <sub>6</sub> H <sub>5</sub> (CH <sub>2</sub> ) <sub>3</sub> COOH, anion	0.910	3.59	0.04	3.01	1.3329	0.0000	2.2184	-6.90	-6.83
104	C <sub>6</sub> H <sub>5</sub> (CH <sub>2</sub> ) <sub>3</sub> COOH	0.760	1.29	0.61	0.57	1.3544	0.0000	0.0000	-5.05	-5.02
105	C <sub>6</sub> H <sub>5</sub> (CH <sub>2</sub> ) <sub>4</sub> COOH, anion	0.920	3.63	0.04	3.10	1.4718	0.0000	2.2794	-6.35	-6.65
106	C <sub>6</sub> H <sub>5</sub> (CH <sub>2</sub> ) <sub>4</sub> COOH	0.770	1.24	0.57	0.60	1.4933	0.0000	0.0000	-4.50	-4.77
107	C <sub>6</sub> H <sub>5</sub> (CH <sub>2</sub> ) <sub>7</sub> COOH, anion	0.940	3.87	0.07	3.26	1.8965	0.0000	2.4256	-5.91	-5.95
108	C <sub>6</sub> H <sub>5</sub> (CH <sub>2</sub> ) <sub>7</sub> COOH	0.790	1.27	0.57	0.62	1.7771	0.0000	0.0000	-4.06	-4.26
109	Salicylic acid, anion <sup>c</sup>	1.050	3.19	0.08	2.74	0.9689	0.0000	2.2641	-7.04	-6.59
110	Indomethacin, anion <sup>c</sup>	2.390	5.62	0.10	4.38	2.5084	0.0000	2.9899	-7.22	-7.21
111	Diclofenac, anion <sup>c</sup>	1.960	5.31	0.03	3.35	2.0035	0.0000	2.6243	-7.00	-6.21
112	Naproxen, anion <sup>c</sup>	1.660	5.07	0.02	3.11	1.7606	0.0000	2.4261	-6.71	-6.43
113	Piroxicam, anion <sup>c</sup>	2.710	6.81	0.00	3.78	2.2285	0.0000	2.7356	-7.50	-7.37
114	Salicylic acid <sup>c</sup>	0.900	0.85	0.73	0.37	0.9904	0.0000	0.0000	-5.07	-5.08
115	Indomethacin <sup>c</sup>	2.240	1.47	0.58	1.43	2.5299	0.0000	0.0000	-5.39	-5.12
116	Diclofenac <sup>c</sup>	1.810	1.85	0.55	0.77	2.0250	0.0000	0.0000	-5.30	-4.51
117	Naproxen <sup>c</sup>	1.510	2.02	0.60	0.67	1.7821	0.0000	0.0000	-4.97	-4.81
118	Piroxicam <sup>c</sup>	2.560	2.71	0.00	1.21	2.2500	0.0000	0.0000	-6.02	-5.52

<sup>a</sup>Values of solute descriptors can be calculated or estimated as detailed in Ref. 14.

<sup>b</sup> $K_p$  in units of cm/s.

<sup>c</sup>Measured by Singh and Roberts<sup>18</sup>; piroxicam ( $pK_a = 5.46$ ) is slightly less than 99% ionized at pH 7.4, so we made a minor correction to the reported value (#113) using Eq. 5 to subtract the contribution of neutral piroxicam.



Compound	R
1a	-CH <sub>2</sub> CH <sub>2</sub> CONH <sub>2</sub>
1b	-CH <sub>2</sub> CH <sub>2</sub> CON(CH <sub>3</sub> ) <sub>2</sub>
1c	-CH <sub>2</sub> CH <sub>2</sub> COOCH <sub>3</sub>
1d	-CH <sub>2</sub> CH <sub>2</sub> COOH
1e	-(CH <sub>2</sub> ) <sub>4</sub> CH <sub>2</sub> COOH
1f	-(CH <sub>2</sub> ) <sub>4</sub> CH <sub>2</sub> CONH <sub>2</sub>
1g	-(CH <sub>2</sub> ) <sub>4</sub> CH <sub>2</sub> OH
1h	-CH <sub>2</sub> CH <sub>3</sub>
1i	-(CH <sub>2</sub> ) <sub>4</sub> CH <sub>2</sub> COOCH <sub>3</sub>
1j	-(CH <sub>2</sub> ) <sub>4</sub> CH <sub>3</sub>
1k	-(CH <sub>2</sub> ) <sub>6</sub> CH <sub>3</sub>

**Figure 1.** Chemical structures of the hydrocortisone esters, 1a–1k.

where  $SP = \log K_p$ , to all 118 compounds or species, using the multiple linear regression analysis of  $\log K_p$  against the seven solute descriptors. The obtained LFER model is as follows:

$$\begin{aligned} \log K_p &= -5.420(\pm 0.211) - 0.102(\pm 0.296)E - 0.457(\pm 0.231)S \\ &- 0.324(\pm 0.337)A - 2.680(\pm 0.300)B + 2.066(\pm 0.249)V \\ &- 1.938(\pm 0.485)J^+ + 2.548(\pm 0.337)J^- \\ N &= 118, R^2 = 0.861, SD = 0.462, F = 97.3 \end{aligned} \quad (6)$$

Here, 95% confidence limits are given in parentheses;  $N$  is the number of compounds or species studied;  $R$  is the correlation coefficient;  $SD$  is the standard deviation, and  $F$  is the Fisher  $F$ -statistic.

In the construction of Eq. 6, we had to make the approximations that a neutral–anion ratio of 70 applied to the five acids (#1–5) in Table 1 and that for the remaining 13 compounds in Table 1, we could ignore the contribution from the neutral form altogether. Now that we have an equation for  $\log K_p$ , we can use it to calculate the contribution of the ionic and neutral

forms for all 18 compounds. For the five acids (#1–5), and for all 10 acids, the new ratio was found to be 61, so that our assumption of a ratio of 70 is valid. In the case of the nine bases (#10–18, Table 1), we can now calculate the value of  $\log K_p$  for the neutral species from Eq. 6 and the descriptors for the neutral species and deduce that, indeed, the neutral species make a negligible contribution to  $\log K_p$ . We point out that we have also constructed an equation for  $\log K_p$  taking a neutral–anion ratio of 100 for the five acids (#1–5) in Table 1 and obtain an equation identical to Eq. 6. The latter, therefore, does not depend on the exact value of the ratio at all.

Equation 6 is quite comparable to Eq. 3 obtained only for neutral species with the coefficients in the two equations reasonably close; the  $SD$  value in Eq. 6 is 0.462, which is almost the same as that for Eq. 3 (0.469). A plot of observed values of  $\log K_p$  versus calculated values of  $\log K_p$  on Eq. 6 is shown in Figure 2. The data points for the anions and cations scatter randomly over the line of unit slope.

The five neutral phenyl fatty acids and their corresponding anions (#99–108 in Table 2) fit Eq. 6 very well; the average absolute residual is only 0.202 log units. For all 10 acids, the ratio of neutral to ionic  $K_p$  values is 61. The same analysis was applied to the bases in Table 2. For the seven *N*-alkylbenzylamines, the ratio is 57, but for alprenolol and propranolol, the ratios are much larger at 340 and 975, respectively. Our view is that neutral acids and bases permeate across the epidermis very much faster than the corresponding ionized species, but that the actual ratio depends on their structures. Kasting and Bowman<sup>24</sup> have determined the passive permeation of the sodium ion across human skin as  $4.6 \times 10^{-7}$  cm/min, which corresponds to  $\log K_p = -8.12$  with  $K_p$  in units of cm/s. Abraham and Acree<sup>13</sup> have obtained descriptors for the sodium ion, and if these are combined with the coefficients of Eq. 6, we predict  $\log K_p = -7.41$ , in good agreement with the experimental value. A value of  $-7.84$  for  $\log K_p$  for passive permeation of the tetraethylammonium ion can be obtained from a graph given by Peck et al.<sup>25</sup> Our predicted value is  $-6.48$  in fair agreement with experiment. This is the first time that permeation of an ion across a membrane has been predicted just from the physicochemical properties of the ion and membrane.

The system coefficients  $j^+$  and  $j^-$  in Eq. 6 show that the additional ion–skin interaction plays an important role in ionic permeation process. However, it should be noted that skin permeation of ionic species is influenced by all the terms in Eq. 6 and not just by the terms in  $J^+$  and  $J^-$ .

The predictive standard deviation (PSD) obtained from the leave-one-out statistics is a useful estimate

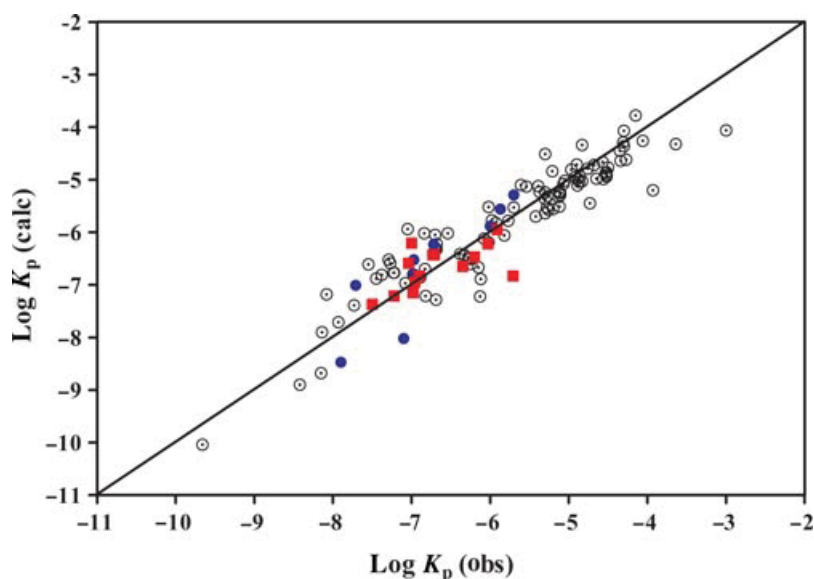


**Figure 2.** A plot of calculated values of  $\log K_p$  on Eq. 6 versus the observed values of  $\log K_p$ .  $\circ$ , neutral species;  $\blacksquare$ , anions from carboxylic acids;  $\bullet$ , cations (protonated bases).

of the predictive power of the regression models, especially for our case that includes data for ionic species.<sup>26,27</sup> The PSD value for Eq. 6 is 0.502, which is possibly close to what can be achieved without overfitting. It is difficult to predict  $\log K_p$  to less than 0.5 log unit for large and varied data sets as discussed previously.<sup>11</sup> Moreover, the data set we used includes both neutral species and ionic species.

It is of interest to investigate the connection between the human skin permeation process and water–organic solvent or water–artificial membrane partitions (Table 3) by comparison of the seven system coefficients ( $e$ ,  $s$ ,  $a$ ,  $b$ ,  $v$ ,  $j^+$ , and  $j^-$ ). It is one of our aims

to build a physicochemical model based on lipophilicity indices from biomimic partitioning systems for predicting  $K_p$ . Note that in Table 3, the retention factors  $k_{cer}$  in cerasome electrokinetic chromatography (EKC), measured by Zhang et al.,<sup>16</sup> are proportional to partition coefficients between water and cerasome (made of skin lipids), as cerasome EKC is actually the water–cerasome partition system based on capillary electrophoresis.

In order to compare a reasonable number of systems simultaneously, we use the analysis method of Abraham and Martins,<sup>11</sup> where the coefficients are regarded as points in seven-dimensional space. The

**Table 3.** Coefficients in General LFER Equations for Human Skin Permeation and a Series of Water–Solvent/Artificial Membrane Partitions;  $d'$  Values Compared with Skin Permeation (Neutral Molecules and Ions) and to Skin Partition (Neutral Molecules)

Solvent/Membrane	$c$	$e$	$s$	$a$	$b$	$v$	$j^+$	$j^-$	$d'$	
									Perm <sup>a</sup>	Part <sup>a</sup>
Methanol	0.276	0.334	-0.714	0.243	-3.320	3.549	-2.609	3.027	1.97	2.13
Ethanol	0.222	0.471	-1.035	0.326	-3.596	3.857	-3.170	3.085	2.63	2.62
1-Propanol	0.139	0.405	-1.029	0.247	-3.767	3.986	-3.077	2.834	2.68	2.80
1-Butanol	0.152	0.438	-1.177	0.096	-3.919	4.122	-3.605	2.685	3.09	3.03
1-Hexanol	0.115	0.492	-1.164	0.054	-3.971	4.131	-3.100	2.940	2.90	3.06
Propanone	0.313	0.312	-0.121	-0.608	-4.753	3.942	-2.288	0.078	3.80	3.37
Acetonitrile	0.413	0.077	0.326	-1.566	-4.391	3.364	-2.243	0.101	3.59	3.15
NMP	0.147	0.532	0.275	0.840	-4.794	3.674	-1.797	0.105	3.92	3.34
DMSO	-0.194	0.327	0.791	1.260	-4.540	3.361	-3.387	0.132	4.16	3.24
EG	-0.270	0.578	-0.511	0.715	-2.619	2.729	-1.300	2.363	1.56	1.29
PC	0.004	0.168	0.504	-1.283	-4.407	3.421	-1.989	0.341	3.41	3.09
Wet 1-octanol, $\log P_{oct}$	0.088	0.562	-1.054	0.034	-3.460	3.814	-3.023	2.580	2.40	2.50
Cerasome, $\log k_{cer}^b$	-1.922	0.200	-0.629	-0.109	-1.451	1.757	0.334	1.958	2.70	0.86
Water–skin partition	0.341	0.341	-0.206	-0.024	-2.178	1.850	0.000	0.000	0.80 <sup>c</sup>	0.00
Skin permeation, $\log K_p$	-5.420	-0.103	-0.457	-0.324	-2.680	2.066	-1.939	2.548	0.00	0.80

<sup>a</sup>Reference system; “perm” means skin permeation and “part” means water–skin partition.

<sup>b</sup>Retention factors in cerasome EKC in log units.

<sup>c</sup>For neutral compounds only,  $j^+ = j^- = 0$ .

NMP, *N*-methylpyrrolidinone; DMSO, dimethyl sulfoxide; EG, ethylene glycol; PC, propylene carbonate.

distance between the points,  $d'$ , calculated by simple trigonometry, is then a measure of how close are the sets of coefficients. As the coefficients have specific chemical meanings, the smaller the value of  $d'$ , the closer are the coefficients in a chemical sense and the closer are the systems in a chemical sense. Abraham and Martins<sup>11</sup> suggested that for a system to be a good chemical model,  $d'$  should be less than around 0.5–0.8 units. Values of  $d'$  with skin permeation as the reference system are shown in Table 3.

From Table 3, we find that skin permeation is not closely related chemically to any of the partitioning systems for which an ionic equation is available, not even to the water–cerasome system. Abraham and Martins<sup>11</sup> have obtained an equation for water–skin partition,  $\log K_{sc}$ , but for neutral solutes only. However, we can calculate  $d'$  with water–skin partition as the standard system, although for neutral solutes only (Table 3). Now cerasome ( $d' = 0.86$ ) is a reasonable model. Methanol ( $d' = 2.13$ ), and ethylene glycol ( $d' = 1.29$ ) also have low values of  $d'$ —lower than for partition into aprotic solvents or less polar solvents—which suggests that neutral compounds partition into rather polar parts of skin.

We can consider skin permeation in terms of partition from water into skin followed by diffusion across the under layer of skin, as described by Eq. 7,

$$\log K_p = \log K_{sc} + \log \frac{D_{sc}}{h} \quad (7)$$

in which  $D_{sc}$  is the diffusion coefficient in the SC of thickness  $h$ .  $\log K_{sc}$  has been supposed to correlate with  $\log P_{oct}$  for neutral species,<sup>28</sup> and the latter to be related to the water–liposome partition coefficient  $\log K_{lw}$ .<sup>29</sup> However, it is known that  $\log P_{oct}$  is not a very good model for water–skin partition, with  $d'$  as 2.08 units (Table 3), and so we analyze Eq. 7 without use of the  $\log P_{oct}$  model. Several authors have suggested that there are two parallel pathways through the SC, for example, Wang et al.<sup>30</sup> wrote (in their nomenclature) Eq. 8 as follows:

$$P_{sc/w} = (P_{sc/w})^{comp} + (P_{sc/w})^{polar} \quad (8)$$

However, it is not possible to dissect  $\log K_p$  into two constituent terms just through an equation such as Eq. 8. To make any progress through Eq. 8, Wang et al.<sup>30</sup> had to calculate the first term from a set of physicochemical parameters.

It would be very interesting if we had data on partitioning into skin by anions and cations because we could then dissect ionic effects on permeation into partition and diffusion and so determine structural effects on the diffusion of ionic species. In the absence of actual  $\log K_{sc}$  data, we can use partition into cera-

**Table 4.** Retarding Factors for Permeation of Ionic Species Through Skin by Comparison to the Corresponding Neutral Compounds; Comparison with Permeation through the Blood-Brain Barrier

Species	N	Retarding Factors		
		Diffusion <sup>a</sup>	Partition	Total
Skin Permeation				
Neutral compounds	95	0	0.0	0
Acid anions	14	13	4.7	61
Base cations	7	82	0.66	54
Alprenolol cation <sup>b</sup>	1	1200	0.28	340
Propranolol cation <sup>b</sup>	1	5250	0.18	955
Water–Brain Permeation				
Neutral compounds	24	0.0	0.0	0
Acid anions	3	6.9	15.0	105
Base cations	21	5.9	2.2	13

<sup>a</sup>Diffusion in skin and in the blood–brain barrier.

<sup>b</sup>Diffusion and partition values calculated with reference to the neutral alprenolol and propranolol bases.

some, Eq. 9,<sup>16</sup>

$$\log k_{cer} = -1.922 + 0.200E - 0.629S - 0.109A \\ -1.451B + 1.757V + 0.334J^+ + 1.958J^- \quad (9)$$

as an estimate of partitioning into skin and then obtain relative values of  $\log D_{sc}$ , Eq. 10, by subtraction of Eq. 9 from Eq. 6. The constant term in Eq. 10 is unknown, but in the present context is irrelevant.

$$\log D_{sc}(\text{est}) = c - 0.302E + 0.172S - 0.215A \\ -1.229B + 0.309V - 2.272J^+ + 0.590J^- \quad (10)$$

From Eqs. 6, 9, and 10, we can then deduce the effect of ionization, by comparison with neutral solutes, on the overall permeation and the separate partition and diffusion process. This is given in Table 4 in terms of the retarding factors for the ionized solutes. The retarding factor is the effect of an ionic species in reducing the rate of permeation by comparison to the corresponding neutral species.

The poor permeability of anions is partly due to poor partition into the SC but mostly due to slow diffusion of the ionized species (by comparison to the corresponding neutral species). For cations, poor permeability is entirely due to very slow diffusion (again by comparison to the neutral species). This is quite different to diffusion in water, where ionic species diffuse at about the same rate as the corresponding neutral compounds, see Eq. 11.<sup>31</sup>

$$\log D(\text{in water}) = 0.31 - 0.027A - 0.360V \\ +0.096J^+ - 0.004J^- \quad (11)$$

A possible explanation for ionic slow diffusion is as follows: The ionized forms definitely bind closer



to the bilayer interface than the neutral form. The solute moves in the lipid bilayers with preference toward lateral diffusion regardless of the solute size and location. The highly ordered lipid chains near the bilayer interface result in the steric resistance of solutes.<sup>32,33</sup> As a result, the ionic species encounters a larger retarding effect to their movement.

The only other permeation process for which data on neutral molecules and ions has been examined is permeation from saline through the blood–brain barrier,<sup>14</sup> see Eq. 12.

$$\begin{aligned} \log PS(\text{blood} - \text{brain barrier}) \\ = -1.268 - 0.047E - 0.876S - 0.719A - 1.571B \\ + 1.767V + 0.469J^+ + 1.663J^- \end{aligned} \quad (12)$$

Abraham<sup>14</sup> suggested that water–ethanol mixtures, such as 40% ethanol (v/v), were reasonable models for partition into polar areas of the blood–brain barrier, but this was for neutral molecules only. Since then, Abraham and Acree<sup>34</sup> have obtained equations for the partition of both neutral molecules and ions, so that we can now use such an equation, Eq. 13, as a model for partition into the blood–brain barrier. Then, as before, an equation for diffusion, Eq. 14, can be obtained by subtraction of coefficients.

$$\begin{aligned} \log P(\text{water} - 40\% \text{ ethanol}) \\ = -0.221 + 0.131E - 0.159S + 0.171A \\ - 1.809B + 1.918V - 1.271J^+ + 1.676J^- \end{aligned} \quad (13)$$

$$\begin{aligned} \log D(\text{blood} - \text{brain barrier}) \\ = c - 0.178E - 0.717S - 0.890A + 0.238B \\ - 0.151V + 1.740J^+ - 0.013J^- \end{aligned} \quad (14)$$

The effect of ionization can now be dissected into partition and diffusion, as before, again with respect to neutral molecules as shown in Table 4. Comparison of the two sets of data shows that base cations are particularly retarded on diffusion through the SC. We suggest that diffusion of the base cations is made difficult by the presence of negatively charged groups in the SC. It is known that the intercellular lipid multilayers in the SC, consisting mainly of ceramides, cholesterol, and fatty acids, are the main pathway for most molecules. The ionizable fatty acids impart a negative charge to the intercellular pathway.<sup>35</sup> Hence, when the cations diffuse in highly ordered lipid layers, their movement is retarded under the electrostatic attraction of negatively charged head groups in lipids.

## CONCLUSION

It has been possible to extend the LFER model for human skin permeation of neutral solutes, Eq. 3, to include the permeation of anions and cations. From our experimental  $K_p$  for ionic species, one extra term ( $j^+J^+$ ) was obtained for cations and another extra term ( $j^-J^-$ ) was obtained for anions, leading to Eq. 6. The PSD of this equation is 0.502, which is quite good for a set of 118 compounds including neutral species and ionic species. Neutral acids and bases permeate through human skin faster than their corresponding ionic species, but the ratio of neutral to ionic permeation depends on the actual structures. The skin permeation process cannot be mimicked perfectly by water–phase/artificial membrane partitions, as the latter contains no physicochemical information on lateral diffusion in the SC. The poor permeation of ionic species is mainly due to their slow diffusion across the SC, especially for a number of base cations.

Equation 6 indicates that an increase in volume of a solute by itself will lead to an increase in  $\log K_p$ . This is in line with a number of equations that correlate  $\log K_p$  with  $\log P_{\text{oct}}$  for neutral species, and which yield a positive coefficient for the independent variable  $\log P_{\text{oct}}$ . For example, Buchwald and Bodor<sup>36</sup> give the following equation for 98 compounds,

$$\log K_p(\text{cm/s}) = -6.93 + 0.46 \log P_{\text{oct}} \quad (15)$$

The relationship between  $\log P_{\text{oct}}$  and volume is well known and for 613 compounds is given by Eq. 16,<sup>37</sup>

$$\begin{aligned} \log P_{\text{oct}} = 0.088 + 0.562E - 1.054S + 0.034A \\ - 3.460B + 3.814V \end{aligned} \quad (16)$$

As  $\log K_p$  depends positively on  $\log P_{\text{oct}}$ , and because  $\log P_{\text{oct}}$  depends positively on volume, it is entirely consistent to find that  $\log K_p$  depends positively on volume.

## ACKNOWLEDGMENTS

We are very pleased to acknowledge the helpful discussions of Professor Ulrich Schäfer in Saarland University and of a reviewer.

## REFERENCES

- Geinoz S, Guy RH, Testa B, Carrupt PA. 2004. Quantitative structure–permeation relationships (QSPeRs) to predict skin permeation: A critical evaluation. *Pharm Res* 21(1):83–92.
- Abraham MH, Acree WE Jr. 2010. The transfer of neutral molecules, ions and ionic species from water to wet octanol. *Phys Chem Chem Phys* 12(40):13182–13188.
- Abraham MH, Zhao YH. 2005. Characterisation of the water/o-nitrophenyl octyl ether system in terms of the

- partition of nonelectrolytes and of ions. *Phys Chem Chem Phys* 7(12):2418–2422.
4. Abraham MH. 2003. The determination of air/water partition coefficients for alkyl carboxylic acids by a new indirect method. *J Environ Monit* 5(5):747–752.
  5. Abraham MH, Acree WE Jr. 2005. Characterisation of the water–isopropyl myristate system. *Int J Pharm* 294(1–2): 121–128.
  6. Sprunger L, Blake-Taylor BH, Wairegi A, Acree WE Jr., Abraham MH. 2007. Characterization of the retention behavior of organic and pharmaceutical drug molecules on an immobilized artificial membrane column with the Abraham model. *J Chromatogr A* 1160(1–2):235–245.
  7. Wang Y, Sun J, Liu H, Liu J, Zhang L, Liu K, He Z. 2009. Predicting skin permeability using liposome electrokinetic chromatography. *Analyst* 134(2):267–272.
  8. Gil-Agusti M, Esteve-Romero J, Abraham MH. 2006. Solute–solvent interactions in micellar liquid chromatography: Characterization of hybrid micellar systems of sodium dodecyl sulfate–pentanol. *J Chromatogr A* 1117(1):47–55.
  9. Burns ST, Agbodjan AA, Khaledi MG. 2002. Characterization of solvation properties of lipid bilayer membranes in liposome electrokinetic chromatography. *J Chromatogr A* 973(1–2):167–176.
  10. Zhao YH, Le J, Abraham MH, Hersey A, Eddershaw PJ, Luscombe CN, Butina D, Beck G, Sherborne B, Cooper I, Platts JA. 2001. Evaluation of human intestinal absorption data and subsequent derivation of a quantitative structure–activity relationship (QSAR) with the Abraham descriptors. *J Pharm Sci* 90(6):749–784.
  11. Abraham MH, Martins F. 2004. Human skin permeation and partition: General linear free-energy relationship analyses. *J Pharm Sci* 93(6):1508–1523.
  12. Zhao YH, Abraham MH, Hersey A, Luscombe CN. 2003. Quantitative relationship between rat intestinal absorption and Abraham descriptors. *Eur J Med Chem* 38(11–12):939–947.
  13. Abraham MH, Acree WE Jr. 2010. Equations for the transfer of neutral molecules and ionic species from water to organic phases. *J Org Chem* 75(4):1006–1015.
  14. Abraham MH. 2011. The permeation of neutral molecules, ions, and ionic species through membranes: Brain permeation as an example. *J Pharm Sci* 100(5):1690–1701.
  15. Abraham MH, Acree WE Jr. 2010. The transfer of neutral molecules, ions and ionic species from water to ethylene glycol and to propylene carbonate; descriptors for pyridinium cations. *New J Chem* 34(10):2298–2305.
  16. Zhang K, Chen M, Scriba GK, Abraham MH, Fahr A, Liu X. 2011. Linear free energy relationship analysis of retention factors in cerasome electrokinetic chromatography intended for predicting drug skin permeation. *J Pharm Sci* 100(8):3105–3113.
  17. Meindl WR, Von Angerer E, Schoenenberger H, Ruckdeschel G. 1984. Benzylamines: Synthesis and evaluation of antimycobacterial properties. *J Med Chem* 27(9):1111–1118.
  18. Singh P, Roberts MS. 1994. Skin permeability and local tissue concentrations of nonsteroidal anti-inflammatory drugs after topical application. *J Pharmacol Exp Ther* 268(1):144–151.
  19. Hirvonen J, Rytting JH, Paronen P, Urtti A. 1991. Dodecyl N,N-dimethylamino acetate and azone enhance drug penetration across human, snake, and rabbit skin. *Pharm Res* 8(7):933–937.
  20. Roberts MS, Anderson RA, Swarbrick J. 1977. Permeability of human epidermis to phenolic compounds. *J Pharm Pharmacol* 29(11):677–683.
  21. Bronaugh RL, Congdon ER. 1984. Percutaneous absorption of hair dyes: Correlation with partition coefficients. *J Invest Dermatol* 83(2):124–127.
  22. Gwak HS, Choi JS, Choi HK. 2005. Enhanced bioavailability of piroxicam via salt formation with ethanolamines. *Int J Pharm* 297(1–2):156–161.
  23. Roy SD, Flynn GL. 1990. Transdermal delivery of narcotic analgesics: pH, anatomical, and subject influences on cutaneous permeability of fentanyl and sufentanil. *Pharm Res* 7(8):842–847.
  24. Kasting GB, Bowman LA. 1990. DC electrical properties of frozen, excised human skin. *Pharm Res* 7(2):134–143.
  25. Peck KD, Ghanem AH, Higuchi WI. 1995. The effect of temperature upon the permeation of polar and ionic solutes through human epidermal membrane. *J Pharm Sci* 84(8):975–982.
  26. Cruciani G, Baroni M, Clementi S, Costantino G, Riganelli D, Skagerberg B. 1992. Predictive ability of regression-models.1. Standard-deviation of prediction errors (Sdep). *J Chemometr* 6(6):335–346.
  27. Hawkins DM. 2004. The problem of overfitting. *J Chem Inf Comput Sci* 44(1):1–12.
  28. Johnson ME, Blankschtein D, Langer R. 1997. Evaluation of solute permeation through the stratum corneum: Lateral bilayer diffusion as the primary transport mechanism. *J Pharm Sci-U.S.* 86(10):1162–1172.
  29. Burns ST, Khaledi MG. 2002. Rapid determination of liposome–water partition coefficients (K<sub>lw</sub>) using liposome electrokinetic chromatography (LEKC). *J Pharm Sci* 91(7):1601–1612.
  30. Wang TF, Kasting GB, Nitsche JM. 2006. A multiphase microscopic diffusion model for stratum corneum permeability. I. Formulation, solution, and illustrative results for representative compounds. *J Pharm Sci* 95(3):620–648.
  31. Hills EE, Abraham MH, Hersey A, Bevan CD. 2011. Diffusion coefficients in ethanol and in water at 298 K: Linear free energy relationships. *Fluid Phase Equilib* 303(1):45–55.
  32. Mitragotri S. 2003. Modeling skin permeability to hydrophilic and hydrophobic solutes based on four permeation pathways. *J Control Release* 86(1):69–92.
  33. Mitragotri S, Johnson ME, Blankschtein D, Langer R. 1999. An analysis of the size selectivity of solute partitioning, diffusion, and permeation across lipid bilayers. *Biophys J* 77(3):1268–1283.
  34. Abraham MH, Acree WE Jr. Equations for the partition of neutral molecules, ions and ionic species from water to water–ethanol mixtures. *J Soln Chem* (in press).
  35. Michniak BB, Meidan V, Al-Khalili M, Wertz PW. 2005. Skin: Physiology and penetration pathways. In *Delivery system handbook for personal care and cosmetic products: Technology, applications, and formulations*; Rosen MR, Ed. Norwich: William Andrew, pp 78–95.
  36. Buchwald P, Bodor N. 2001. A simple, predictive, structure-based skin permeability model. *J Pharm Pharmacol* 53(8):1087–1098.
  37. Abraham MH, Chadha HS, Whiting GS, Mitchell RC. 1994. Hydrogen bonding. 32. An analysis of water–octanol and water–alkane partitioning and the delta log P parameter of Seiler. *J Pharm Sci* 83(8):1085–1100.

### **3.3 Publication 3**

#### **Comparison of Lipid Membrane-Water Partitions with Various Organic Solvent-Water Partitions of Neutral Species and Ionic Species**

*Keda Zhang, Kewei Yang, Gerhard K. E. Scriba, Michael H. Abraham, Alfred Fahr, Xiangli Liu*

Journal of Pharmaceutical Sciences, being revised.

**The built PDF after submission was shown in the dissertation: 46 ~ 67 (22 pages)**



**Comparison of Lipid Membrane-Water Partitions with  
Various Organic Solvent-Water Partitions of Neutral Species  
and Ionic Species**

Journal:	<i>Journal of Pharmaceutical Sciences</i>
Manuscript ID:	12-574
Wiley - Manuscript type:	Research Article
Date Submitted by the Author:	01-Jul-2012
Complete List of Authors:	Zhang, Keda; Friedrich-Schiller-Universität Jena, Department of Pharmaceutical Technology Yang, Kewei; Friedrich-Schiller-Universität Jena, Department of Pharmaceutical Technology Scriba, Gerhard; University of Jena, Pharmaceutical Chemistry; Abraham, Michael; University College London, Chemistry Fahr, Alfred; Friedrich – Schiller University of Jena, Pharmaceutical Technology Liu, Xiangli; Friedrich-Schiller-Universität Jena, Department of Pharmaceutical Technology
Keywords:	Liposomes, Log P, Physicochemical properties, QSPR, Permeability

SCHOLARONE™  
Manuscripts

1  
2  
3  
4  
5 **Comparison of Lipid Membrane-Water Partitions with Various**  
6 **Organic Solvent-Water Partitions of Neutral Species and Ionic**  
7 **Species**  
8  
9

10  
11 Keda Zhang<sup>1</sup>, Kewei Yang<sup>1</sup>, Gerhard K. E. Scriba<sup>2</sup>, Michael H. Abraham<sup>3\*</sup>,

12  
13  
14 Alfred Fahr<sup>1</sup>, Xiangli Liu<sup>1\*</sup>  
15  
16

17  
18  
19 **Running heads:** Comparison of Membrane-water and Solvent-Water Partitioning Systems of  
20  
21 Neutral and Ionic Species  
22  
23

24  
25 <sup>1</sup> Department of Pharmaceutical Technology, Friedrich-Schiller-Universität Jena, 07743 Jena,  
26 Germany  
27

28 <sup>2</sup> Department of Pharmaceutical Chemistry, Friedrich-Schiller-Universität Jena, 07743 Jena,  
29 Germany  
30

31 <sup>3</sup> Department of Chemistry, University College London, London WC1H 0AJ, UK  
32  
33

34  
35 \*Corresponding authors:

36 Xiangli Liu

37 (Telephone: 49-3641-949903; Fax: 49-3641-949902; E-mail: [Xiangli.Liu@uni-jena.de](mailto:Xiangli.Liu@uni-jena.de))  
38

39 Michael H. Abraham  
40

41 (Telephone: 44-20-7679-4639; Fax: 44-20-7679-7463; E-mail: [m.h.abraham@ucl.ac.uk](mailto:m.h.abraham@ucl.ac.uk))  
42  
43  
44  
45  
46  
47  
48  
49  
50  
51  
52  
53  
54  
55  
56  
57  
58  
59  
60

## Abstract

Lipid membrane-water partitions (e.g., immobilized artificial membrane systems where the lipid membrane is a phospholipid monolayer bound to gel beads), were compared to various organic solvent-water partitions using linear free energy relationships. The results show that lipid membranes exhibit a considerably different chemical environment from those of organic solvents. For both neutral species and ionic species, partitions into the more polar hydroxylic solvents are chemically closer to partition into the lipid membrane as compared to partitions into the less polar hydroxylic solvents and into aprotic solvents. This means that solutes partition into the polar parts of lipid membranes, regardless of whether they are charged or not. In addition, cerasome (i.e., liposome composed mainly of stratum corneum lipids) was compared with regular phospholipid liposomes as a possible model for human stratum corneum in partitions. It was found that the cerasome-water partition exhibits a better chemical similarity to skin permeation. This is probably due to the unique structures of ceramides that occur in cerasome and in the stratum corneum lipid domain.

**KEY WORDS:** log P; liposomes; IAM; LEKC; physicochemical properties; LFER; QSPR; ionic species; partition; permeability

## Introduction

The *n*-octanol-water partition coefficient (as  $\log P_{\text{oct}}$ ) is widely used as an estimate for partitions of chemicals into biological membranes, but it is now recognized that biological membranes vary so much in character that it is impossible for any given solvent-water system to be a useful model for all membranes.<sup>1</sup> In addition, recent work on ionic partition into biological membranes suggests that the *n*-octanol-water system is not satisfactory as a model for ionic partition.<sup>2,3</sup> Consequently, the liposome-water partitioning system has been developed as a promising model for biological partition process because of the highly-ordered lipid bilayer microstructure of liposome. Workers have observed that ionic species partition significantly better into liposome than into *n*-octanol,<sup>4-8</sup> while the partition coefficients of neutral species were found to be comparable but not equal in liposome-water and *n*-octanol-water systems.<sup>6,7</sup> Recently, Zhang et al.<sup>9</sup> demonstrated that cerasome (i.e., liposome consisting mainly of stratum corneum (SC) lipids)-water system is chemically rather different from various organic solvent-water systems, using linear free energy relationships (LFERs) as a method of analysis. It was further shown that the cerasome-water partition is a reasonable chemical model for the SC-water partition, although this conclusion was deduced for neutral species only.<sup>10</sup>

Even so, it is of considerable interest to compare neutral liposomes with organic solvents, which are neutral, on solute interactions from a physicochemical point of view, given that cerasome is negatively charged. So far, there has been no easy-to-use way to measure a large number of neutral liposome-water partition parameters of neutral and ionic species, which are required for a rigorous physicochemical analysis. The current techniques used to characterize lipid membrane-water partitions and their advantages and disadvantages are summarized in Table 1. The use of immobilized artificial membranes (IAMs) is a rapid reliable method to characterize neutral lipid membrane-water partitions for both neutral and ionic species.

1  
2  
3 However, immobilized lipid monolayers in IAM are known to differ from lipid bilayers in  
4 liposomes in terms of the lateral mobility of lipids and the density of the polar phospholipid  
5 head-groups.<sup>11,12</sup>  
6  
7

8  
9 The focus of this work is to compare the physicochemical nature of neutral IAM systems  
10 and liposome-water partitions with organic solvent-water partitions using LFERs, as well as  
11 some biological membrane systems, for which the ionic LFER equations are available. In  
12 addition, we also investigated what the crucial difference is between lipid monolayers in IAM  
13 and lipid bilayers in liposomes as regards interactions with solutes. Recently, Liu et al.<sup>13</sup> have  
14 already measured a large number of neutral and charged compounds in a IAM system, where  
15 phosphatidylcholines (PC) were immobilized to gel beads. In the present work, we measured  
16 the partitions of most of these compounds in liposomes made up of 3-*sn*-phosphatidylcholine  
17 (POPC) and 3-*sn*-Phosphatidyl-L-serine (PS) (80:20, mol/mol), using liposome electrokinetic  
18 chromatography (LEKC). We made use of these data to achieve the above aim.  
19  
20  
21  
22  
23  
24  
25  
26  
27  
28  
29  
30  
31  
32

## 33 **Materials and Methods**

### 34 **Chemicals**

35  
36 A series of (4-methylbenzyl)alkylamines were synthesized according to known  
37 procedures.<sup>14</sup> The other compounds in Table 2 were purchased from Sigma-Aldrich  
38 (Steinheim, Germany), together with 3-*sn*-phosphatidylcholine (from synthetic) and 3-*sn*-  
39 phosphatidyl-L-serine (from bovine brain). Decanophenone was obtained from Alfa Aesar  
40 (Karlsruhe, Germany). Methanol and chloroform were purchased from Carl Roth (Karlsruhe,  
41 Germany).  
42  
43  
44  
45  
46  
47  
48  
49  
50

### 51 **Liposome Preparation**

52  
53 All liposomes were prepared once by the extrusion method. Briefly, the desired amounts  
54 of POPC and PS (80:20, mol/mol) were dissolved in chloroform/methanol mixture (9:1, v/v)  
55  
56  
57  
58  
59  
60



1  
2  
3 in a 1L round bottom flask. A thin lipid film was formed by removing organic solvents under  
4  
5 vacuum at 45°C with a rotary evaporator. The resulting film was hydrated and dispersed in  
6  
7 100 ml 10 mM phosphate buffer pH 7.4 by continuous shaking for 60 min at 45°C to yield  
8  
9 multilamellar vesicles (MLVs) with a lipid concentration of 3 mM. Then the MLVs were  
10  
11 extruded through a polycarbonate filter (100 nm pore size; Poretics, Livermore, USA) 20  
12  
13 times at room temperature using a LiposoFast LF-50 (Avestin, Ottawa, Canada) under an  
14  
15 external pressure of 3.5 bar. The final product was a homogeneous liposome dispersion of  
16  
17 large unilamellar vesicles (LUVs), for which the average particle size and zeta potential were  
18  
19 79.4 ( $\pm 0.5$ ) nm with a polydispersity index of 0.084 and -27.1 ( $\pm 1.0$ ) mV, respectively,  
20  
21 measured using a Zetasizer Nano ZS (Malvern, Herrenberg, Germany). The liposome  
22  
23 dispersion was very stable for at least two months at 4°C (unreported data), and thus used in  
24  
25 the whole work.  
26  
27  
28

### 30 LEKC

31  
32  
33 The LEKC experiments were carried out using a HPCE 1600AX (Agilent, Waldbronn,  
34  
35 Germany) equipped with a diode array detector (DAD). 58.5/50 cm uncoated fused-silica  
36  
37 capillaries of 50  $\mu\text{m}$  id and 375  $\mu\text{m}$  od (BGB Analytic, Schloßböckelheim, Germany) were  
38  
39 employed throughout this study. A new capillary was rinsed with 1.0 M aqueous sodium  
40  
41 hydroxide for 20 min, water for 5 min, 1.0 M hydrochloride acid for 20 min and water for  
42  
43 5min. The samples were analyzed at +20 kV, with a hydrodynamic injection at 50 mbar for  
44  
45 3s. The capillary was kept at 37°C and the detection wavelengths were set at 210 nm, 225 nm,  
46  
47 and 245 nm. The LEKC procedures were performed and the retention factors of neutral and  
48  
49 charged solutes were separately calculated, as described in our previous work.<sup>9</sup>  
50  
51  
52

### 53 LEFR

54  
55  
56 An LEFR equation proposed by Abraham<sup>15</sup> has been successfully used to characterize  
57  
58 numerous equilibrium systems, including *in vivo* and *in vitro* partition processes and transport  
59  
60

1  
2  
3 processes, and to predict the corresponding equilibrium coefficients, including partition  
4 coefficients (e. g.  $\log P_{\text{oct}}$  or  $\log P_{\text{lip}}$ ) and rate coefficients (e. g. skin permeability  $\log K_p$ ), see  
5  
6  
7 Eq. (1):  
8

$$9 \quad SP = c + eE + sS + aA + bB + vV \quad (1)$$

10  
11  
12 SP represents an equilibrium coefficient, such as  $\log P$ , for a series of solutes in a given  
13 system. The independent variables are physicochemical properties or descriptors of the  
14 solutes as follows: E is the excess molar refraction in  $(\text{cm}^3\text{mol}^{-1})/10$ , S is the solute  
15 dipolarity/polarizability, A and B are the overall hydrogen bond acidity and basicity,  
16 respectively, and V is the McGowan characteristic molecular volume in  $(\text{cm}^3\text{mol}^{-1})/100$ . Eq.  
17  
18 (1) was set up for processes involving neutral species only. Abraham and Acree<sup>16-19</sup> found  
19 that in order to apply Eq. (1) to ionic species it was necessary to introduce a new descriptor  
20 for cations,  $J^+$ , and a new descriptor for anions,  $J^-$ , leading to Eq. (2):  
21  
22  
23  
24  
25  
26  
27  
28  
29

$$30 \quad SP = c + eE + sS + aA + bB + vV + j^+J^+ + j^-J^- \quad (2)$$

31  
32  
33 Note that  $J^+$  is zero for anions,  $J^-$  is zero for cations, and both are zero for neutral species,  
34 in which case Eq. (2) reverts to Eq. (1). All the solute descriptors can be calculated or  
35 estimated as detailed previously.<sup>3,16,18,19</sup> The descriptors for ions and ionic species are on the  
36 same scales as those for neutral molecules, so that Eq. (2) can include ions, ionic species and  
37 neutral molecules. Some values of the descriptors used in Eq. (2) are shown in Table 2. The  
38 coefficients in Eq. (2), that is, c, e, s, a, b, v,  $j^+$  and  $j^-$  are obtained by multiple linear  
39 regression (MLR). They are not just fitting coefficients, but serve to characterize the given  
40 system.  
41  
42  
43  
44  
45  
46  
47  
48  
49  
50  
51

## 52 Results and Discussion

53  
54  
55 A set of 35 compounds (including neutral and ionic species) was analyzed by LEKC,  
56 where the liposome vesicles consist of neutral POPC and negatively charged PS. The  
57  
58  
59  
60

1  
2  
3 retention factors ( $\log k_{LEKC}$ ) for these compounds are given in Table 2.  $\log k_{LEKC}$  acts as a  
4  
5 partition index for the lipid membrane-water partition since  $k_{LEKC}$  is proportional to the  
6  
7 corresponding partition coefficient, as is the case for other retention factors and capacity  
8  
9 factors, below. Liu et al.<sup>20</sup> have reported capacity factors ( $\log K_s$ ) for 22 fully ionized solutes  
10  
11 in ILC, where unilamellar liposome vesicles composed of egg phosphatidylcholines (PC)  
12  
13 were immobilized to gel beads. The values of  $\log K_s$  for the solutes present in both databases  
14  
15 can be used to compare interactions of ionic species with charged liposomes and neutral  
16  
17 liposomes. A plot of  $\log k_{LEKC}$  versus  $\log K_s$  for ionic species is shown in Fig. 1. It is clear  
18  
19 that the data points for cations and anions scatter over two almost parallel lines, with the line  
20  
21 for the cations about two log units higher than the line for the anions. This is in agreement  
22  
23 with a previous observation that electrostatic interaction influences the partition of ionic  
24  
25 species into liposomes.<sup>21</sup> The inclusion of negatively charged PS head-groups enhances the  
26  
27 interaction with positively charged solutes and weakens the interaction with negatively  
28  
29 charged solutes. Such electrostatic interactions exist in neutral phospholipid (e.g., PC)  
30  
31 membrane as well.<sup>6</sup>

32  
33  
34  
35  
36 The capacity factors ( $\log k_{IAM}$ ) of a number of compounds were measured by Liu et al.<sup>13</sup>  
37  
38 on an IAM.PC.DD2 column at pH 7.0, of which some are shown in Table 2. Liu et al.<sup>13</sup>  
39  
40 showed that a plot of  $\log K_s$  against  $\log k_{IAM}$  for 22 charged solutes resulted in two parallel  
41  
42 lines, depending on the solute charge.<sup>20</sup> This was attributed to the different densities of the  
43  
44 phospholipid head-groups of lipid membranes in the two systems. In contrast with  $\log k_{LEKC}$ ,  
45  
46  $\log k_{IAM}$  exhibits a strikingly closer relationship with  $\log K_s$ . It is expected that neutral  
47  
48 membranes in IAM and ILC bring about no markedly different electrostatic interaction with  
49  
50 ionic species. This also indicates that the effect of the charge of phospholipid head-groups is  
51  
52 much greater than the effect of their density on ionic partition.  
53  
54  
55

56  
57 A plot of  $\log k_{LEKC}$  versus  $\log k_{IAM}$ , for the compounds in Table 2 except ibuprofen  
58  
59 (anion) where we have no experimental value of  $\log k_{IAM}$ , results in an overall poor  
60

1  
2  
3 correlation, see Fig. 2. This is as might be expected. Cations partition better and anions  
4  
5 partition worse into negatively charged phospholipids than into neutral phospholipids,  
6  
7 whereas the partitions of neutral species hardly vary with the charge of the phospholipids. As  
8  
9 a result, the data points for neutral species locate below those for cations and above those for  
10  
11 anions, see Fig. 2. This result reflects the importance of electrostatic interaction in the lipid  
12  
13 membrane-water partitions of ionic species. Note that the incorporation of PS leads to a  
14  
15 negligible change on the partitions of neutral species into PC liposomes, as seen from the  
16  
17 work of Österberg et al.<sup>21</sup>

20  
21 To compare the IAM system with organic solvent-water systems, we applied Eq. (2) to  
22  
23 all 49 compounds studied by Liu et al.,<sup>13</sup> including 21 neutral solutes and 28 ionized solutes.  
24  
25 The resulting equation is given as Eq. (3).

$$\begin{aligned} \log k_{IAM} = & -0.736 (\pm 0.336) + 0.398 (\pm 0.279) E - 0.509 (\pm 0.256) S - 0.059 (\pm 0.498) A \\ & - 2.630 (\pm 0.460) B + 2.948 (\pm 0.406) V - 0.822 (\pm 0.586) J^+ + 2.854 (\pm 0.520) J^- \quad (3) \\ N = & 49, R^2 = 0.906, SD = 0.316, F = 55 \end{aligned}$$

33  
34 In this and the following equations, 95% confidence limits are given in parentheses; N is  
35  
36 the number of compounds or data points;  $R^2$  is the squared correlation coefficient; SD is the  
37  
38 standard deviation, and F is the F-statistic. A similar analysis of the LEKC system for all 36  
39  
40 compounds leads to Eq. (4).

$$\begin{aligned} \log k_{LEKC} = & -1.768 (\pm 0.401) + 0.535 (\pm 0.442) E - 0.775 (\pm 0.240) S - 0.199 (\pm 0.344) A \\ & - 2.424 (\pm 0.605) B + 2.640 (\pm 0.455) V + 0.094 (\pm 0.489) J^+ + 2.688 (\pm 0.663) J^- \quad (4) \\ N = & 36, R^2 = 0.923, SD = 0.319, F = 48 \end{aligned}$$

47  
48 Abraham and Acree<sup>1</sup> have shown, for neutral compounds only, that permeation through  
49  
50 membranes is very varied, and that no one solvent-water partitioning system can be used as a  
51  
52 general model for all membranes. We can now compare membrane systems and solvent-  
53  
54 water systems using equations that include not just neutral compounds but ionic species as  
55  
56 well. We use a similar method to that of Abraham and Acree<sup>1</sup> in which a principal component  
57  
58

1  
2  
3 analysis, PCA, is carried out on the seven coefficients in Eq. (2),  $e$ ,  $s$ ,  $a$ ,  $b$ ,  $v$ ,  $j^+$  and  $j^-$ , that  
4 characterize the given systems. The coefficients of the systems compared are given in Table 3;  
5 systems # 1-6 are the membrane systems and systems # 7-32 are various solvent-water  
6 partitioning systems. In the present case, the first two principal components (PCs) account for  
7 74% of the total variance in the dataset. A plot of the scores of the second PC versus the first  
8 PC reveals how chemically close the systems are in terms of the distance between points in  
9 the two dimensional plot, see Fig. 3.  
10  
11  
12  
13  
14  
15  
16  
17

18 The points for the aprotic solvents, # 21- 31, cluster together and are far away from all the  
19 membrane systems. Wet octanol, # 17, is also far away from the membrane systems, so that  
20 its use as a membrane model is highly questionable. The very polar ethanol-water mixtures, #  
21 12 and # 13 are very good models for human skin permeation (# 1), and the slightly less polar  
22 mixtures, # 14 and # 15 are reasonable models for partition into cerasome (# 2) and for  
23 permeation from saline through the blood-brain barrier (# 4). The ethanol-water mixtures #  
24 10 and # 11 are not quite as polar as # 14 and # 15, but are reasonable models for the LEKC  
25 and the IAM systems, # 5 and # 6, as is also the ethylene glycol-water system (# 32).  
26 Abraham and Acree<sup>1</sup> have obtained similar results for neutral compounds, so that we can now  
27 suggest that both neutral compounds and ionic species partition into the polar parts of lipid  
28 membrane. However on the whole, there is no “ideal” solvent that can be used as a general  
29 model for lipid membranes.  
30  
31  
32  
33  
34  
35  
36  
37  
38  
39  
40  
41  
42  
43  
44

45 Zhang et al.<sup>9</sup> have set up an equation for the cerasome electrokinetic chromatography  
46 (EKC) in order to estimate SC-water partition (Table 3). From Fig. 3, it can be seen that the  
47 point for the cerasome-water partition (# 2) is closer to the point for permeation through the  
48 SC (# 1) than are the points for other lipid membrane-water partitions. A quantitative  
49 assessment can be carried out by calculating the actual seven-dimensional distances,  
50  $D(\text{PCA})_7$ , between points from the scores for PC1-PC7, as given in Table 3. These show that  
51 the cerasome point (# 2) is quite near to that for permeation through the SC (# 1) and that  
52  
53  
54  
55  
56  
57  
58  
59  
60

1  
2  
3 cerasome owns a better chemical similarity than the membrane systems (# 5 and # 6).  
4  
5 Cerasome is a unique liposome whose roles in modeling the SC cannot be replaced by regular  
6  
7 phospholipid liposomes in partitions. This is probably due to the unusual structures of  
8  
9 ceramides, the major type of lipids found in the SC. Ceramides consist of derivatives of  
10  
11 sphingosines bases linked to a variety of fatty acids via amide bonds. Clearly, the polar head-  
12  
13 groups in ceramides act as both acceptors and donors of hydrogen bonds by the hydroxyl and  
14  
15 amino groups as compared to those in phospholipids, which act only as acceptors of  
16  
17 hydrogen bonds.<sup>24</sup> Ceramides therefore should generate strong hydrogen bonding with  
18  
19 solutes that are hydrogen bond bases. Furthermore, the aliphatic chains in ceramides are  
20  
21 mostly long-chain and saturated, and hence lead to high phase transition temperatures.  
22  
23 Ceramides are thus mostly in a solid crystalline or gel state at physiological temperature,  
24  
25 which exhibits lower partition coefficients than the state of liquid crystalline membranes  
26  
27 present at higher temperatures.<sup>25,26</sup>  
28  
29  
30  
31

## 32 Conclusion

33  
34  
35 In this study, lipid membrane-water partitions were compared to various organic  
36  
37 solvent-water partitions for both neutral and ionic species. It was found that partition into  
38  
39 lipid membranes is chemically markedly different from partitions into organic solvents,  
40  
41 although partitions into aqueous ethanol can provide useful models for membrane partition.  
42  
43 Although the lipid membrane studied is actually the lipid monolayer bound to gel beads in  
44  
45 IAM, there are only small differences between such lipid monolayers and lipid bilayers in  
46  
47 liposome caused by the different densities of the phospholipid head-groups. In addition, our  
48  
49 results suggest that solutes, no matter whether they are charged or not, partition into the polar  
50  
51 parts of lipid membranes. Cerasome was compared with regular phospholipid liposomes as a  
52  
53 possible model for the SC in partitions. The results show that cerasome differs considerably  
54  
55 from phospholipid liposomes, and provides a better chemical correlation with skin  
56  
57  
58  
59  
60

1  
2  
3 permeation, probably due to the unique structure of ceramides that are present in both  
4  
5 cerasome and the SC lipid domain.  
6  
7  
8

## 9 10 **References**

- 11  
12 1. Abraham MH, Acree WE, Jr. 2012. Linear free energy relationships for  
13 water/hexadec-1-ene and water/deca-1,9-diene partitions, and for permeation through lipid  
14 bilayers; comparison of permeation systems. submitted.  
15  
16
- 17  
18 2. Abraham MH, Austin RP. 2012. The effect of ionized species on microsomal binding.  
19 Eur J Med Chem 47(1):202-205.  
20  
21
- 22  
23 3. Abraham MH. 2011. The permeation of neutral molecules, ions, and ionic species  
24 through membranes: brain permeation as an example. J Pharm Sci 100(5):1690-1701.  
25  
26
- 27  
28 4. Austin RP, Davis AM, Manners CN. 1995. Partitioning of ionizing molecules  
29 between aqueous buffers and phospholipid vesicles. J Pharm Sci 84(10):1180-1183.  
30  
31
- 32  
33 5. Mason RP, Rhodes DG, Herbette LG. 1991. Reevaluating equilibrium and kinetic  
34 binding parameters for lipophilic drugs based on a structural model for drug interaction with  
35 biological membranes. J Med Chem 34(3):869-877.  
36  
37
- 38  
39 6. Avdeef A, Box KJ, Comer JE, Hibbert C, Tam KY. 1998. pH-metric logP 10.  
40 Determination of liposomal membrane-water partition coefficients of ionizable drugs. Pharm  
41 Res 15(2):209-215.  
42  
43
- 44  
45 7. Fruttero R, Caron G, Fornatto E, Boschi D, Ermondi G, Gasco A, Carrupt PA, Testa  
46 B. 1998. Mechanisms of liposomes/water partitioning of (p-methylbenzyl)alkylamines.  
47 Pharm Res 15(9):1407-1413.  
48  
49
- 50  
51 8. Balon K, Riebesehl BU, Muller BW. 1999. Drug liposome partitioning as a tool for  
52 the prediction of human passive intestinal absorption. Pharm Res 16(6):882-888.  
53  
54  
55  
56  
57  
58  
59  
60

- 1  
2  
3 9. Zhang K, Chen M, Scriba GK, Abraham MH, Fahr A, Liu X. 2011. Linear free  
4 free energy relationship analysis of retention factors in cerasome electrokinetic chromatography  
5 intended for predicting drug skin permeation. *J Pharm Sci* 100(8):3105-3113.  
6  
7
- 8  
9  
10 10. Zhang K, Chen M, Scriba GK, Abraham MH, Fahr A, Liu X. 2012. Human skin  
11 permeation of neutral species and ionic species: extended linear free-energy relationship  
12 analyses. *J Pharm Sci* 101(6):2034-2044.  
13  
14
- 15  
16 11. Ong S, Liu H, Pidgeon C. 1996. Immobilized-artificial-membrane chromatography:  
17 measurements of membrane partition coefficient and predicting drug membrane permeability.  
18 *J Chromatogr A* 728(1-2):113-128.  
19  
20
- 21  
22 12. Rand RP, Parsegian VA. 1989. Hydration forces between phospholipid-bilayers.  
23 *Biochim Biophys Acta* 988(3):351-376.  
24  
25
- 26  
27 13. Liu X, Hefesha H, Scriba G, Fahr A. 2008. Retention behavior of neutral and  
28 positively and negatively charged solutes on an immobilized-artificial-membrane (IAM)  
29 stationary phase. *Helv Chim Acta* 91(8):1505-1512.  
30  
31
- 32  
33 14. Meindl WR, Von Angerer E, Schoenenberger H, Ruckdeschel G. 1984. Benzylamines:  
34 synthesis and evaluation of antimycobacterial properties. *J Med Chem* 27(9):1111-1118.  
35  
36
- 37  
38 15. Abraham MH. 1993. Scales of solute hydrogen-bonding - their construction and  
39 application to physicochemical and biochemical processes. *Chem Soc Rev* 22(2):73-83.  
40  
41
- 42  
43 16. Abraham MH, Acree WE, Jr. 2010. The transfer of neutral molecules, ions and ionic  
44 species from water to ethylene glycol and to propylene carbonate; descriptors for pyridinium  
45 cations. *New J Chem* 34(10):2298-2305.  
46  
47
- 48  
49 17. Abraham MH, Acree WE, Jr. 2010. The transfer of neutral molecules, ions and ionic  
50 species from water to wet octanol. *Phys Chem Chem Phys* 12(40):13182-13188.  
51  
52
- 53  
54 18. Abraham MH, Acree WE, Jr. 2010. Equations for the transfer of neutral molecules  
55 and ionic species from water to organic phases. *J Org Chem* 75(4):1006-1015.  
56  
57  
58  
59  
60



- 1  
2  
3 19. Abraham MH, Acree WE, Jr. 2010. Solute descriptors for phenoxide anions and their  
4 use to establish correlations of rates of reaction of anions with iodomethane. *J Org Chem*  
5 75(9):3021-3026.  
6  
7  
8  
9  
10 20. Liu X, Fan P, Chen M, Hefesha H, Scriba G, Gabel D, Fahr A. 2010. Drug-  
11 membrane interaction on immobilized liposome chromatography compared to immobilized  
12 artificial membrane (IAM), liposome/water, and octan-1-ol/water systems. *Helv Chim Acta*  
13 93(2):203-211.  
14  
15  
16  
17  
18 21. Osterberg T, Svensson M, Lundahl P. 2001. Chromatographic retention of drug  
19 molecules on immobilised liposomes prepared from egg phospholipids and from chemically  
20 pure phospholipids. *Eur J Pharm Sci* 12(4):427-439.  
21  
22  
23  
24  
25 22. Abraham MH, Acree WE, Jr. 2012. Equations for the partition of neutral molecules,  
26 ions and ionic species from water to water-ethanol mixtures. *J Soln Chem* 41(4):730-740.  
27  
28  
29 23. Abraham MH, Zhao YH. 2005. Characterisation of the water/o-nitrophenyl octyl  
30 ether system in terms of the partition of nonelectrolytes and of ions. *Phys Chem Chem Phys*  
31 7(12):2418-2422.  
32  
33  
34  
35  
36 24. Moore DJ, Rerek ME, Mendelsohn R. 1997. FTIR spectroscopy studies of the  
37 conformational order and phase behavior of ceramides. *J Phys Chem B* 101(44):8933-8940.  
38  
39  
40 25. Bano M. 2000. Determination of partition coefficient by the change of main phase  
41 transition. *Gen Physiol Biophys* 19(3):279-293.  
42  
43  
44  
45 26. Sarmiento AB, Delima MCP, Oliveira CR. 1993. Partition of dopamine antagonists  
46 into synthetic lipid bilayers - the effect of membrane-structure and composition. *J Pharm*  
47 *Pharmacol* 45(7):601-605.  
48  
49  
50  
51  
52  
53  
54  
55  
56  
57  
58  
59  
60

## Legend to Figures

**Figure 1.** A plot of  $\log k_{\text{LEKC}}$  (POPC<sub>80</sub>/PS<sub>20</sub>) in LEKC versus  $\log K_s$  (egg PC) in ILC: ■ cations (protonated bases), the regression equation:  $y = 0.8699x - 0.6710$ ,  $R^2 = 0.9521$ ; ◆ anions (deprotonated acids), the regression equation:  $y = 0.7228x - 2.362$ ,  $R^2 = 0.9649$ .

**Figure 2.** A plot of  $\log k_{\text{LEKC}}$  (POPC/PS) in LEKC versus  $\log k_{\text{IAM}}$  (IAM.PC.DD2 column) in IAM: ■ cations (protonated bases), the regression equation:  $y = 0.9133x - 0.9529$ ,  $R^2 = 0.9450$ ; ◆ anions (deprotonated acids), the regression equation:  $y = 0.9783x - 2.654$ ,  $R^2 = 0.9606$ ; ● smaller neutral molecules, the regression equation:  $y = 1.001x - 1.412$ ,  $R^2 = 0.9780$ ; ▲ larger neutral molecules (steroids), the regression equation:  $y = 0.9876x - 2.302$ ,  $R^2 = 0.4925$ .

**Figure 3.** A plot of the scores of the second principal component (PC 2) against the first principal component (PC 1); ● membrane systems, ○ solvent-water partitions.

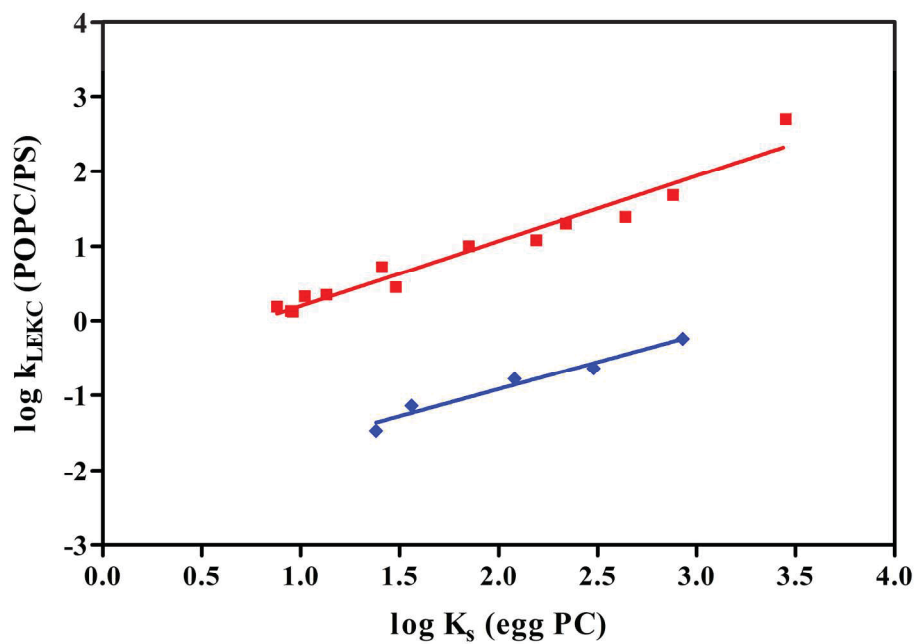


Figure 1. A plot of log k<sub>LEKC</sub> (POPC80/PS20) in LEKC versus log K<sub>s</sub> (egg PC) in ILC: ■ cations (protonated bases), the regression equation:  $y = 0.8699x - 0.6710$ ,  $R^2 = 0.9521$ ; ◆ anions (deprotonated acids), the regression equation:  $y = 0.7228x - 2.362$ ,  $R^2 = 0.9649$ .  
94x66mm (600 x 600 DPI)

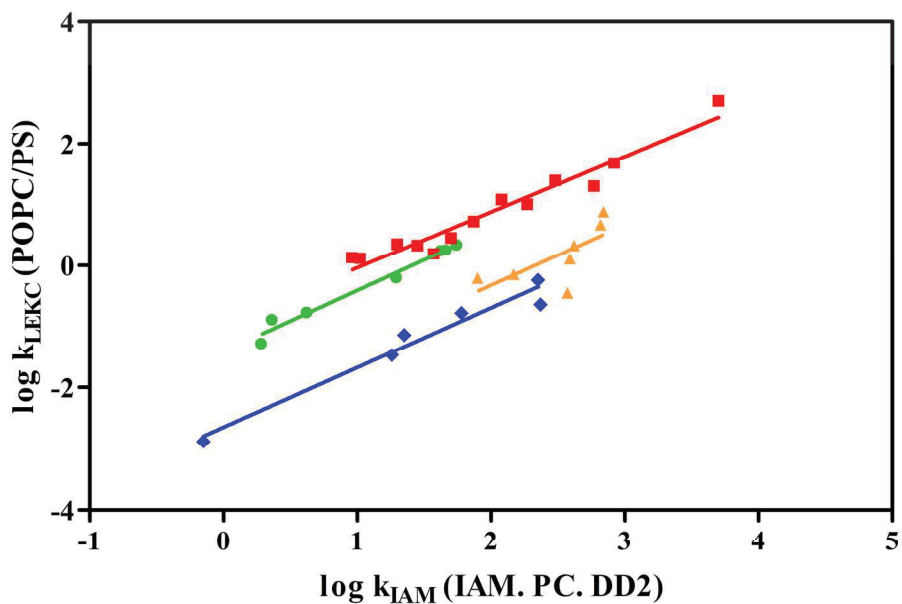


Figure 2. A plot of log k<sub>LEKC</sub> (POPC/PS) in LEKC versus log k<sub>IAM</sub> (IAM. PC. DD2) in IAM: ■ cations (protonated bases), the regression equation:  $y = 0.9133x - 0.9529$ ,  $R^2 = 0.9450$ ; ◆ anions (deprotonated acids), the regression equation:  $y = 0.9783x - 2.654$ ,  $R^2 = 0.9606$ ; ● smaller neutral molecules, the regression equation:  $y = 1.001x - 1.412$ ,  $R^2 = 0.9780$ ; ▲ larger neutral molecules (steroids), the regression equation:  $y = 0.9876x - 2.302$ ,  $R^2 = 0.4925$ .  
89x59mm (600 x 600 DPI)

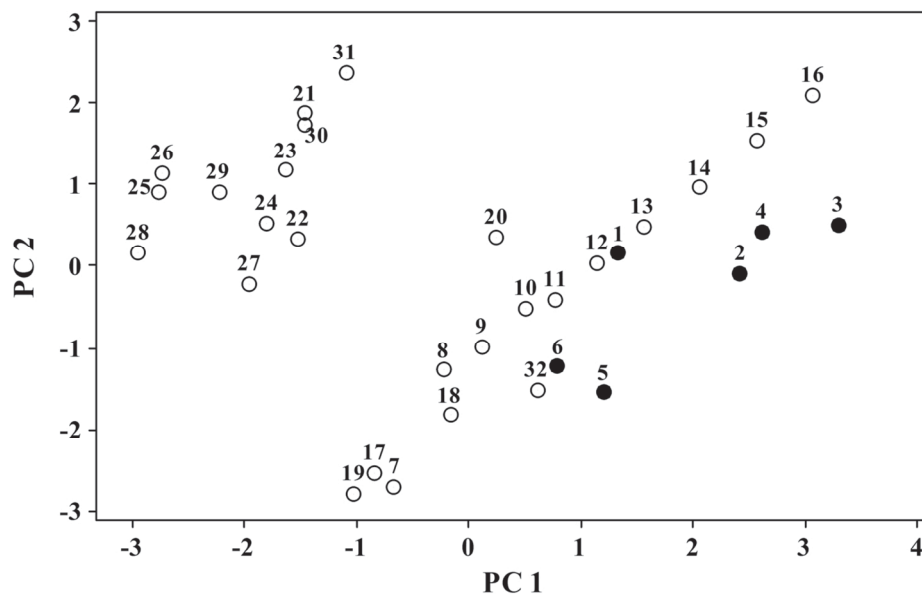


Figure 3. A plot of the scores of the second principal component (PC 2) against the first principal component (PC 1); ● membrane systems, ○ solvent-water partitions.

137x91mm (300 x 300 DPI)

**Table 1.** Current techniques for analyzing the lipids-water partitions and their respective characters

Techniques	Advantages	Disadvantages	Others
Shake Equilibrium	Standard approaches	Time-consuming; tedious; laborious; unwieldy	Traditional techniques (e. g. dialysis method, centrifugation method, ultrafiltration method)
Potentiometric Titration	Relatively higher speed; log $P_{lip}$ values for both ionic and neutral species <sup>a</sup>	Only suitable for ionizable solutes; time-consuming; tedious; laborious	—
Immobilized Artificial Membrane (IAM) Chromatography	Speed; high-reproducibility; small sample amount; low purity requirement	Lipid monolayer with lack of lateral mobility of lipids and density of phospholipid head-groups	Set up on high-performance liquid chromatography (HPLC)
Immobilized Liposome Chromatography (ILC)	Speed, high-reproducibility; small sample amount; low purity requirement	Unstable; irreproducible column preparation; unsuitable for lipophilic solutes (long retention times for many neutral molecules)	Set up on HPLC
Liposome Electrokinetic Chromatography (LEKC)	Speed; high-reproducibility; small sample amount; low purity requirement	Unsuitable for neutral solutes with neutral liposomes used	Set up on capillary electrophoresis (CE)

<sup>a</sup> log  $P_{lip}$  represents the partition coefficient between liposome and water.

**Table 2.** Compounds and species used in this work, their solute descriptors, and the corresponding equilibrium coefficients

NO.	Compounds	E	S	A	B	V	J <sup>+</sup>	J <sup>-</sup>	log P <sub>oct</sub> <sup>a</sup>	log k <sub>LEKC</sub> <sup>b</sup>	log k <sub>IAM</sub> <sup>c</sup>	log K <sub>s</sub> <sup>d</sup>
1	Cortisolone	1.910	3.45	0.36	1.60	2.7389	0.0000	0.0000	2.52	-0.15	2.17	—
2	Corticosterone	1.860	3.43	0.40	1.63	2.7389	0.0000	0.0000	1.94	-0.21	1.90	—
3	Estrone	1.730	2.05	0.50	1.08	2.1558	0.0000	0.0000	3.13	0.67	2.82	—
4	Estriol	1.970	1.74	1.06	1.63	2.2575	0.0000	0.0000	2.54	-0.45	2.57	—
5	17-Hydroxyprogesterone	1.640	3.35	0.25	1.31	2.6802	0.0000	0.0000	3.17	0.33	2.62	—
6	Testosterone	1.540	2.59	0.32	1.19	2.3827	0.0000	0.0000	3.29	0.11	2.59	—
7	Progesterone	1.450	3.29	0.00	1.14	2.6215	0.0000	0.0000	3.87	0.88	2.84	—
8	Aniline	0.955	0.96	0.26	0.41	0.8162	0.0000	0.0000	0.90	-1.01	0.26	—
9	Nitrobenzene	0.871	1.11	0.00	0.28	0.8906	0.0000	0.0000	1.85	-0.60	0.99	—
10	Resorcinol	0.980	1.11	1.09	0.52	0.8338	0.0000	0.0000	0.80	-0.89	0.36	—
11	Benzyl alcohol	0.803	0.87	0.39	0.56	0.9160	0.0000	0.0000	1.10	-1.28	0.28	—
12	Phenol	0.805	0.89	0.60	0.30	0.7751	0.0000	0.0000	1.47	-0.77	0.62	—
13	4-Chlorophenol	0.915	1.08	0.67	0.20	0.8975	0.0000	0.0000	2.39	0.24	1.62	—
14	Styrene	0.849	0.65	0.00	0.16	0.9552	0.0000	0.0000	2.95	0.25	1.66	—
15	Toluene	0.601	0.52	0.00	0.14	0.8573	0.0000	0.0000	2.73	-0.20	1.29	—
16	Ethylbenzene	0.613	0.51	0.00	0.15	0.9982	0.0000	0.0000	3.15	0.34	1.74	—
17	Aspirin, anion	0.931	3.91	0.04	3.03	1.2664	0.0000	2.1227	1.13	-2.99	-0.15	—
18	Flurbiprofen, anion	1.590	4.56	0.07	3.36	1.8174	0.0000	2.5383	3.81	-0.78	1.78	2.08
19	Ketoprofen, anion	1.800	5.49	0.01	3.39	1.9564	0.0000	2.4851	2.77	-1.47	1.26	1.38
20	Naproxen, anion	1.660	5.07	0.02	3.11	1.7606	0.0000	2.4260	3.06	-1.14	1.35	1.56
21	Indomethacin, anion	2.390	5.62	0.10	4.38	2.5084	0.0000	2.9899	4.27	-0.64	2.37	2.48
22	Mefenamic acid, anion	1.800	4.71	0.09	3.14	1.8996	0.0000	2.6427	5.12	-0.24	2.35	2.93
23	Ibuprofen, anion	0.880	3.50	0.08	3.31	1.7556	0.0000	2.4188	3.87	-0.73	—	—
24	4-MeC <sub>6</sub> H <sub>4</sub> CH <sub>2</sub> NHMe, cation	0.650	2.58	1.42	0.00	1.2604	1.2835	0.0000	1.96	0.13	0.96	0.95
25	4-MeC <sub>6</sub> H <sub>4</sub> CH <sub>2</sub> NHEt, cation	0.640	2.66	1.44	0.00	1.4013	1.2994	0.0000	2.38	0.12	1.02	0.96
26	4-MeC <sub>6</sub> H <sub>4</sub> CH <sub>2</sub> NHPr, cation	0.630	2.63	1.37	0.00	1.5422	1.3290	0.0000	2.96	0.35	1.30	1.13
27	4-MeC <sub>6</sub> H <sub>4</sub> CH <sub>2</sub> NHBu, cation	0.620	2.62	1.34	0.00	1.6831	1.3349	0.0000	3.49	0.72	1.87	1.41
28	4-MeC <sub>6</sub> H <sub>4</sub> CH <sub>2</sub> NH(CH <sub>2</sub> ) <sub>4</sub> Me, cation	0.610	2.60	1.34	0.00	1.8240	1.3136	0.0000	4.26	1.00	2.27	1.85
29	4-MeC <sub>6</sub> H <sub>4</sub> CH <sub>2</sub> NH(CH <sub>2</sub> ) <sub>5</sub> Me, cation	0.600	2.60	1.36	0.00	1.9649	1.2956	0.0000	4.96	1.30	2.77	2.34
30	4-MeC <sub>6</sub> H <sub>4</sub> CH <sub>2</sub> NH(CH <sub>2</sub> ) <sub>6</sub> Me, cation	0.590	2.63	1.36	0.00	2.1058	1.2969	0.0000	5.12	1.68	2.92	2.88
31	Metoprolol, cation	1.020	5.35	2.16	0.00	2.2819	2.3476	0.0000	1.95	0.33	1.45	1.02
32	Oxprenolol, cation	1.160	5.09	2.35	0.00	2.2389	2.2029	0.0000	2.51	0.45	1.70	1.48
33	Penbutolol, cation	0.775	4.66	1.98	0.00	2.6195	1.9630	0.0000	4.62	2.70	3.70	3.45
34	Propranolol, cation	1.690	4.31	2.07	0.00	2.1695	2.4319	0.0000	3.48	1.39	2.48	2.64
35	Alprenolol, cation	1.100	4.46	1.78	0.00	2.1802	2.2574	0.0000	3.10	1.08	2.08	2.19
36	Acebutolol, cation	1.450	6.69	3.62	0.00	2.7771	2.2965	0.0000	2.02	0.19	1.57	0.88

<sup>a</sup> from Zhang et al.<sup>10</sup><sup>b</sup> measured in this work.<sup>c</sup> from Liu et al.<sup>13</sup><sup>d</sup> from Liu et al.<sup>20</sup>

**Table 3.** Coefficients in Eq. (2) for a number of membrane systems (# 1-6) and solvent-water partitions (# 7-32); D(PCA)7 values compared with skin permeation

System	No.	SP	c	e	s	a	b	v	j+	j-	D(PCA)7
Skin permeation <sup>a</sup>	1	log K <sub>p</sub>	-5.402	-0.102	-0.457	-0.324	-2.680	2.066	-1.938	2.548	0.00
Cerasome <sup>b</sup>	2	log k	-1.922	0.200	-0.629	-0.109	-1.451	1.757	0.334	1.958	2.65
Microsomal binding <sup>c</sup>	3	log k	-1.221	0.000	-0.763	0.437	-0.444	1.452	0.283	1.215	3.00
BBB-Permeation <sup>d</sup>	4	log PS	-1.268	-0.047	-0.876	-0.719	-1.571	1.767	0.469	1.663	2.48
POPC <sub>80</sub> /PS <sub>20</sub> <sup>e</sup>	5	log k <sub>LEKC</sub>	-1.768	0.535	-0.775	-0.199	-2.424	2.640	0.094	2.688	3.63
PC <sup>e</sup>	6	log k <sub>IAM</sub>	-0.736	0.398	-0.509	-0.059	-2.630	2.948	-0.822	2.854	2.76
100% EtOH <sup>f</sup>	7	log P	0.222	0.471	-1.035	0.326	-3.596	3.857	-3.172	3.146	3.79
90% EtOH	8	log P	0.243	0.213	-0.575	0.262	-3.450	3.545	-2.794	2.705	2.37
80% EtOH	9	log P	0.172	0.175	-0.465	0.260	-3.212	3.323	-2.466	2.722	2.00
70% EtOH	10	log P	0.063	0.085	-0.368	0.311	-2.936	3.102	-2.203	2.550	1.52
60% EtOH	11	log P	-0.040	0.138	-0.335	0.293	-2.675	2.812	-1.858	2.394	1.52
50% EtOH	12	log P	-0.142	0.124	-0.252	0.251	-2.275	2.415	-1.569	2.051	1.47
40% EtOH	13	log P	-0.221	0.131	-0.159	0.171	-1.809	1.918	-1.271	1.676	1.78
30% EtOH	14	log P	-0.269	0.107	-0.098	0.133	-1.316	1.414	-0.941	1.290	2.24
20% EtOH	15	log P	-0.252	0.042	-0.040	0.096	-0.823	0.916	-0.677	0.851	2.78
10% EtOH	16	log P	-0.173	-0.023	-0.001	0.065	-0.372	0.454	-0.412	0.401	3.39
Wet octanol <sup>g</sup>	17	log P	0.088	0.562	-1.054	0.034	-3.460	3.814	-3.023	2.580	4.01
Methanol	18	log P	0.276	0.334	-0.714	0.243	-3.320	3.549	-2.609	3.027	2.80
Hexan-1-ol	19	log P	0.115	0.492	-1.164	0.054	-3.971	4.131	-3.100	2.940	4.07
Formamide	20	log P	-0.171	0.070	0.308	0.589	-3.152	2.432	-3.152	2.432	2.26
Acetonitrile	21	log P	0.413	0.077	0.326	-1.566	-4.391	3.364	-2.243	0.101	3.50
N-Methylpyrrolidinone	22	log P	0.147	0.532	0.275	0.840	-4.794	3.674	-1.797	0.105	4.71
Dimethylsulfoxide	23	log P	-0.194	0.327	0.791	1.260	-4.540	3.361	-3.387	0.132	4.71
Propanone	24	log P	0.313	0.312	-0.121	-0.608	-4.753	3.942	-2.288	0.078	3.85
1,2-Dichloroethane	25	log P	0.183	0.294	-0.134	-2.801	-4.291	4.180	-3.429	-0.025	4.62
Dichloromethane	26	log P	0.319	0.102	-0.187	-3.058	-4.090	4.324	-3.984	0.086	4.56
o-Nitrophenyl octyl ether	27	log P	0.121	0.600	-0.495	-2.246	-3.879	3.574	-2.314	0.350	4.63
Nitrobenzene	28	log P	-0.152	0.525	0.081	-2.332	-4.494	4.187	-3.373	0.777	4.88
Benzonitrile	29	log P	0.097	0.285	0.059	-1.605	-4.562	4.028	-2.729	0.136	4.04
Propylene carbonate	30	log P	0.004	0.168	0.504	-1.283	-4.407	3.421	-1.989	0.341	3.65
Sulfolane	31	log P	0.000	0.147	0.601	-0.318	-4.541	3.290	-1.200	-0.792	4.22
Ethylene glycol	32	log P	-0.270	0.578	-0.511	0.715	-2.619	2.729	-1.300	2.363	3.55

<sup>a</sup> from Zhang et al.<sup>10</sup>

<sup>b</sup> from Zhang et al.<sup>9</sup>

<sup>c</sup> from Abraham and Austin.<sup>2</sup>



1  
2  
3  
4  
5  
6  
7  
8  
9  
10  
11  
12  
13  
14  
15  
16  
17  
18  
19  
20  
21  
22  
23  
24  
25  
26  
27  
28  
29  
30  
31  
32  
33  
34  
35  
36  
37  
38  
39  
40  
41  
42  
43  
44  
45  
46  
47  
48  
49  
50  
51  
52  
53  
54  
55  
56  
57  
58  
59  
60

<sup>d</sup> Permeation from saline through the blood-brain barrier.<sup>3</sup>

<sup>e</sup> obtained in this study.

<sup>f</sup> Partitions from water to vol % ethanol-water mixtures.<sup>22</sup>

<sup>g</sup> Partitions from water to various solvents.<sup>16-18,22,23</sup>

For Peer Review

## 4. Discussion

---

LFER is a quite useful tool, not only to reveal the physicochemical nature of equilibrium systems but also to predict the corresponding equilibrium coefficients. In this study, LFER serves as the core analytical method, as being used to compare different partitioning systems by comparison of system coefficients, which can be used to characterize the given systems, and to predict  $\log K_p$  of both neutral and ionic species. In line with the aims of this study, I will discuss here: comparison of partitioning systems (centered around the SC-water partition), LFER analysis for skin permeability of both neutral and ionic species, and application of the Potts-Guy model on ionic species.

### **4.1 Comparison of Partitioning Systems**

In Publication 1 and Publication 3, the compounds with a broad structural diversity were selected and their retention factors were measured in LEKC, where cerasome and liposome (POPC<sub>80</sub>/PS<sub>20</sub>) were used as the investigated liposomes, respectively. The retention factor in LEKC serves as a partition index since it is proportional to the corresponding partition coefficient, as is the case for lipophilicity indices in ILC and IAM chromatography.

Abraham and Acree (2010a, b, c, d) have obtained solute descriptors for many anions derived from acids by deprotonation and for many cations derived from bases by addition of a proton. In cases where the descriptors were not determined, we used the equations set out by Abraham and Acree (2010a) for the calculation of descriptors. Once the descriptors for the relevant species are available, the dependent variable, in this case the retention factors, can be regressed against them for the LFER equation on the lines of Eq. 1.9, see Publication 1 and Publication 3.

In order to better compare liposomes with organic solvents, which are electrically neutral, on solute interaction, it is very necessary to make use of neutral liposome. Given that there has been no easy-to-use way so far to measure a number of neutral liposome-water partition parameters of

## Discussion

neutral species, which are required for LFER analysis, a neutral IAM from Liu et al. (2008) was used as a substitute for neutral liposome. In addition, it was investigated what the crucial difference is between immobilized lipid monolayers in IAM and lipid bilayers in liposomes in partition processes. Liu et al. (2008) have recently measured a diversity of neutral and ionized compounds on an IAM.PC.DD2 column, where phosphatidylcholines (PC) were bound to gel beads. Eq. 1.9 was also applied to the capacity factors obtained in this IAM system, see Publication 3. Using the LFER equations obtained above, we carried out the following comparisons of much interest.

### ***4.1.1 Comparison Methods of LEER Coefficients***

A quantitative method for comparison of coefficients is to consider the seven coefficients of any system (that is,  $e$ ,  $s$ ,  $a$ ,  $b$ ,  $v$ ,  $j^+$  and  $j^-$ ) as a point in seven-dimensional space. The distance between the points,  $d'$ , calculated by straightforward trigonometry, is then a measure of how close are the sets of coefficients. As the coefficients have specific chemical meanings, the smaller the value of  $d'$ , the closer are the coefficients in a chemical sense and the closer are the systems in a chemical sense. Abraham and Martins (2004) suggested that for a system to be a good model,  $d'$  should be less than around 0.5-0.8 units.

Another useful way to compare the coefficients in a set of equations is to perform a principal component analysis (PCA). The seven coefficients are converted into seven linearly uncorrelated principal components (PCs) via an orthogonal transformation, which contain exactly the same information. The first two principal components (PC1 and PC2) can generally account for most of the entire information. A plot of the scores of PC1 against PC2 reveals how 'close' the equations are in terms of chemical interactions.

These two methods have their respective focuses, and were employed in this study as needed. The former emphasizes the relationship between any two systems but lacks an overall view of

## Discussion

these relationships. In contrast, the latter shows full characterization of the relationships among all the systems but cannot exactly give the correlation extent of two systems.

### ***4.1.2 Comparison of Lipid Membrane-Water Systems with Organic Solvent-Water Systems***

In Publication 1 and Publication 3, lipid membrane-water partitions were compared with organic solvent-water partitions using LFER equations for ionic species. The results show lipid membranes (including neutral IAM) exhibit a considerably different chemical environment from those of organic solvents. Furthermore, partitions into the more polar hydroxylic solvents are chemically closer to partitions into lipid membranes as compared to partitions into the less polar hydroxylic solvents and into aprotic solvents. Abraham and Acree (2012) have recently obtained similar results for neutral species, so that we can now suggest that both neutral and ionic species partition into the polar parts of lipid membrane. However on the whole, there is no ‘ideal’ solvent that can be used as a general model for lipid membranes.

Additionally, we compared partition into IAM with partition into liposomes in Publication 3. Lipid monolayers in IAM are known to differ from lipid bilayers in liposomes in terms of lateral mobility of lipids and density of the polar phospholipid head-groups (Ong et al., 1996; Rand and Parsegian, 1989). However, it was found that such structural differences just bring about a negligible change on partition properties. Therefore, neutral IAM may be a good surrogate for neutral liposome in partition processes.

### ***4.1.3 Uniqueness of Cerasome on Modeling the Stratum Corneum in Partitions***

The SC-water partition was compared with cerasome-water and organic solvent-water partitions in Publication 2, although for neutral species only. However, it can be seen that cerasome is a reasonable model for the SC in partitions, with a much lower  $d'$  value (0.86) than those for organic solvents, and phospholipid liposomes (containing cholesterol or not) whose values have not been published. Furthermore, the cerasome-water partition shows a better chemical correla-

## Discussion

tion to skin permeation than other lipid membrane-water partitions and microsomal binding, see Publication 3. Hence, cerasome is a unique liposome whose roles on modeling the SC cannot be replaced by regular phospholipid liposomes. This is probably due to the unusual structures of ceramides, the major type of lipids in the SC. Ceramides consist of derivatives of sphingosine bases linked to a variety of fatty acids via amide bonds. Clearly, the polar head-groups in ceramides serve as both acceptors and donors of hydrogen bonds by the hydroxyl and amino groups as compared to those in phospholipids, which act only as acceptors of hydrogen bonds (Moore et al., 1997). Ceramides therefore should give rise to strong hydrogen bonding with solutes that are hydrogen bond bases. Besides, the aliphatic chains in ceramides are mostly long-chain and saturated, and hence lead to high phase transition temperatures. Ceramides are thus mostly in a solid crystalline or gel state at physiological temperature, which exhibits lower partition coefficients than the state of liquid crystalline membranes (Bano, 2000; Sarmiento et al., 1993).

### ***4.1.4 Correlation between Skin Permeation and Partitioning Systems***

It was found that skin permeation is not closely related chemically to any of the organic solvent-water partitions, not even to the cerasome-water partition, see Publication 2. However, this is not unexpected. Skin permeation can be considered in terms of partition from water into skin followed by diffusion across the under layer of skin. Here, these partitioning systems maybe provide an estimate for the skin-water partition, but could not contain information on diffusion through skin. It was suggested that for neutral species, transport within the SC owns a strong size dependence for small solutes (< 300 Da) and a weak size dependence for larger solutes (Johnson et al., 1996; Johnson et al., 1997; Mitragotri, 2000). Further, the results of this study suggest that the diffusion process for ionic species is more complicated than that for neutral species (see Section 4.2). This means that, diffusion coefficients across the SC may vary very much with solutes.

It is thus clear that only partitioning system (even the skin-water partition) fails to account for the main variance of skin permeation.

### **4.2 LFER Analysis for Skin Permeability of Both Species**

The values of  $\log K_p$  for 18 ionizable compounds (including 9 acids and 9 bases) through human epidermis were measured using Franz diffusion cells in Publication 2. After combining these data with the experimental  $\log K_p$  database for neutral molecules compiled by Abraham and Martins (2004) and reliable  $\log K_p$  data for ionic species in literature, the MLR analysis of  $\log K_p$  against the seven solute descriptors yields a LFER equation for skin permeation of both neutral and ionic species, with  $R^2 = 0.861$  and  $SD = 0.462$  log units. Here and elsewhere,  $R^2$  is the squared correlation coefficient and SD is the standard deviation.

#### **4.2.1 Assessment of Predictive Power**

This equation was found to be quite comparable to the Abraham-Martins model, Eq. 1.10, which involves neutral molecules only, with the coefficients in the two equations reasonably close; their SD values are almost the same. This proves that inclusion of the additional descriptors ( $J^+$  and  $J^-$ ) in LFER makes sense for ionic species. A plot of experimental values of  $\log K_p$  versus calculated values of  $\log K_p$  on this equation is given in Publication 2. The data points for the anions and cations scatter randomly over the line of unit slope. That is, ionic species fit the equation very well.

The predictive standard deviation (PSD) derived from the leave-one-out statistics, is a useful estimate of the predictive power of the regression models, especially for our case that comprises the data for ionic species (Cruciani et al., 1992; Hawkins, 2004). The PSD value for our equation is 0.502, which is possibly close to what can be achieved without overfitting. This may be sufficient for many purposes. Abraham and Martins (2004) pointed out that it is difficult to predict  $\log K_p$  to less than around 0.5 log unit for large and varied data sets. This is understandable if the intrinsic variability of the experimental  $\log K_p$  from different groups is taken into account. The

## Discussion

$\log K_p$  for passive permeation of the sodium ion and the tetraethylammonium ion across human skin were predicted using our equation. The predicted values are in fair agreement with the experimental values. This is the first time that permeation of an ion across a membrane has been predicted just from the physicochemical properties of the ion and membrane. This equation can also be applied to estimate  $\log K_p$  values for partly ionized solutes based on the respective contributions of neutral and ionic species.

### ***4.2.2 Effects of Ionization on the Overall Permeation and the Separate Partition and Diffusion***

As shown in Eq. 1.2, if we had data on partitioning into skin by anions and cations, we could dissect ionic effects on permeation into partition and diffusion. In the absence of actual  $\log K_{sc}$  data, we can use partition into cerasome as an estimate for partition into skin and then deduce an equation for  $\log D_{sc}$  of ionic species, by subtraction of coefficients in known equations for skin permeation and partition into cerasome. From these above equations, we can then obtain the effects of ionization, by comparison with neutral solutes, on the overall permeation and the separate partition and diffusion processes. The results show that neutral acids and bases permeate across human skin very much faster than the corresponding ionized species, but the actual  $K_p$  ratio depends on their structures. Moreover, the poor permeability of anions is partly due to poor partition into the SC but mostly due to slow diffusion of the ionized species (by comparison to the neutral species). For cations, poor permeability is entirely due to very slow diffusion (again by comparison to the neutral species). All of the details are given in Publication 2.

As for ionic slow diffusion, a possible explanation is as follows: The ionized form definitely binds closer to the lipid bilayer interface in the SC than the neutral form. The solute moves in the lipid bilayers with preference towards lateral diffusion regardless of the solute size and location. The highly-ordered lipid chains near the bilayer interface result in the steric resistance of solutes

## Discussion

(Mitragotri, 2003; Mitragotri et al., 1999). As a result, the ionic species encounters a larger retarding effect to their movement.

Further, we suggest that diffusion of the base cations is made more difficult by the presence of negatively charged head-groups in the SC. As one of the major lipids in the SC, the only ionizable fatty acids impart a net negative charge to the intercellular lipid bilayers (Michniak-Kohn et al., 2005). When the cations diffuse in the lipid layers, their movement will be retarded under the electrostatic attraction of negatively charged head-groups in lipids.

### ***4.3 Application of the Potts-Guy Model***

Potts and Guy (1992) proposed a QSPR model for  $\log K_p$  based on partition parameters between water and model vehicles for the SC and molecular volume (see Eq. 1.1). As we introduced, this equation was deduced from Eq. 1.2. It is known that organic solvent-water partitions are not very good models for the skin-water partition. We can now use the partition into cerasome (as  $\log k_{7.4}$  in Publication 1) as a model to investigate the application of Eq. 1.1 on predicting  $\log K_p$  of both neutral and ionic species. Here, the McGowan approximation for molecular volume (that is,  $V$ ) is adopted. A MLR analysis of  $\log K_p$  against  $\log k_{7.4}$  and  $V$  for neutral and ionized compounds that are present both in our data sets for  $\log K_p$  and  $\log k_{7.4}$  (see Publication 2 and Publication 1), leading to Eq. 4.1.  $N$  is here the number of compounds or data points.

$$\log K_p (\text{cm s}^{-1}) = -4.437 + 0.164 \log k_{7.4} - 0.759 V \quad (4.1)$$
$$R^2 = 0.293, \text{SD} = 1.079, N = 41$$

It is obvious that only  $\log k_{7.4}$  and  $V$  cannot explain the nature of skin permeation very well. But, this is not surprising. In the Potts-Guy model,  $\log D_{sc}$  was suggested to be linearly, inversely related to molecular volume. Such a relationship may be very useful for estimation of  $\log K_p$  values of neutral species, as Eq. 4.2 shows, which is from the above regression for neutral species



## Discussion

only. However, it is purely empirical in nature and gives little information as to the actual structural features of solutes that influence diffusion in the SC.

$$\log K_p (\text{cm s}^{-1}) = -2.221 + 1.488 \log k_{7,4} - 0.852V \quad (4.2)$$
$$R^2 = 0.826, \text{SD} = 0.561, N = 22$$

Our previous discussion indicated that the effect of ionization on diffusion through the SC is striking for ionizable compounds. This is markedly different from diffusion in water, where ionic species diffuse at about the same rate as the corresponding neutral compounds (Hills et al., 2011). As a result, the empirical relationship between  $\log D_{sc}$  and molecular volume breaks down for ionic species. We can now conclude that, the Potts-Guy model cannot be used to predict  $\log K_p$  for ionic species.

### **4.4 Contribution of this Study**

On the whole, this study has successfully achieved the initial aims, and mainly contributes to the progress of science in several aspects below:

- 1) It was demonstrated that liposomes are chemically far apart from organic solvents as for interaction with solutes, and thus that organic solvents cannot be used as a general model for liposomes.
- 2) It was confirmed that liposomes can model the SC on partition properties very well, and that the use of the proper lipid composition is rather significant for its chemical similarity with the SC. In addition, the commercially available cerasome can be considered as a reasonable model.
- 3) A LFER equation for skin permeation for both neutral and ionic species was constructed, which can be used to predict  $\log K_p$  and characterize skin permeation. It is the first model so far that can predict  $\log K_p$  of ionic species; and moreover, it is simple and easy-to-use.

## Discussion

- 4) It was found that neutral acids and bases permeate through human skin much faster than their corresponding ionized forms, but that the ratio of neutral to ionic permeation is dependent upon the actual structure. And the poor permeation of ionic species is mainly due to their slow diffusion across the SC, especially for base cations.
- 5) It was indicated that the Potts-Guy model based on partition parameters in model vehicles (even in liposomes) for the SC and molecular volume does not work for estimation of  $\log K_p$  of ionic species.

## 5. Summary

---

The skin forms an extremely efficient barrier between internal organs and the external environment, but also provides an attractive administration route. Skin permeability (as  $\log K_p$ ) is a critical parameter for estimating transdermal delivery of chemicals in contact with the skin in pharmaceuticals and cosmetics. Given the fact that measurement of  $\log K_p$  is quite time-consuming and laborious, various mathematical models based on understanding of the fundamental mechanisms underlying skin permeation have been proposed to estimate the otherwise unavailable  $\log K_p$ . However, there has been no model up to now for prediction of  $\log K_p$  of ionic species. In order to solve this problem, we proposed and investigated two potential solutions in this study: one is the Potts-Guy model on the basis of partition parameters in liposome-water systems and molecular volume (MV), and the other is the extended linear free-energy relationship (LFER), which can be used to predict biological membrane permeability of ionic species.

In this study, the compounds with a broad structural diversity were selected and their retention factors were measured in liposome electrokinetic chromatography (LEKC), where cerasomes composed mainly of the stratum corneum (SC) lipids and liposomes (POPC<sub>80</sub>/PS<sub>20</sub>) were used as the pseudo-stationary phases, respectively. These two negatively charged membrane systems and a neutral immobilized artificial membrane (IAM) system from literature as a surrogate for neutral liposome-water partition were compared with various organic solvent-water partitioning systems using LFERs. It was observed that liposomes display a greatly different chemical environment from those of organic solvents, and no organic solvent can thus provide a general model for liposomes in partition processes. What is more, the correlation between the skin-water partition and organic solvent/liposome-water partitions was also investigated. The results show that cerasome exhibits a better chemical similarity with the skin as compared to phospholipid

## Summary/Zusammenfassung

liposomes and all organic solvents. Further, the cerasome-water partition correlates better to skin permeation than other liposome-water partitions and microsomal binding. This is probably due to the unique structures of ceramides that occur in SC and consequently in cerasomes.

The  $\log K_p$  values of nine acid anions and nine base cations were measured in this study. The data were used to construct a LFER equation for skin permeation of neutral species and ionic species, together with experimental  $\log K_p$  for both species in literature. The resulting equation, with a  $R^2$  value of 0.861 and a SD value of 0.462 log units, can be used to predict  $\log K_p$  for neutral species and ionic species, as well as partly ionized solutes. The predicted values for the passive permeation of the sodium ion and the tetraethylammonium ion are in good accord with the experimental values. It was found that neutral acids and bases are much more permeable than their ionized forms, and that the ratio depends on the actual structure. Using the cerasome-water partition as a substitute for the skin-water partition, the effect of ionization of solutes on skin permeation was separated to those on partition and diffusion processes. The poor permeability of ionic species is largely due to slow diffusion through the SC, especially for base cations.

In addition, the Potts-Guy model based on the retention factors obtained in cerasome electrokinetic chromatography (EKC) and MV was discussed. It was found that such a model cannot be applied to predict  $\log K_p$  for ionic species because MV fails to account for their diffusion through the SC, even empirically.

In conclusion, LFER is a very useful tool for predicting skin permeation, not only for neutral species but also for ionic species, whereas the Potts-Guy model may be useful for neutral species but is not applicable for ionic species.

# Zusammenfassung

---

Die Haut bildet eine äußerst effiziente Barriere zwischen dem Körperinneren und der äußeren Umwelt und stellt aber auch einen attraktiven Applikationsweg dar. Die Hautpermeabilität (dargestellt als  $\log K_p$ ) ist dabei auf dem Gebiet der Pharmazie und Kosmetik ein entscheidender Parameter, um das transdermale Hautpenetrations- bzw. Hautpermeationsverhalten eines Stoffes nach dermalen Applikation abzuschätzen. Direkte Messungen des  $\log K_p$  sind zeitaufwendig und mühsam. In der vorliegenden Arbeit wurden verschiedene, auf dem Verständnis grundlegender Mechanismen der Hautpermeation basierende, mathematische Modelle vorgeschlagen, um nicht verfügbare  $\log K_p$ -Werte zu generieren. Bisher gab es jedoch kein Modell, um den  $\log K_p$  von ionisierten Molekülen vorherzusagen. Um dieses Problem zu lösen, haben wir in dieser Arbeit zwei Lösungsmöglichkeiten für die Vorhersage von  $\log K_p$ -Werten geladener Substanzen vorgeschlagen und im Weiteren diskutiert: Zum einen das Potts-Guy-Modell auf der Basis von Verteilungsparametern in Liposom/Wasser-Systemen und dem Molekülvolumen (MV), zum anderen die erweiterte lineare freie Energie-Beziehung (linear free energy relationship; LFER), die verwendet werden kann, um die Permeabilität geladener Stoffe durch biologische Membranen vorherzusagen.

In dieser Arbeit wurden Verbindungen mit einer breiten strukturellen Vielfalt ausgewählt und ihre Retentionsfaktoren mit Hilfe von Liposom-Elektrokinetik-Chromatographie (liposome electrokinetic chromatography; LEKC) gemessen, wobei Cerasomen, hauptsächlich bestehend aus Lipiden des Stratum corneums (SC), bzw. Liposomen (POPC<sub>80</sub>/PS<sub>20</sub>) als pseudostationäre Phase dienten. Diese beiden negativ geladenen Membransysteme sowie ein System aus neutralen künstlichen immobilisierten Membranen (immobilized artificial membranes; IAM) stellvertretend für eine neutrale Liposomen/Wasser-Verteilung wurden mit verschiedenen

## Summary/Zusammenfassung

Verteilungssystemen zwischen organischen Lösungsmitteln und Wasser unter Anwendung der LFER verglichen. Es wurde beobachtet, dass Liposomen eine sich von organischen Lösungsmitteln stark unterscheidende chemische Umgebung besitzen. Daher stellen organische Lösungsmittel kein allgemein gültiges Modell für Liposomen in Bezug auf Verteilungsprozesse dar. Der Zusammenhang zwischen der Haut/Wasser-Verteilung und der organischen Lösungsmittel/Liposom-Wasser-Verteilung wurde ebenfalls untersucht. Die Ergebnisse zeigen, dass Cerasomen im Vergleich zu herkömmlichen Liposomen aus Phospholipiden sowie allen organischen Lösungsmitteln eine höhere chemische Ähnlichkeit mit der Haut aufweisen. Darüber hinaus konnte für die Cerasomen/Wasser-Verteilung eine bessere Korrelation mit der Hautpermeation nachgewiesen werden, als für die Liposomen-Wasser-Verteilung oder die mikrosomale Bindung. Grund hierfür ist wahrscheinlich die einzigartige Struktur der Ceramide, die im Stratum corneum wie auch hier in den Cerasomen vorhanden ist.

Die  $\log K_p$ -Werte von neun sauren, anionischen Molekülen und neun basischen, kationischen Molekülen wurden in dieser Arbeit gemessen. Aus den generierten Daten wurde in Verbindung mit  $\log K_p$  Werten aus der Literatur eine LFER-Gleichung für die Hautpermeation von neutralen und ionischen Molekülen entwickelt. Die resultierende Gleichung mit einem  $R^2$  von 0,861 und einer Standardabweichung von 0,462 log Einheiten kann sowohl zur Vorhersage des  $\log K_p$ -Wertes für neutrale und ionische Moleküle, als auch für Vorhersage des  $\log K_p$ -Wertes teilweise ionisierter Substanzen verwendet werden. Die abgeschätzten Werte für die passive Permeation des Natrium-Ions und des Tetraethylammonium-Ions stimmen mit den experimentellen Werten gut überein. Es wurde erkannt, dass neutrale Säuren und Basen viel stärker permeieren als die dazugehörigen ionisierten Formen und dass das Verhältnis von der jeweiligen Struktur abhängt. Unter Verwendung der Cerasome/Wasser-Verteilung als Ersatz für die Haut-Wasser-Verteilung wurde der Effekt der Ionisierung der gelösten Substanzen auf die

## Summary/Zusammenfassung

Hautpermeation von den Effekten auf die Verteilung und Diffusionsprozesse getrennt. Die schlechte Permeation ionischer Moleküle beruht im Wesentlichen auf der langsamen Diffusion durch das SC, vor allem für basische Kationen.

Darüber hinaus wurde das Potts-Guy Modell basierend auf den Retentionsfaktoren, welche mittels Cerasome Electrokinetic Chromatography (EKC) bestimmt wurden, und MV diskutiert. Es wurde herausgefunden, dass ein solches Modell nicht für die Schätzung von  $\log K_p$ -Werten ionischer Moleküle angewendet werden kann, da MV daran scheitert, die Diffusion durch das SC zu erfassen - auch empirisch.

Zusammenfassend lässt sich sagen, dass LFER ein nützliches Hilfsmittel ist, um die Hautpermeation nicht nur für neutrale, sondern auch für ionische Moleküle voraussagen, wohingegen das Potts-Guy Modell gegebenenfalls für neutrale, aber nicht für ionische Moleküle anwendbar ist.

## 6. References

---

Abraham, M.H., 1993. Scales of solute hydrogen-bonding - their construction and application to physicochemical and biochemical processes. *Chem Soc Rev* 22, 73-83.

Abraham, M.H., 2011. The permeation of neutral molecules, ions, and ionic species through membranes: brain permeation as an example. *J Pharm Sci* 100, 1690-1701.

Abraham, M.H., Acree, W.E., Jr., 2010a. Equations for the transfer of neutral molecules and ionic species from water to organic phases. *J Org Chem* 75, 1006-1015.

Abraham, M.H., Acree, W.E., Jr., 2010b. Solute descriptors for phenoxide anions and their use to establish correlations of rates of reaction of anions with iodomethane. *J Org Chem* 75, 3021-3026.

Abraham, M.H., Acree, W.E., Jr., 2010c. The transfer of neutral molecules, ions and ionic species from water to ethylene glycol and to propylene carbonate; descriptors for pyridinium cations. *New J Chem* 34, 2298-2305.

Abraham, M.H., Acree, W.E., Jr., 2010d. The transfer of neutral molecules, ions and ionic species from water to wet octanol. *Phys Chem Chem Phys* 12, 13182-13188.

Abraham, M.H., Acree, W.E., Jr., 2012. Linear free energy relationships for water/hexadec-1-ene and water/deca-1,9-diene partitions, and for permeation through lipid bilayers; comparison of permeation systems. First published on the web 18 Jun 2012.

Abraham, M.H., Martins, F., 2004. Human skin permeation and partition: general linear free-energy relationship analyses. *J Pharm Sci* 93, 1508-1523.

Ackermann, C., Flynn, G.L., 1987. Ether water partitioning and permeability through nude-mouse skin in vitro .1. Urea, thiourea, glycerol and glucose. *Int J Pharm* 36, 61-66.

Acree, W.E., Jr., Grubbs, L.M., Abraham, M.H., 2012. Prediction of partition coefficients and permeability of drug molecules in biological systems with Abraham model solute descriptors derived from measured solubilities and water-to-organic solvent partition coefficients, in: Acree, W.E., Jr. (Ed.), *Toxicity and Drug Testing*. InTech, Rijeka, Croatia, pp. 91-128.



## References

- Avdeef, A., Box, K.J., Comer, J.E., Hibbert, C., Tam, K.Y., 1998. pH-metric logP 10. Determination of liposomal membrane-water partition coefficients of ionizable drugs. *Pharm Res* 15, 209-215.
- Bangham, A.D., Standish, M.M., Miller, N., 1965a. Cation permeability of phospholipid model membranes: effect of narcotics. *Nature* 208, 1295-1297.
- Bangham, A.D., Standish, M.M., Watkins, J.C., 1965b. Diffusion of univalent ions across the lamellae of swollen phospholipids. *J Mol Biol* 13, 238-252.
- Bano, M., 2000. Determination of partition coefficient by the change of main phase transition. *Gen Physiol Biophys* 19, 279-293.
- Beigi, F., Yang, Q., Lundahl, P., 1995. Immobilized-liposome chromatographic analysis of drug partitioning into lipid bilayers. *J Chromatogr A* 704, 315-321.
- Blank, I.H., Scheuplein, R.J., 1969. Transport into and within Skin. *Brit J Dermatol* 81, 4-&.
- Bodde, H.E., Vandenbrink, I., Koerten, H.K., Dehaan, F.H.N., 1991. Visualization of in vitro percutaneous penetration of mercuric-chloride - transport through intercellular space versus cellular uptake through desmosomes. *J Control Release* 15, 227-236.
- Brekkan, E., Lundqvist, A., Lundahl, P., 1996. Immobilized membrane vesicle or proteoliposome affinity chromatography. Frontal analysis of interactions of cytochalasin B and D-glucose with the human red cell glucose transporter. *Biochemistry* 35, 12141-12145.
- Brown, M.B., Martin, G.P., Jones, S.A., Akomeah, F.K., 2006. Dermal and transdermal drug delivery systems: current and future prospects. *Drug Deliv* 13, 175-187.
- Burns, S.T., Agbodjan, A.A., Khaledi, M.G., 2002. Characterization of solvation properties of lipid bilayer membranes in liposome electrokinetic chromatography. *J Chromatogr A* 973, 167-176.
- Burns, S.T., Khaledi, M.G., 2002. Rapid determination of liposome-water partition coefficients ( $K_{lw}$ ) using liposome electrokinetic chromatography (LEKC). *J Pharm Sci* 91, 1601-1612.
- Cruciani, G., Baroni, M., Clementi, S., Costantino, G., Riganeli, D., Skagerberg, B., 1992. Predictive ability of regression-models .1. Standard-deviation of prediction errors (Sdep). *J Chemometrics* 6, 335-346.

## References

- Diamond, J.M., Katz, Y., 1974. Interpretation of nonelectrolyte partition-coefficients between dimyristoyl lecithin and water. *J Membr Biol* 17, 121-154.
- Elias, P.M., 1983. Epidermal lipids, barrier function, and desquamation. *J Invest Dermatol* 80, 44s-49s.
- Flynn, G.L., 1990. Physicochemical determinants of skin absorption, in: Gerrity, T.R., Henry, C.J. (Eds.), *Principles of Route-to-Route Extrapolation for Risk Assessment*. Elsevier, New York, pp. 93-127.
- Hawkins, D.M., 2004. The problem of overfitting. *J Chem Inf Comput Sci* 44, 1-12.
- Hills, E.E., Abraham, M.H., Hersey, A., Bevan, C.D., 2011. Diffusion coefficients in ethanol and in water at 298 K: linear free energy relationships. *Fluid Phase Equilibr* 303, 45-55.
- Holbrook, K.A., Odland, G.F., 1974. Regional differences in the thickness (cell layers) of the human stratum corneum: an ultrastructural analysis. *J Invest Dermatol* 62, 415-422.
- Johnson, M.E., Berk, D.A., Blankschtein, D., Golan, D.E., Jain, R.K., Langer, R.S., 1996. Lateral diffusion of small compounds in human stratum corneum and model lipid bilayer systems. *Biophys J* 71, 2656-2668.
- Johnson, M.E., Blankschtein, D., Langer, R., 1997. Evaluation of solute permeation through the stratum corneum: lateral bilayer diffusion as the primary transport mechanism. *J Pharm Sci* 86, 1162-1172.
- Kaliszan, R., 1999. Chromatography and capillary electrophoresis in modelling the basic processes of drug action. *Trac-Trend Anal Chem* 18, 400-410.
- Khaleque, M.A., Oho, T., Okumura, Y., Mitani, M., 2000. Controlled detachment of immobilized liposomes on polymer gel support. *Chem Lett*, 1402-1403.
- Kitson, N., Thewalt, J., Lafleur, M., Bloom, M., 1994. A model membrane approach to the epidermal permeability barrier. *Biochemistry* 33, 6707-6715.
- Law, S., Wertz, P.W., Swartzendruber, D.C., Squier, C.A., 1995. Regional variation in content, composition and organization of porcine epithelial barrier lipids revealed by thin-layer chromatography and transmission electron microscopy. *Arch Oral Biol* 40, 1085-1091.

## References

- Liu, X., Hefesha, H., Scriba, G., Fahr, A., 2008. Retention behavior of neutral and positively and negatively charged solutes on an immobilized-artificial-membrane (IAM) stationary phase. *Helv Chim Acta* 91, 1505-1512.
- Lu, G.W., Flynn, G.L., 2009. Cutaneous and transdermal delivery-processes and systems of delivery, in: Florence, A.T., Siepmann, J. (Eds.), *Modern Pharmaceutics*, 5th edition. Informa Healthcare USA, New York, pp. 43-100.
- Lundahl, P., Beigi, F., 1997. Immobilized liposome chromatography of drugs for model analysis of drug-membrane interactions. *Adv Drug Deliver Rev* 23, 221-227.
- Lundqvist, A., Brekkan, E., Lagerquist, C., Haneskog, L., Lundahl, P., 1997. Frontal affinity chromatographic analysis of membrane protein reconstitution. *Mat Sci Eng C-Biomim* 4, 221-226.
- Mannhold, R., van de Waterbeemd, H., 2001. Substructure and whole molecule approaches for calculating log P. *J Comput Aid Mol Des* 15, 337-354.
- Menon, G.K., Elias, P.M., 1997. Morphologic basis for a pore-pathway in mammalian stratum corneum. *Skin Pharmacol* 10, 235-246.
- Michaels, A.S., Chandrasekaran, S.K., Shaw, J.E., 1975. Drug permeation through human skin - theory and in vitro experimental measurement. *Aiche J* 21, 985-996.
- Michniak-Koln, B.B., Meidan, V., Al-Khalili, M., Wertz, P.W., 2005. Skin: physiology and penetration pathways, in: Rosen, M.R. (Ed.), *Delivery System Handbook for Personal Care and Cosmetic Products: Technology, Applications, and Formulations*. William Andrew, Norwich, pp. 78-95.
- Mitragotri, S., 2000. In situ determination of partition and diffusion coefficients in the lipid bilayers of stratum corneum. *Pharm Res* 17, 1026-1029.
- Mitragotri, S., 2003. Modeling skin permeability to hydrophilic and hydrophobic solutes based on four permeation pathways. *J Control Release* 86, 69-92.
- Mitragotri, S., Anissimov, Y.G., Bunge, A.L., Fransch, H.F., Guy, R.H., Hadgraft, J., Kasting, G.B., Lane, M.E., Roberts, M.S., 2011. Mathematical models of skin permeability: an overview. *Int J Pharm* 418, 115-129.

## References

- Mitragotri, S., Blankschtein, D., Langer, R., 1996. Transdermal drug delivery using low-frequency sonophoresis. *Pharm Res* 13, 411-420.
- Mitragotri, S., Edwards, D.A., Blankschtein, D., Langer, R., 1995. A mechanistic study of ultrasonically-enhanced transdermal drug delivery. *J Pharm Sci* 84, 697-706.
- Mitragotri, S., Johnson, M.E., Blankschtein, D., Langer, R., 1999. An analysis of the size selectivity of solute partitioning, diffusion, and permeation across lipid bilayers. *Biophys J* 77, 1268-1283.
- Moore, D.J., Rerek, M.E., Mendelsohn, R., 1997. FTIR spectroscopy studies of the conformational order and phase behavior of ceramides. *J Phys Chem B* 101, 8933-8940.
- Nemanic, M.K., Elias, P.M., 1980. In situ precipitation: a novel cytochemical technique for visualization of permeability pathways in mammalian stratum corneum. *J Histochem Cytochem* 28, 573-578.
- Ong, S., Liu, H., Pidgeon, C., 1996. Immobilized-artificial-membrane chromatography: measurements of membrane partition coefficient and predicting drug membrane permeability. *J Chromatogr A* 728, 113-128.
- Ong, S., Pidgeon, C., 1995. Thermodynamics of solute partitioning into immobilized artificial membranes. *Anal Chem* 67, 2119-2128.
- Ongpipattanakul, B., Francoeur, M.L., Potts, R.O., 1994. Polymorphism in stratum corneum lipids. *Biochim Biophys Acta* 1190, 115-122.
- Peck, K.D., Ghanem, A.H., Higuchi, W.I., 1994. Hindered diffusion of polar molecules through and effective pore radii estimates of intact and ethanol treated human epidermal membrane. *Pharm Res* 11, 1306-1314.
- Pidgeon, C., 1990a. Immobilized artificial membranes, U.S. Patent 4,931,498.
- Pidgeon, C., 1990b. Method for solid phase membrane mimetics, U.S. Patent 4,927,879.
- Pidgeon, C., Stevens, J., Otto, S., Jefcoate, C., Marcus, C., 1991. Immobilized artificial membrane chromatography: rapid purification of functional membrane proteins. *Anal Biochem* 194, 163-173.

## References

- Pidgeon, C., Venkataram, U.V., 1989. Immobilized artificial membrane chromatography: supports composed of membrane lipids. *Anal Biochem* 176, 36-47.
- Potts, R.O., Francoeur, M.L., 1990. Lipid biophysics of water loss through the skin. *Proc Natl Acad Sci USA* 87, 3871-3873.
- Potts, R.O., Guy, R.H., 1992. Predicting skin permeability. *Pharm Res* 9, 663-669.
- Rand, R.P., Parsegian, V.A., 1989. Hydration forces between phospholipid-bilayers. *Biochim Biophys Acta* 988, 351-376.
- Raykar, P.V., Fung, M.C., Anderson, B.D., 1988. The role of protein and lipid domains in the uptake of solutes by human stratum corneum. *Pharm Res* 5, 140-150.
- Sandberg, M., Lundahl, P., Greijer, E., Belew, M., 1987. Immobilization of phospholipid-vesicles on alkyl derivatives of agarose-gel beads. *Biochim Biophys Acta* 924, 185-192.
- Sarmiento, A.B., Delima, M.C.P., Oliveira, C.R., 1993. Partition of dopamine antagonists into synthetic lipid bilayers - the effect of membrane-structure and composition. *J Pharm Pharmacol* 45, 601-605.
- Scheuplein, R.J., 1965. Mechanism of percutaneous absorption. I. Routes of penetration and the influence of solubility. *J Invest Dermatol* 45, 334-346.
- Scheuplein, R.J., 1967. Mechanism of percutaneous absorption. II. Transient diffusion and the relative importance of various routes of skin penetration. *J Invest Dermatol* 48, 79-88.
- Scheuplein, R.J., Blank, I.H., 1971. Permeability of the skin. *Physiol Rev* 51, 702-747.
- Scheuplein, R.J., Blank, I.H., 1973. Mechanism of percutaneous absorption. IV. Penetration of nonelectrolytes (alcohols) from aqueous solutions and from pure liquids. *J Invest Dermatol* 60, 286-296.
- Sznitowska, M., Janicki, S., Williams, A.C., 1998. Intracellular or intercellular localization of the polar pathway of penetration across stratum corneum. *J Pharm Sci* 87, 1109-1114.
- Taillardat-Bertschinger, A., Carrupt, P.-A., Barbato, F., Testa, B., 2003. Immobilized artificial membrane HPLC in drug research. *J Med Chem* 46, 655-665.
- Wallsten, M., Yang, Q., Lundahl, P., 1989. Entrapment of lipid vesicles and membrane protein-lipid vesicles in gel bead pores. *Biochim Biophys Acta* 982, 47-52.

## References

- Wang, Y., Sun, J., Liu, H., Liu, J., Zhang, L., Liu, K., He, Z., 2009. Predicting skin permeability using liposome electrokinetic chromatography. *Analyst* 134, 267-272.
- Wiedmer, S.K., Jussila, M.S., Riekkola, M.L., 2004. Phospholipids and liposomes in liquid chromatographic and capillary electromigration techniques. *Trac-Trend Anal Chem* 23, 562-582.
- Wiedmer, S.K., Shimmo, R., 2009. Liposomes in capillary electromigration techniques. *Electrophoresis* 30 Suppl 1, S240-257.
- Williams, A.C., Barry, B.W., 1992. Skin absorption enhancers. *Crit Rev Ther Drug Carrier Syst* 9, 305-353.
- Williams, M.L., Elias, P.M., 1987. The extracellular matrix of stratum corneum: role of lipids in normal and pathological function. *Crit Rev Ther Drug Carrier Syst* 3, 95-122.
- Xian, D.L., Huang, K.L., Liu, S.Q., Xiao, J.Y., 2008. Quantitative retention-activity relationship studies by liposome electrokinetic chromatography to predict skin permeability. *Chinese J Chem* 26, 671-676.
- Yang, Q., Liu, X.Y., Ajiki, S., Hara, M., Lundahl, P., Miyake, J., 1998. Avidin-biotin immobilization of unilamellar liposomes in gel beads for chromatographic analysis of drug-membrane partitioning. *J Chromatogr B Analyt Technol Biomed Life Sci* 707, 131-141.
- Yang, Q., Liu, X.Y., Yoshimoto, M., Kuboi, R., Miyake, J., 1999. Covalent immobilization of unilamellar liposomes in gel beads for chromatography. *Anal Biochem* 268, 354-362.
- Yang, Q., Lundahl, P., 1994. Steric immobilization of liposomes in chromatographic gel beads and incorporation of integral membrane-proteins into their lipid bilayers. *Anal Biochem* 218, 210-221.
- Zhang, Y., Zhang, R., Hjerten, S., Lundahl, P., 1995. Liposome capillary electrophoresis for analysis of interactions between lipid bilayers and solutes. *Electrophoresis* 16, 1519-1523.

## 7. Abbreviations

---

A	Overall hydrogen bond acidity
B	Overall hydrogen bond basicity
BBB	Blood-brain barrier
CE	Capillary electrophoresis
Cerasome EKC	Cerasome electrokinetic chromatography
$D_{sc}$	Diffusion coefficient through stratum corneum
E	Excess molar refraction in $(\text{cm}^3 \text{mol}^{-1})/10$
HPLC	High-performance liquid chromatography
$h_{sc}$	Diffusion path length in stratum corneum
IAM	Immobilized artificial membrane
ILC	Immobilized liposome chromatography
$k_{7,4}$	Retention factor obtained in cerasome electrokinetic chromatography
$K_p$	Skin permeability
$K_{sc}$	Partition coefficient in stratum corneum
LEKC	Liposome electrokinetic chromatography
LFER	Linear free-energy relationship
MLR	Multiple linear regression
MV	Molecular volume
MW	Molecular weight
N	Number of data points or compounds
P	Partition parameters into vehicles that model the stratum corneum

## Abbreviations

P <sub>lip</sub>	Liposome-water partition coefficient
P <sub>oct</sub>	n-Octanol-water partition coefficient
PC	Phosphatidylcholine or Principal component
PCA	Principal component analysis
POPC	3-sn-Phosphatidylcholine
PS	3-sn-Phosphatidyl-L-serine
PSD	Predictive standard deviation
QSPR	Quantitative structure-permeability relationship
R <sup>2</sup>	Squared correlation coefficient
S	Solute dipolarity/polarizability
SC	Stratum corneum
SD	Standard deviation
SP	Equilibrium coefficient for a series of solutes in a given system
V	McGowan characteristic molecular volume in (cm <sup>3</sup> mol <sup>-1</sup> )/100



## 8. Acknowledgements

---

My sincere and profound gratitude goes first and foremost to Prof. Dr. Alfred Fahr, my supervisor, for his thoughtful and in-depth guidance. His deep understanding of lipids and membranes in general and passionate attitude towards science have had a great impact on me. During the past three years, I have been truly impressed on his creativity and imagination. Furthermore, the confidence and faith he put on me walked me through all the stages of my Ph.D. life.

I am also greatly indebted to my co-supervisor, PD. Dr. Xiangli Liu, for her careful teaching on experimental techniques, illuminating advices and professional supervision. She led me to the exciting and attractive study field – quantitative structure-activity relationship, and always encouraged me to touch more research topics and enlarge my horizon. Without her great help, I would not have finished this dissertation.

Then, I would like to express my sincere gratitude to Prof. Dr. Michael Abraham, who taught me how to apply the linear free-energy relationship model. His kind help and suggestion lifted up my thought and knowledge.

A lot of thanks go to Prof. Dr. Gerhard K. E. Scriba and his colleagues, who kindly provided the use of capillary electrophoresis instrument and taught me many skills. To work together with them is an enjoyable, unforgettable experience in my Ph.D. study.

Further, I am very grateful to Prof. Dr. Ulrich F. Schäfer and Peter Meiers. They taught me a lot on how to measure skin permeability *in vitro*, and more importantly let me know what the rigorous scholarship is, which benefits me so much.

I wish to express my warm thanks to my colleagues who helped me directly or indirectly in my work and life: Kewei Yang, Ming Chen, Erica D’Aguano, Amaraporn Roopdee, Maximillian Sperlich, Stephen Holzschuh, Kalpa Nagarseker, Kathrin Kaeß, Mukul Ashtikar, Kirsten Dahse,

## Acknowledgements

Kristin Rüdél, Khaled Shalaby Ahmed, Hossam Hefesha, Susann Schröder, Ronny Rürger, Gorge Pester, Markus Rabenhold, Christiane Decker, Ramona Brabetz, Alexander Mohn, Angela Herre, Jana Thamm. I feel very lucky that I had them around me in my life. My experience in Germany is so beautiful because of them!

I give my deepest gratitude to my beloved parents for their selfless love, care and support in my whole life. They are forever the harbor of my heart and the source of my motivation. My love to them is more than to anything else.

Last but not least, I would like to appreciate all the reviewers for the time, patience and attention spent selflessly on my dissertation.

# Curriculum Vitae

---

## Personal Information

**Name:** Keda Zhang  
**Date of Birth:** August 25, 1986  
**Nationality:** Chinese  
**Address:** Lessingstr. 8 (Pharm), 07743 Jena, Germany  
**Telephone:** + 49 3641 949929 (office)  
**E-mail:** [keda.zhang@uni-jena.de](mailto:keda.zhang@uni-jena.de)

## Education

- 1) **Aug. 2009 – present:** PhD candidate in Pharmaceutics  
Institute of Pharmacy, Friedrich-Schiller-University Jena, Germany  
Thesis: **Predicting Skin Permeability of Neutral Species and Ionic Species**  
Advisors: Prof. Dr. Alfred Fahr, PD. Dr. Xiangli. Liu
- 2) **Jul. 2007 – Aug. 2009:** Master degree of science in Medicinal Chemistry  
School of Pharmacy, Wuhan University, China  
Thesis: **Design and Synthesis of 4 $\beta$ -Amino-5 $\alpha$ -androstanes**  
Advisor: Prof. Dr. Xianming Hu
- 3) **Sep. 2003 – Jul. 2007:** Bachelor degree of science in Applied Chemistry  
School of Science, Wuhan University of Technology, China  
Thesis: **Synthesis and Characterization of Monosaccharide-Grafted Polycarboxylate Superplasticizer**  
Advisor: Prof. Dr. Jiaheng Lei

## Research Experience

### **Doctoral Research:**

Projects include:

- Investigation on simple mathematical models for predicting skin permeability of both neutral and ionic species, including the linear free-energy relationship (LFER) model and the model

## Curriculum Vitae

based on partition parameters in liposomes and molecular weight; measurements of retention factors of both species in liposome electrokinetic chromatography (LEKC); measurements of skin permeability of ionic species *in vitro*.

- Estimation of binding strength of DY-676 (a fluorescent label for biomolecules) with lipid membranes by immobilized artificial membrane (IAM) chromatography.
- Estimation of the lipophilicity  $\log P_{\text{oct}}$  for temoporfin (a highly lipophilic drug) by reversed-phase high-performance liquid chromatography (RP-HPLC).

### **Master Research:**

Projects include:

- Synthesis and characterization of 4 $\beta$ -androstanes.
- Synthesis and characterization of *N*-hydroxy-L-arginine (NOHA) with L-glutamine as starting material.
- Extraction and purification of anthocyanins from balaton tart cherry powder.

### **Bachelor Research:**

Projects include:

- Synthesis and characterization of monosaccharide-grafted polycarboxylate superplasticizer.
- Study on extraction techniques of salt lake lithium resources in China.

### **Publications**

1. **Keda Zhang**, Kewei Yang, Gerhard K. E. Scriba, Michael H. Abraham, Alfred Fahr, Xiangli Liu. Comparison of lipid membrane-water partitions with various organic solvent-water partitions. *Journal of Pharmaceutical Sciences*, 2012, being revised.
2. **Keda Zhang**, Ming Chen, Gerhard K. E. Scriba, Michael H. Abraham, Alfred Fahr, Xiangli Liu. Human skin permeation of neutral species and ionic species: Extended linear free-energy relationship analyses. *Journal of Pharmaceutical Sciences*, 2012, 101(6): 2034-2044
3. **Keda Zhang**, Ming Chen, Gerhard K. E. Scriba, Michael H. Abraham, Alfred Fahr, Xiangli Liu. Linear free energy relationship analysis of retention factors in cerasome electrokinetic chromatography intended for predicting drug skin permeation. *Journal of Pharmaceutical Sciences*, 2011, 100(8): 3105-3113

## Curriculum Vitae

4. Xianbing Ke, Hao Hu, **Keda Zhang**, Wenjin Xu, Qifeng Zhu, Lamei Wu and Xianming Hu. Significant steroids: Effective and general synthesis of 4 $\alpha$ - and 4 $\beta$ -amino-5 $\alpha$ -androstanes. *Chemical Communications*, 2009, 9, 1037-1039
5. **Keda Zhang**, Lei Lei, Xianming Hu. Research on extraction and purification of anthocyanins from balaton tart cherry powder. *6<sup>th</sup> International Symposium for Chinese Medicinal Chemists*, Shanghai, China, 2008.
6. Hui Wu, **Keda Zhang**, Jie Wu, Ke Li, Jiaheng Lei. Development of extraction technology research of salt lake lithium resources in China. *Chemistry and Bioengineering*, 2006, 23(8): 4-6, in Chinese.

### **Presentations:**

1. **Oral presentation:** Linear free energy relationship analysis of retention factors in cerasome electrokinetic chromatography intended for predicting drug skin permeation. 21<sup>th</sup> Mountain/Sea Liposome Workshop, Oberjoch, Germany, 2011.
2. **Poster presentation:** Linear free energy relationship analysis of retention factors in cerasome electrokinetic chromatography intended for predicting drug skin permeation. Controlled Released Society German Chapter Annual Meeting, Jena, Germany, 2011.

### **Patents:**

1. Jiaheng Lei, Yong Liu, Liping Guo, Hui Wu, **Keda Zhang**. Monosaccharide-grafted polycarboxylate superplasticizer and preparation method thereof. May 7<sup>th</sup>, 2008: CN 101172805 A

# Statement

I am very familiar with the Promotionsordnung of the Faculty of Biology and Pharmacy in the Friedrich-Schiller-University Jena. All parts of the dissertation were produced by myself. Hereby I declare that this dissertation does not contain any material previously submitted for a degree or diploma at another university or any material previously written or published by any other person, except where due acknowledgement or reference has been made in the text. I also declare that I did not enlist the assistance of any dissertation counseling agent, and that I did not provide any direct or indirect monetary benefit to any third party for work connected to my dissertation.

Jena,

Keda Zhang